DNA 2772T

ADA 058-367

DNA EMP AWARENESS COURSE NOTES

Third Edition

IIT Research Institute
10 West 35th Street
Chicago, Illinois 60616

October 1977

Topical Report

CONTRACT No. DNA 001-75-C-0074

THIS WORK SPONSORED BY THE DEFENSE NUCLEAR AGENCY
UNDER RDT&E RMSS CODE X323075469 Q75QAXEC09201 H2590D.

Prepared for

Director
DEFENSE NUCLEAR AGENCY
Washington, D. C. 20305

A comparison of the waveform and spectrum of the high altitude burst and the induction fields of a lightning stroke are shown in the figure.

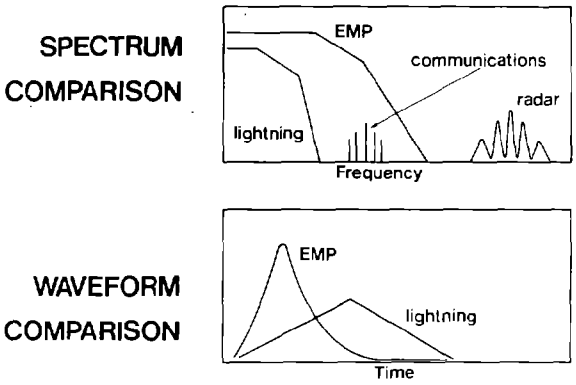

Although a lightning stroke can have a fast rise time, low energy precursor before the main stroke, the main stroke is a high amplitude (100 kV/m or greater), 1 to 5 microsecond rise time and hundreds of microseconds fall time. An enormous amount of energy is contained in the main stroke. The induction field, however, which is of concern to systems nearby a lightning discharge is on the order of 1 kV/m electric field. This induction field is non-radiating and therefore a localized field.

In the high altitude burst case, the fields radiated onto the earth's surface are of the order of 50 kV/m electric field with rise times of the order of 10 nanoseconds. The wave is a radiating EM wave which results in an extremely large distribution on the earth's surface in contrast to the localized nature of lightning. For a burst over the continental U.S., the fields on the surface are predominantly horizontally polarized E fields. Since the burst location is outside the ionosphere, the coverage on the earth's surface is limited by the line-of-sight tangent radius to the earth's surface. The figure shows the approximate coverage on the earth for a 100 km (small circle) and 300 km (large circle) height of burst over the central U.S.

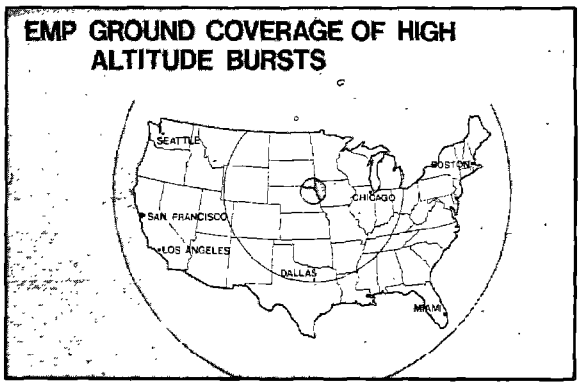

These fields are not uniform in amplitude or waveform over the entire area but depend on burst location and the earth's geomagnetic field, as we will see in Section III of the course. It should also be recognized that no other weapons effects accompany the EMP from a high-altutude burst.

Due to the fast rise times of the EMP, the spectral energy is distributed throughout the spectrum through the lower microwave band. Most man-made sources occupy only a narrow part of the spectrum.

In the case of the near surface (0-2 km) burst within the deposition (source) region, non-radiating fields on the order of 100 kV/m electric fields (or higher) with rise times of tens of nanoseconds (approximately 50 ns) are realized. Outside the deposition region, a radiating EM wave is realized. The fields of this radiating wave at a distance of 10 km from the burst location are quite comparable to the close-by fields of the lightning stroke. That is, rise times of approximately 1 to 5 microseconds and peak amplitude of 1 kV/m electric field. These fields fall off as 1/R (R being the distance from the burst point) with distance from the burst. These fields are essentially vertical polarized electric fields.

In other words, EMP is sufficiently different from any other electromagnetic environment usually encountered that protection practices and components for non-EMP environments -- radio-frequency interference, lightning, radar, etc., are not directly applicable for EMP problems.

Laboratory tests have demonstrated that vacuum tube systems are many times more resistant to permanent damage from EMP than semiconductor systems, and 60 Hz motors even more resistant than vacuum tubes; but even motors can be damaged if connected to a very large energy-collecting structure.

The replacement of "harder" vacuum tube systems by "softer" transistors or integrated circuit systems was an aspect which was never considered during the atmospheric test period. This evolution of systems using components that require inherently less power has resulted in an increased susceptibility to EMP.

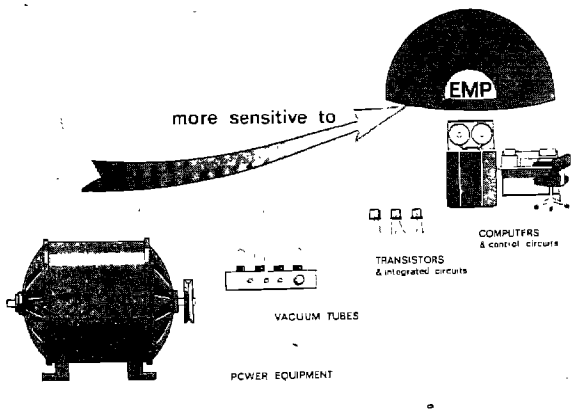

Digital computers are extremely sensitive to EMP. Here it makes little difference whether vacuum tubes or transistors are used. It can affect operation of a computer by introducing false signals or by erasing information stored in memory banks. Very small amounts of energy may perturb such things as the flight path of a missile, momentarily disrupt display devices, temporarily upset the operation of many other types of electronic gear, etc.

Tests on systems have demonstrated an "avalanche effect", wherein very small amounts of EMP can "dump" huge amounts of stored electrical energy which normally occurs within a system. This can set off an electronic/electrical "landslide" which could damage components or jam communications systems. This is somewhat analogous to a tiny spark igniting a forest fire. In fact, EMP-induced "sparks" could well ignite fuel-air vapors or detonate ammunition under the proper conditions. A well-publicized example of an "electrical avalanche" due to a small component failure was the Northeast power system blackout. This, of course, was not induced by EMP.

Most of our electronic systems are designed to be frequency selective, (i.e., operate over a narrow frequency band), and, therefore, respond differently to the EMP spectrum. As we have seen, the EMP spectrum is very broad, but it certainly is finite. Where the energy couples to the system (power line, antenna, etc.) determines the spectral content and the energy transmitted to sensitive components within the system. Therefore, all systems will not be susceptible to EMP nor will they respond in the same manner or to the same extent.

Examples

What does this mean in more specific terms? A few hypothetical system examples may be illustrative. Consider a communications complex. The most likely EMP effect would be temporary interruption of communication service. This can occur even though no permanent damage requiring parts replacement occurs. Where EMP protection was not considered, it has been shown that one EMP pulse could impair service of certain portions of the system for as long as 20 to 40 minutes. Burnout of key components is somewhat less likely, but always a possibility.

In the case of strategic systems and some tactical systems, no impairment of the system can usually be tolerated, even for a few seconds. For example, EMP pickup in the control system of an in-flight missile could perturb the flight so much as to cause breakup of the missile, could disrupt the count-down of missiles being readied for firing, or could impair the command and control during critical times.

In the case of tactical systems, many of these systems are required to survive the effects of the nearby detonations of a low-yield nuclear weapon. Here it makes little sense to invest millions of dollars in blast, thermal, and TREE protection without providing a comparable degree of EMP protection as well.

Consider a hypothetical, anti-aircraft, fire-control, and fighter-director tactical system. One EMP event has the potential to "erase" all of the recorded data supplied by over-the-horizon picket aircraft and ships or distant sensors even though no permanent damage occurs. This one-to-ten minute potential service interruption could allow an enemy bomber enough of an advantage to destroy the system.

Nuclear war without a direct USA involvement is a relevant part of EMP weapon effects scenarios. A nuclear detonation, a continent away, must not functionally damage vital radio communication links from the USA to tactical units -- ships, aircraft and ground units stationed near the conflict.

The photograph dramatically illustrates some of the pseudo-focusing or field-gathering effects. In this case, the EMP field intensity has been "gathered" (or more correctly, enhanced) by a factor of about 100 times. This "pseudo-focusing" was sufficient to ionize the air near the blade tips, as shown in this photograph taken of a rotor blade of a helicoper undergoing nighttime EMP simulation tests.

Summary

The 3,000 mile high altitude electromagnetic EMP effects radii occurs because of:

1. large source region,
2. very intense fields with characteristics never normally encountered,
3. "focusing effect" of energy collection,
4. extreme sensitivity of modern components and subsystems,
5. "house-of-cards" design of systems.

From the foregoing, we can see that EMP susceptibility is a three-factor function:

- Energy collection; collection efficienty (size) of structure,
- Fraction of collected energy applied to sensitive component,
- Sensitivity of component to damage or upset (interruption).

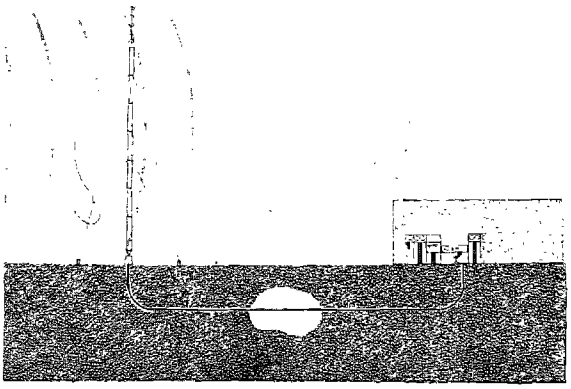

The potential disruption effects of EMP must be considered for all systems because of the ever-increasing dependence on modern sophisticated electronic/electrical systems for both military and civilian uses.

Thus all systems of any importance should incorporate features and techniques to counter the EMP effects, as required. A number of systems have already been demonstrated to be protected and many more systems are currently being EMP-hardened.

Thus, the central issue today is PROTECTION.

It is essential to keep in mind that in a time varying electromagnetic field, the electric field ($\vec{E}$) and the magnetic field ($\vec{H}$) cannot be created independently. Coexistence of the electric and magnetic fields is a prerequisite to the establishment of an electromagnetic field. At low frequencies ($\tilde{<}$ 10 kHz), the electric and magnetic fields are often considered separately for simplification of shielding analysis and design. At these low frequencies this is a very good approximation. True separation of these fields only exists in the static (dc) case, however.

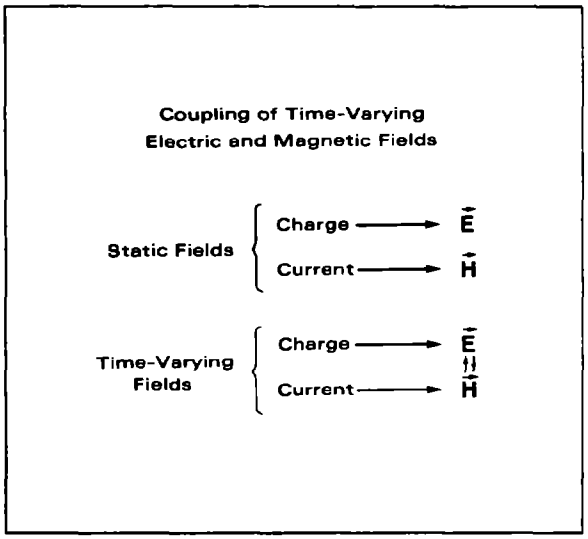

The relationship between the electric and magnetic field is given by:

$$\frac{\vec{E}}{\vec{H}} = \eta$$

where

η = characteristic impedance of the media

η_o = 377 Ω is the characteristic impedance of free space.

The medium also plays an important role in formulating the electromagnetic field. The parameters of the medium provide the necessary link between various electromagnetic quantities. The more important medium parameters and their units, and the role they play are indicated here.

Parameters of the Medium	Relationships Between Field Quantities and Parameters of the Medium
ϵ = Permittivity (Farad/m)	$\vec{D} = \epsilon\vec{E}$
μ = Permeability (Henrys/m)	$\vec{B} = \mu\vec{H}$
σ = Conductivity (Mhos/m)	$\vec{J} = \sigma\vec{E}$

Electric fields are the result of charge separation in the media. For simplicity, consider the generation of a static (dc) electric field. A simple case is that of a parallel plate capacitor. Impressing a voltage (V) across the plates results in a redistribution of charge on the plates as shown. This redistribution of charge results in an electric field ($\vec{E}$) between the plates. The relation between the electric field and the applied voltage, in this case, is given by:

$$\vec{E} = \frac{V}{S} \text{ volts/meter}$$

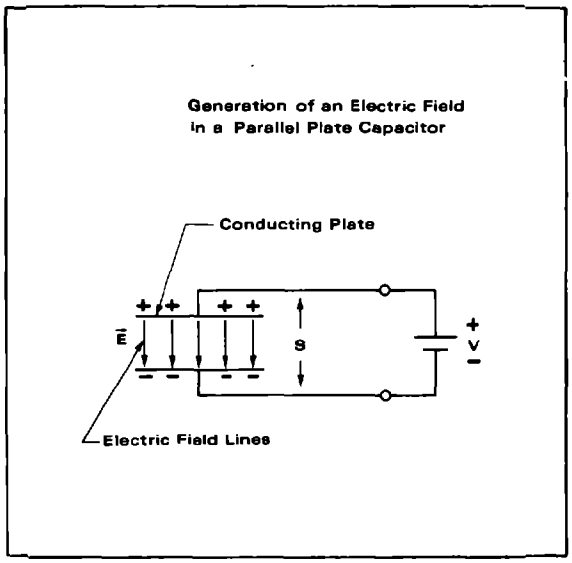

If we have a force which causes charge separation, an electric field is created. In this case, the force was the applied voltage. For example, in the case of EMP generation, as we will see in Section III, the force causing the charge separation is the nuclear detonation and the resulting gamma rays.

The generation of magnetic fields requires current to flow. Again for simplicity, consider the static (dc) case. Consider, for a simple example, the field between two current sheets carrying a total current I. The total current is related to the current density (J_s) by the relation

$$I = J_s S$$

where

S = cross sectional area of the current sheet.

This assumes a uniform current density which holds only for the static case. The resulting magnetic field ($\vec{H}$) between the current sheets is given by:

$$\vec{H} = \frac{\vec{J}_s}{2\pi d} \text{ amps/meter.}$$

In the case of EMP, see Section III, the current flow results from the interaction of the gammas produced by the nuclear detonation with the media.

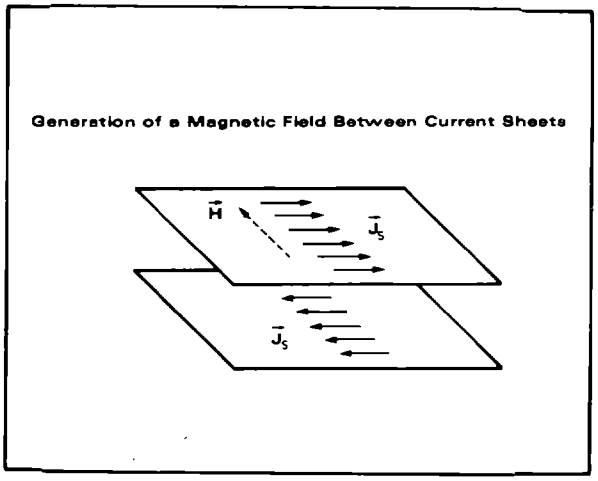

In many cases in field theory, the events occurring at a point, or within an incremental volume, are of interest. In these circumstances, it is desirable to define the relationships between the current and voltage for the incremental volume. These are shown in the figure. The concept of current density is useful. For an incremental volume or area, the current is uniform throughout, and the current is related to the current density by:

$$I = \vec{J}S = \frac{V}{R}$$

where

$\vec{J} = \sigma \vec{E}$

$V = \vec{E}L$

$R = \frac{L}{\sigma S}$

σ = conductivity of the material

R = resistance of the material for the incremental volume

$\vec{E}$ = induced electric field.

Ohm's Law for an Elemental Volume

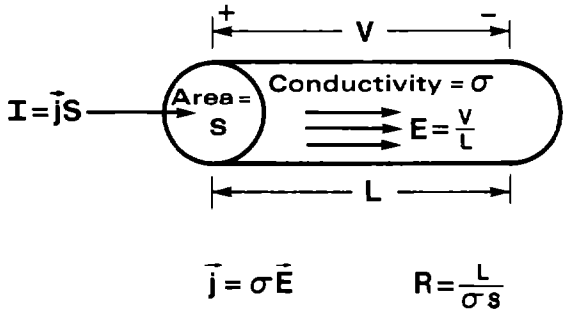

Direction of power flow in a distant EM field is given by the POYNTING vector and can be obtained by use of the right-hand rule, as indicated. Note that the POYNTING vector, $\vec{P}$, gives not only the direction of power flow but also the power density of an EM field in watts/m^2.

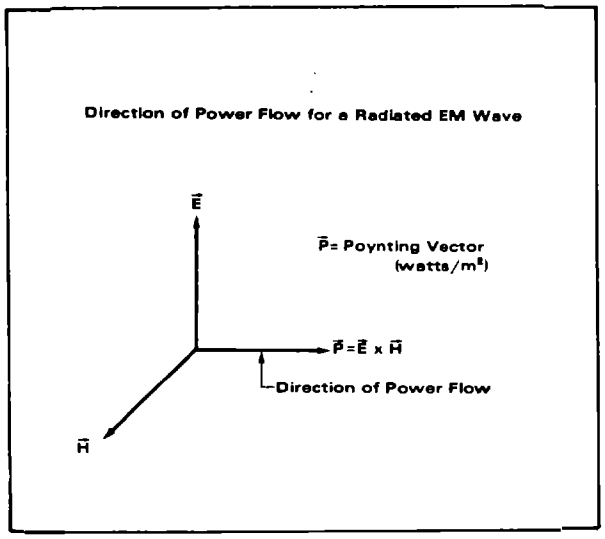

2.3 EMP CHARACTERISTICS

The waveform of the EMP plays an important role in the coupling to systems and the effects on systems. At this time we will define the more important characteristics of the EMP to serve as a base of understanding for subsequent discussions.

Two of the most important parameters are shown in the figure. The rise time (t_r) is defined as the time between the 10 and 90 percent points of the leading edge of the wave. The time to half-value is the time for the wave to decay to half amplitude on the trailing edge of the pulse. These times determine the spectral content of the wave.

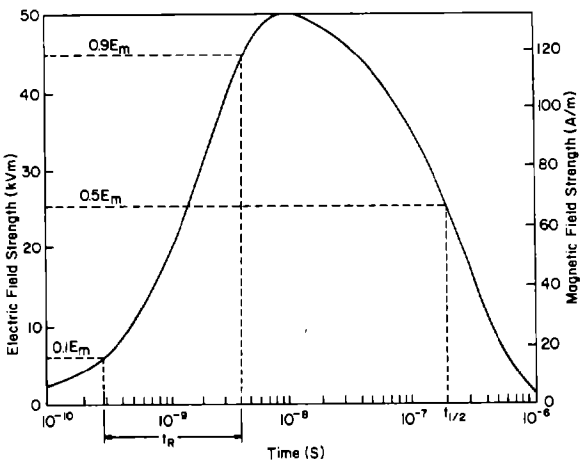

GENERALIZED HIGH-ALTITUDE EMP ELECTRIC AND MAGNETIC-FIELD TIME WAVEFORM

Equally important, in order to determine the coupling to a system, is the polarization of the wave. The polarization is defined on the basis of the $\vec{E}$ field vector. Vertical polarization is when the $\vec{E}$ field vector is normal to the direction or propagation and wholly within the plane of incidence. Horizontal polarization is when the $\vec{E}$ field vector is normal to both the plane of propagation and the plane of incidence.

The angles of incidence are the vertical angle (ψ) between the point of observation and the burst point measured from the location of the point of observation, and the horizontal angle (θ) between the axis of the energy collector and the direction plane of incidence.

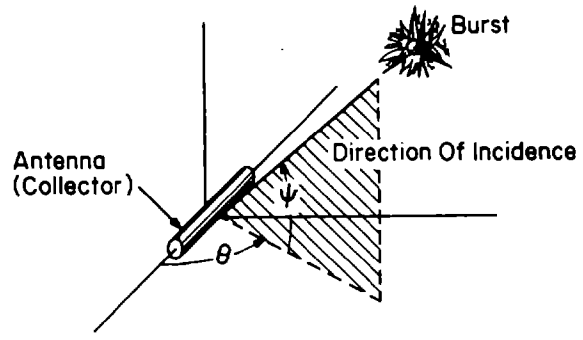

ANGLES OF INCIDENCE

How do the gamma rays cause EMP? The answer is through the Compton interaction process. Compton discovered that photons can collide with electrons, knocking them out of the atoms in which they were originally bound. These Compton collisions are somewhat like the collision of a moving billiard ball with one at rest. The recoil electron, like the ball originally at rest, goes predominantly forward after the collision. Thus, a directed flux of gamma rays produces, by Compton collisions, a directed flux of electrons. This constitutes an electric current, which generates the EMP.

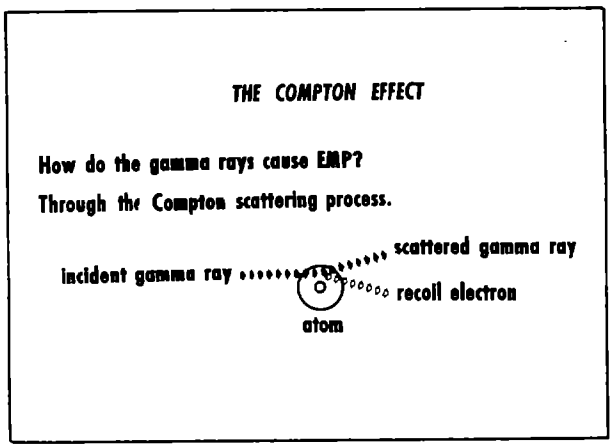

We can now consider some order of magnitude estimates of the energy involved at each state of the EMP generation process. A one megaton bomb releases 4×10^{15} joules of energy. About 0.1% of this energy, or 4×10^{12} joules, may appear as prompt gamma rays. This amount of energy is equivalent to that produced by a hundred megawatt power plant running for about 11 hours. A fair fraction, about one-half of this, goes into the Compton recoil current. Fortunately, most of this energy goes into heating air rather than into the EMP. About 10^{-3} of the gamma energy goes into EMP; thus giving about 10^{-6} of the bomb energy going into the EMP.

3.3 EMP GENERATION

The previous section showed how a nuclear detonation produces the gamma rays and how these in turn produce the Compton electrons. These basic physics principles hold for all burst locations. To generate a radiated EMP, however, other mechanisms exist which differ with burst location. This section will discuss generation of a radiated EMP and its characteristics for the three burst locations.

Deposition Region Fields

The gamma rays emitted by the nuclear detonation are nearly symmetrical, any anisotropy of the emission of the gammas is small and of short duration compared with other factors. The result is the Compton electrons created move radially away from the burst point and there exists a radial symmetric current distribution. The scattering of the electrons leaves behind the heavier positively charged parent molecule. This separation of charge produces a strong radial electric field as shown in the figure.

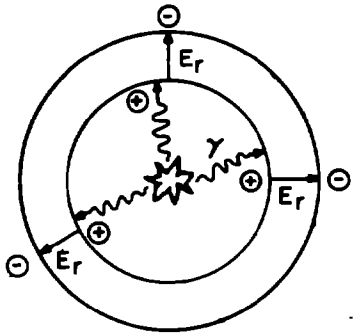

CHARGE SEPARATION MODEL

For this symmetrical condition, no magnetic field is generated and therefore the deposition region fields are nonradiating fields. In the deposition region in early time, the Compton electron current dominates and the radial electric field rises rapidly. Due to additional collisions, the Compton electrons produce secondary electrons which further ionize the air and increase its conductivity. These secondary electrons under the influence of the radial electric field move and produce a conduction current which tends to reduce or limit the local field resulting in the plateau at later time.

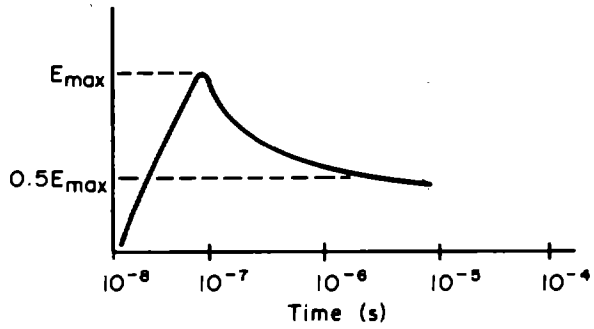

GENERAL TIME WAVEFORM OF E_r IN DEPOSITION REGION

Near Surface Burst EMP

A completely symmetrical system of radial currents produces neither magnetic nor radiated fields. The departure from symmetry, in the case of the near surface burst (less than 2 kilometers above the earth), is provided by the earth/air interface, resulting in a nearly hemispherical deposition region.

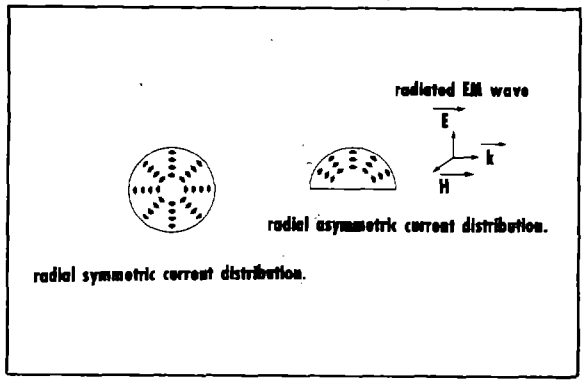

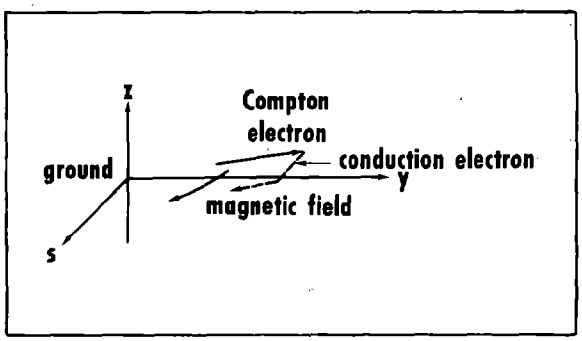

The deposition region is limited in size (3 to 6 km) by the air density and hence the distance the gamma rays can travel. The average distance a gamma ray travels before making a Compton collision is about 200 meters at sea level, although a few may go as far as a few kilometers. The Compton electrons travel outward only a few meters before being stopped by the air. The deposition region is thus more dependent on the absorption of gammas in the atmosphere than on the yield of the weapon.

Within the deposition region, as discussed previously, a strong radial field exists. The radial field has a peak amplitude of approximately 100 kV with a rise time of 10 nanoseconds. The earth tends to short out the radial electric field near it since it is normally a better conductor than air. Near the ground the conduction electrons find an easier path back to the positively charged center by flowing down to the ground and back towards the burst point. The result is a current loop which generates an azimuthal magnetic field.

A vertical electric field is required in connection with the vertical component of conduction current. This vertical electric field can be regarded as connecting Compton electrons in the air with their image charges in the ground. Thus, for a near surface burst, the principle fields in the deposition region are a radial and vertical electric field, and an azimuthal magnetic field.

When viewed from a large distance from the burst point, the net fields are the vertical electric and azimuthal magnetic fields. A vertical dipole can be used as a source model for the radiated EMP in this case. The dipole model is depicted in the figure.

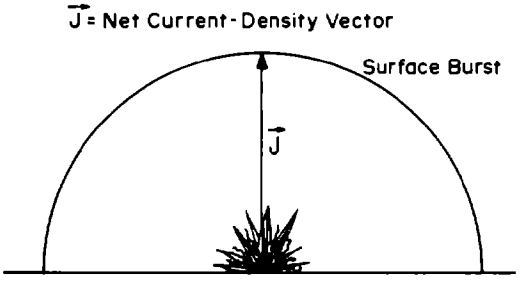

ELECTRIC-DIPOLE MODELS OF SURFACE AND AIR-BURST RADIATED EMP (ADAPTED WITH THE PERMISSION OF THE DEFENSE NUCLEAR AGENCY)

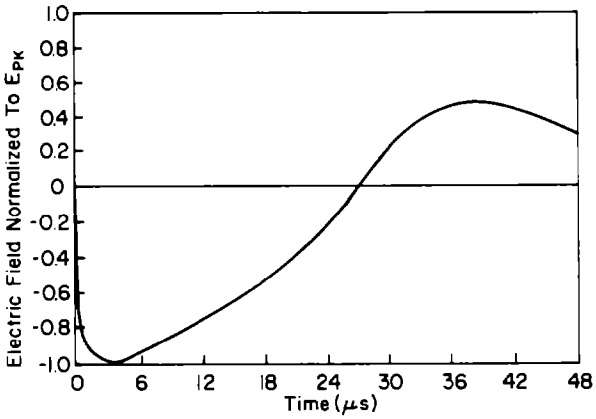

GENERALIZED TIME WAVEFORM OF SURFACE-BURST RADIATED ELECTRIC FIELD (ADAPTED WITH THE PERMISSION OF THE DEFENSE NUCLEAR AGENCY)

The radiated fields are characterized by an oscillating signal. The magnitude of the radiated field falls off inversely proportional to distance from the burst. A rough estimate of the peak electric field strength (E_{pk}), where peak is the largest negative value, is given by:

$$E_{pk} = \frac{10^7}{R} \text{ volts/meter}$$

where R = radial distance from the burst point.

A generalized time waveform is shown. The Fourier transform of this waveform shows the bulk of the energy lies below 1 megahertz. The peak amplitude at a distance of 10 km is about 1000 volts/meter.

The radiated field from a near surface burst is predominantly vertically polarized at the earth's surface.

The relative magnitude of the deposition region fields to the radiated fields, indicate the near surface burst EMP is a serious threat to most systems within the deposition region. Outside the deposition region, the EMP is a principal threat to systems which respond to very low frequencies or have very large energy collectors.

Air Burst EMP

An air burst is defined as a burst occurring at an altitude of 2 to 20 kilometers above the earth. The EMP from an air burst is characterized by a strong radial electric field in the deposition region and a weak radiated field.

The air density, in the range of 2 to 20 kilometers, is relatively dense and quite uniform. This relatively dense air results in a relatively short range for the gamma rays and Compton electrons as in the case of the near surface burst. Consequently, no appreciable turning of the electrons takes place in the geomagnetic field (see the discussion on exoatmospheric EMP), and therefore, this mechanism does not result in a radiated EMP.

Since the air density is also quite uniform, only a small net current asymmetry exists resulting in only a weak radiated EMP. A dipole model, as used for the near surface burst, can also be used here. The radiated fields from the

air burst are similar in shape to those of the near surface burst, with the peak fields at least one order of magnitude less than those of the near surface burst.

Due to the weak radiated fields, the EMP from an air burst is a principle threat to systems which may be within the deposition region, in which case, the other nuclear weapons effects must also be considered.

Exoatmospheric Burst EMP

An exoatmospheric burst is defined as one which takes place at an altitude greater than 40 kilometers above the earth. A typical exoatmospheric burst geometry is depicted in the figure.

EMP FROM HIGH ALTITUDE BURSTS
EXAMPLE OF GEOMETRY BEING CONSIDERED

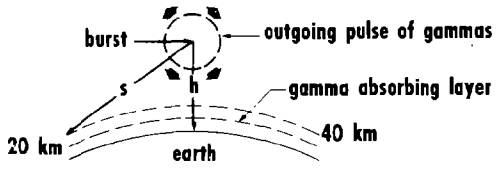

h = height of burst = 400 km
s = distance to horizon = 2,250 km

A high altitude burst illuminates large geographical regions with gamma rays

Above about 40 kilometers altitude, the atmospheric density is sufficiently small that the high energy gammas are not affected appreciably. The atmospheric density is large enough that the gammas are absorbed by Compton scattering below 40 kilometers. The gamma absorption is nearly complete by the time they reach 20 kilometers altitude. The deposition region for a high altitude burst is thus between about 20 to 40 kilometers, which is approximately 65,000 to 130,000 feet.

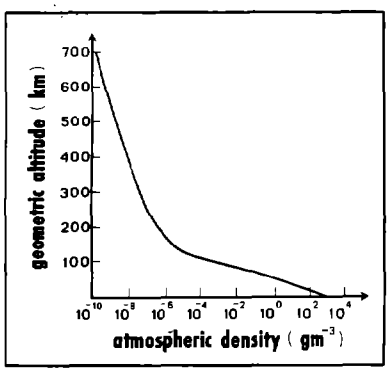

The Compton electrons are scattered forward (downward in this case), within the deposition region as was the case for both the near surface and air bursts. These Compton electrons produce a system of radial currents. As stated previously, a symmetrical system of radial currents will not produce a radiated field. In an exoatmospheric burst situation, there are two mechanisms which produce the radiated field: (1) the asymmetry due to the space/atmosphere interface, and (2) Compton electron turning due to the earth's geomagnetic field. It is the Compton electron turning which dominates since the electrons can travel greater distances, and thus have more time to interact with the geomagnetic field due to the reduced atmospheric density.

The outgoing gammas from the burst form a spherical shell which expands with the velocity of light. Since most of the gammas are emitted in about 10 nanoseconds, the thickness of the shell at any instant is a few meters. When the gamma shell begins to intersect the absorbing layer of the atmosphere, the Compton scattering process begins.

At the altitude of the deposition region, the stopping range of Compton recoil electrons is of the order of 100 meters. In traveling this distance, the Compton electrons are strongly deflected by the geomagnetic field with a gyro radius of about 100 meters. The Compton recoil current therefore has strong components in directions transverse to the gamma propagation direction. This transverse current radiates an electromagnetic wave that propagates in the forward direction.

The outgoing wave keeps up with the gamma shell and is continually augmented by the transverse Compton current until the gammas are all absorbed. Then the

electromagnetic wave goes on alone as a free wave or pulse. Secondary electrons produced by the Comptons make the air conducting. This conductivity attenuates the electromagnetic pulse. The amplitude of EMP is determined by a balance between:

1. Increase due to transverse Compton current.

2. Attenuation due to conductivity.

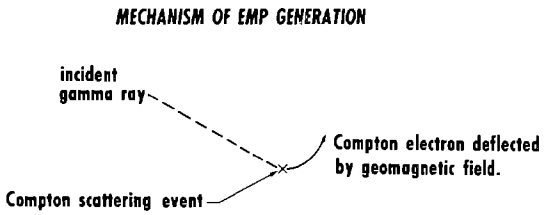

A summary of the process of EMP generation from a high altitude burst can now be given along with important details on the directional dependence.

Gamma rays are scattered from molecules with the emission of Compton electrons in the forward direction with energies on the order of 1/2 million electron volts. The motion of the Compton electrons is modified by the geomagnetic field. They follow a spiral path about the magnetic field lines until they are stopped by collision with atmospheric molecules. As the Compton electrons collide with atmospheric molecules, further ionization occurs and the conductivity increases. The propagation of the EMP depends on the conductivity of the region through which it passes. Dispersion, attenuation, and reflection may occur. The circular component of the Compton electrons represents a magnetic polarization, and the linear component represents an electric polarization.

Both the magnetic and electric polarizations vary with time and, consequently, can radiate electromagnetic energy. This can also be viewed as a collective flow of electrons along the field which radiates in the transversal direction.

Compton electrons that move parallel to the geomagnetic field are not deflected. Thus, the EMP amplitude is small in two directions along the geomagnetic field line passing through the burst point. The EMP amplitude is a maximum on those rays from the burst point which run perpendicular to the geomagnetic field in the deposition region.

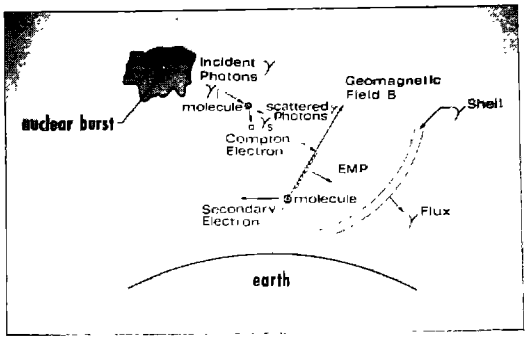

The transverse current components and the resulting radiated fields can be understood by considering a system of elemental dipoles along the line-of-sight from the observation point to the burst point. Each dipole radiates an electromagnetic field (the normal "donut" radiation pattern of a dipole) which add in phase since the EM fields, gammas, and Compton electrons all travel at or near the speed of light.

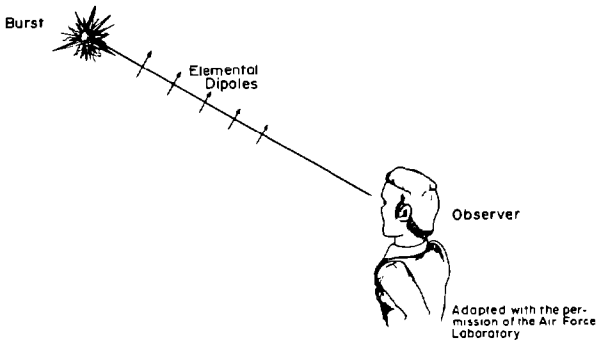

PHASED MAGNETIC DIPOLE ARRAY MODEL

The radiated fields are high intensity fields, have short rise times (wide spectrum) and cover a large area of the earth's surface because of the height and large extent of the deposition region. The geographical coverage as a function of the height of burst can be obtained by considering the tangent radius.

The tangent radius is the arc length between the line from the earth's center to the burst point and the line from the earth's center to the point where a line from the burst point is tangent to the surface of the earth. For a burst at 300 kilometers, the tangent radius is 1920 kilometers, or about 1200 miles. The EMP from the burst can cover this region.

It should be noted that the fields do not end at the tangent radius. For surface systems, this is the farthest point of interest, in most cases, but low amplitude fields may be propagated beyond this point by ducting. For airborne systems, however, the coverage may be much farther depending on the height of the point of observation. As long as there is line-of-sight to the burst point, the EMP will be present.

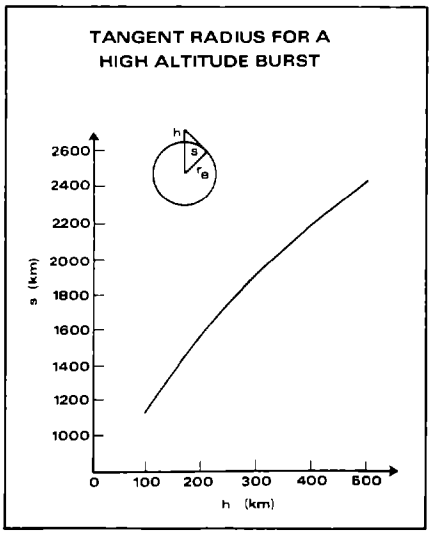

The EMP time waveform varies considerably over the area of coverage. Three cases will be considered: (1) near surface zero, (2) the maximum field point (where a line from the burst point to the maximum field point is orthogonal to the geomagnetic field lines in the deposition region), and (3) at the tangent radius point.

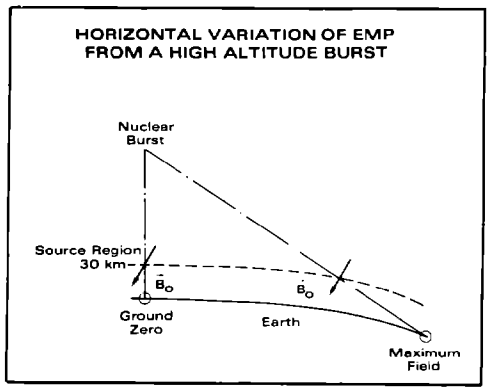

At surface zero, the fields have reduced amplitude (0.25 E_{max}), short rise time (approximately 5 nanoseconds), and time to half value of about 20 nanoseconds. At the maximum field location, the rise time is about 10 nanoseconds and time to half value is about 50 nanoseconds. At the tangent radius, the fields are about 0.5 E_{max}, and rise time to half value greater than 10 nanoseconds and 200 nanoseconds respectively. This distribution, as a function of height of burst and geographic position on the earth, can be determined from the figure. The peak field at any point can be found by aligning magnetic north on the figure with magnetic north at surface zero.

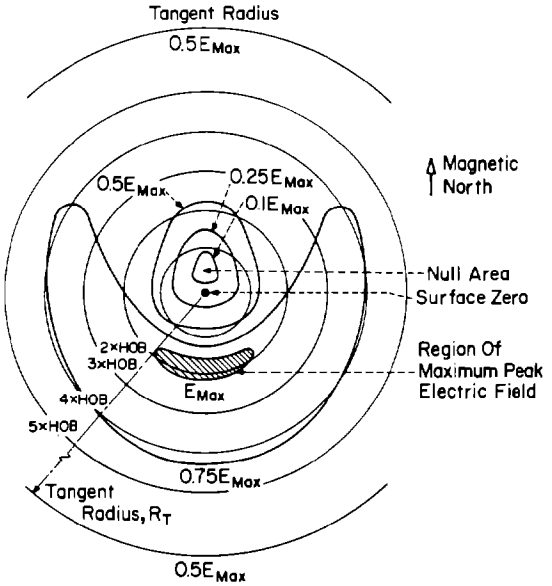

VARIATIONS IN HIGH ALTITUDE EMP PEAK ELECTRIC FIELD ON SURFACE OF CONTINETAL UNITED STATES (ADAPTED WITH THE PERMISSION OF THE DEFENSE NUCLEAR AGENCY)

As a result of this wide variation on the earth's surface and the inability to predict the burst location, the time waveform used preserves the important characteristics of the three waveforms discussed. The composite waveform, therefore, maintains the fast rise time (near surface zero rise time), slow decay (near tangent radius decay), and maximum peak amplitude. The spectrum contains all frequencies of interest. The composite waveform, shown in the figure, can be approximated analytically by a double exponential.

$$E(t) = 5.25 \times 10^4 \left[e^{-\alpha t} - e^{-\beta t}\right]$$

where

$$\alpha = 4 \times 10^6$$

$$\beta = 4.76 \times 10^8$$

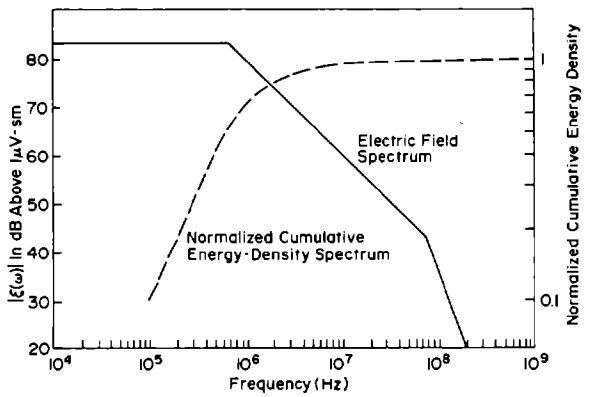

HIGH-ALTITUDE EMP SPECTRUM AND NORMALIZED ENERGY DENSITY SPECTRUM

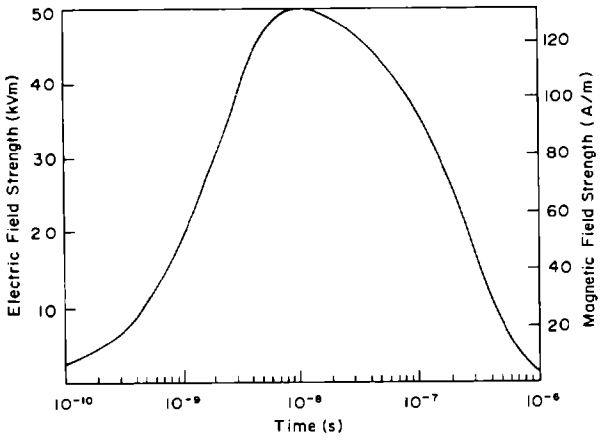

GENERALIZED HIGH-ALTITUDE EMP ELECTRIC-AND-MAGNETIC-FIELD TIME WAVEFORM

The spectrum of this pulse can be obtained by taking the Fourier transform of the time waveform. The significant frequencies extend out to about 150 megahertz with the bulk of the energy (99.9%) below about 100 megahertz.

The polarization of the EMP depends on the locations of both the burst and the observer, and the orientation of the geomagnetic field. The direction of the electric field is normal to both the geomagnetic field at the observer's location, and the direction of incidence. The direction of incidence is radially outward from the burst. For the Continental U.S., a typical dip angle for the geomagnetic field is about 67 degrees.

For this dip angle, and assuming the geomagnetic field lines run north and south, the EMP polarization is horizontal for bursts north or south of the observer. For bursts east or west of the observer, the polarization departs from horizontal by 23 degrees or less. Therefore, the principle polarization for systems based in the U.S. is horizontal.

3.4 EARTH EFFECTS ON TOTAL FIELDS

So far we have discussed the free field which impinges on the surface of the earth due to the radiated EMP. Since these are electromagnetic waves, they will penetrate the surface of the earth and be reflected by it. The amount of penetration or reflection is a function of the frequency (spectrum of the pulse), the polarization, direction of incidence, and earth parameters.

The reflection and transmission coefficient equations are presented in Section V. It should be noted that a phase reversal takes place for the component of the electric field parallel to the conducting surface but not for the normal to the surface component. Near the surface, therefore, for the parallel component, the electric field is reduced, but the magnetic field is increased. Electromagnetic fields also diffuse into the ground. The penetration depth depends on ground conductivity and frequency component considered. A greater ground conductivity leads to a smaller penetration depth. The high-frequency components penetrate less deeply than the low-frequency components of the pulse.

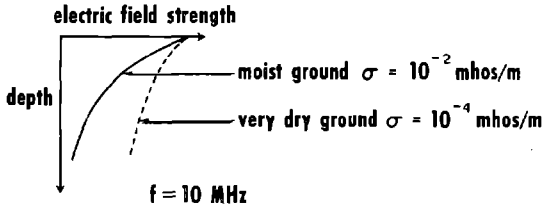

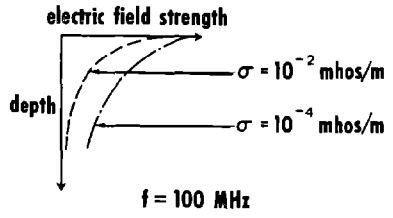

3.5 SYSTEM GENERATED AND INTERNAL EMP

While not the subject of this course, a few words are in order in the area of system generated EMP (SGEMP) and internal EMP (IEMP).

Internal EMP is EMP induced directly in a system by gamma radiation (or X-rays) striking the system. In the case of internal EMP, Compton recoil electrons are produced by interaction of incident gamma radiation with material in the system. This interaction is similar to production of Compton recoil electrons in the atmosphere in the case of external EMP. However, the way in which Compton recoil electrons produce internal EMP differs from that of the Compton recoil electrons in external EMP.

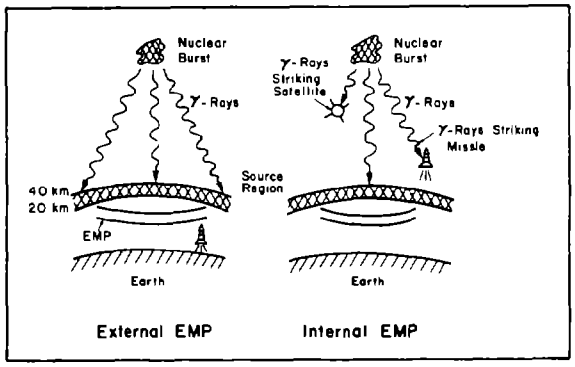

Internal EMP can arise in different ways. One type may be called "cavity EMP" and arises from Compton recoil electrons being driven across the volume of an enclosed cavity. Both electric and magnetic fields are generated. These fields may ring at the cavity frequencies. The fields will induce voltages in circuits contained in the cavity. If the cavity contains air, it may become electrically conducting. This affects the time behavior of the fields.

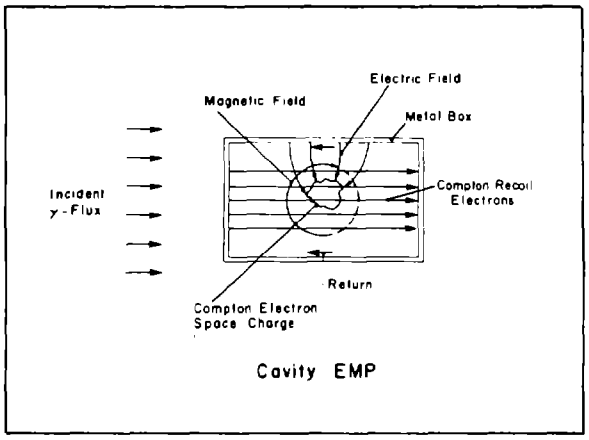

Another internal effect (SGEMP) is "Compton charging." Any object in a gamma flux has some Compton electrons knocked out of it and receives Compton electrons knocked out of other nearby objects. These will usually not balance. The charge added at various locations in a conducting circuit will flow away through the circuit, thus generating an extraneous signal. The charge acquired by insulation may leak away very slowly. In general, the thicker the object, the more charge it acquires.

A coupling structure can also collect energy from an impinging EMP field by magnetic induction. The induced signal from an EMP is equal to the negative time rate of change of the incident magnetic flux. This is an empirically derived fundamental law known as Faraday's Induction Principle. The voltage induced in a loop by a uniform magnetic field is given by

$$v(t) = \mu_o A \frac{d}{dt} H(t)$$

where

μ_o = $4\pi \times 10^{-7}$ is the permeability of free space

A = the area of the loop

H = The component of the magnetic field normal to the plane of the loop.

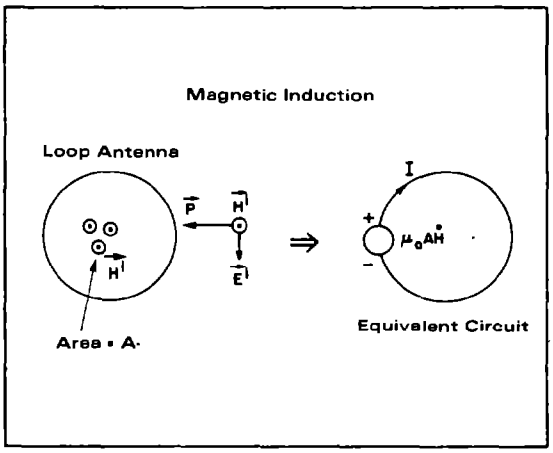

Another important coupling mechanism is that due to the I-Z drop which occurs whenever a coupling structure is imbedded in a lossy medium, e.g., earth, in which EM fields exist. Consider, for example, a bare wire conductor located a distance, d, below the surface of the earth and in the presence of an impinging EMP field as shown. The incident EMP field illuminating the surface of the earth causes conduction currents per meter width to flow in the earth. As a result of the current flow in the earth, a distributed I-Z drop appears along the wire which is equivalent to a voltage source distribution, causing current to flow in the wire conductor. An increment of voltage drop (which can be viewed as a point generator), ΔV, over a distance, Δz, along the conductor is given by

$$\Delta V = Z_T J \Delta z$$

where

J = total earth conduction current per meter width

Z_T = surface transfer impedance of the earth.

The surface transfer impedance is given by

$$Z_T \simeq \frac{\alpha}{\delta} e^{-\alpha z} \exp\left[- d\sqrt{\alpha^2+\beta^2}\right]$$

where

α = propagation constant of the earth

β = free-space propagation constant

δ = earth conductivity

d = depth of burial.

Transmission line theory may now be used to determine the actual current distribution induced on the wire.

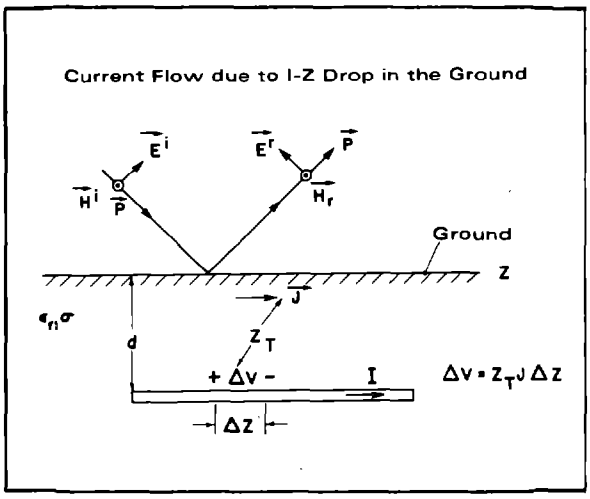

Antennas

Electromagnetic coupling to antennas results from electric and magnetic induction. The induction principle which dominates for a given antenna depends on the antenna's geometrical configuration. At this time we will consider two basic, simple types: (1) the linear antenna (monopoles or dipoles), and (2) the loop antenna. The way energy couples to these simple antennas can serve as a basis for estimating the energy collection by complex antennas and the other conducting structures.

Linear Antennas

When an electromagnetic wave impinges on a linear antenna, the tangential component of the electric field induces charges on the antenna which tend to cancel the incident field. Since these charges are free to move, an antenna current results. In a time varying field, therefore, these charges are constantly in motion and an alternating current flows on the antenna and in the load.

Electric induction on a linear antenna can be viewed as an array of point voltage sources. To obtain the total voltage induced on the antenna, all of the point sources must be summed (integrated) over the length of the antenna. If the antenna is short (antenna length $\leq$ 1/6 the wavelength of the incident signal), it is not necessary to perform the integration. In the case of EMP, since it is a transient signal containing a wide frequency spectrum, the antenna length must be $\leq$ 1/6 the wavelength of the highest frequency component of interest in the spectrum. For typical EMP waveforms, the actual physical length must be less than approximately two (2) feet.

Considerable simplification results when the EMP coupling structure is electrically small, since, for such structures, simple equivalent circuit representations are possible. It is essential, therefore, to establish appropriate criteria on the basis of which it would be possible to determine whether or not a particular coupling structure, i.e., an antenna, is electrically small.

Definitions

D_{max} = maximum dimensions of coupling structure measured from its load terminals to the most distant point on the structure.

f_c = maximum significant frequency component of the EMP spectrum

τ = D_{max}/c -- the time it takes an EM wave to travel the distance D_{max} at the velocity of light c.

Then a coupling structure is electrically small if

$$D_{max} \leq \frac{\lambda_{min}}{6}$$

(Frequency-domain criterion)

or

$$t_r \geq 4\tau$$

(Time domain criterion)

where

$f_c = 0.6/t_r$

t_r = rise time of EMP excitation.

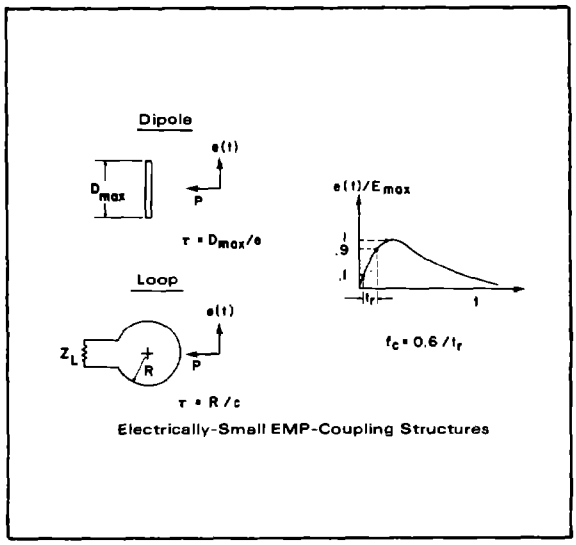

Electrically-Small EMP-Coupling Structures

Loop Antennas

Loop type antennas can couple to an electromagnetic wave through either the electric field or the magnetic field. A voltage will be induced in a loop antenna if a time-varying electric field has a component parallel to one of the sides of the loop, or a time-varying magnetic field component normal to the plane of

the loop. As stated earlier, a time varying magnetic field induces a current in a loop antenna such that the magnetic field produced by the current opposes the applied field.

As in the case of linear antennas, a very simple relationship between the field and the induced voltage exists when the loop is electrically small, or stated another way, the field is uniform throughout the area of the loop. For a loop to be considered small, its diameter must be less than $\lambda_{min}/6$. For typical EMP waveforms, this results in a physical diameter of less than 2 feet for a loop in free space.

Cables

Cabling may be considered in two broad categories: (1) unshielded, and (2) shielded. In the case of unshielded cables, they may be considered as $\dot{E}$ and $\dot{B}$ collectors as previously discussed for linear or loop antennas. Coupling to unshielded cables can also occur through an intermediary conversion impedance (Z_c).

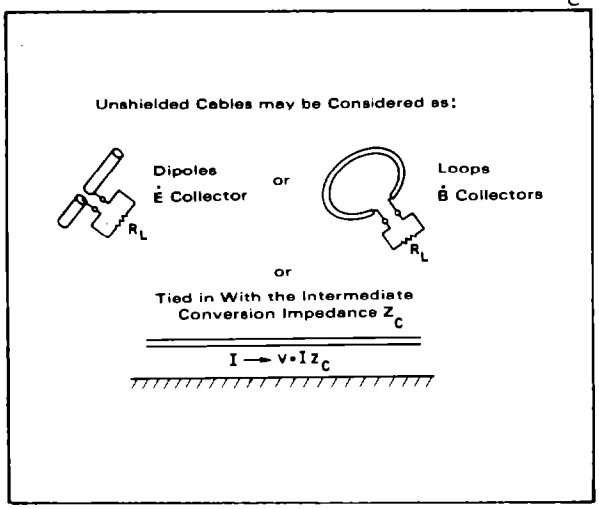

For a cable above, but in proximity to the earth, all three interaction mechanisms are present. The height of the cable above the earth, the earth parameters, and the parameters of the EMP all impact the energy coupled.

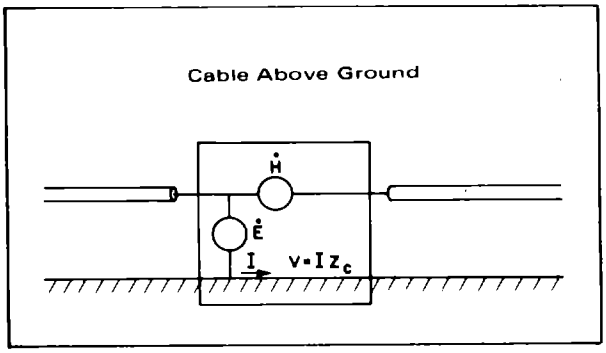

The magnetic induction ($\dot{H}$), results from the flux change between the cable and earth. This induced voltage appears as an incremental series voltage source. The electric induction ($\dot{E}$), results from the displacement current which flows between the cable and the earth due to the stray capacitance. It appears an an incremental shunt current source. The voltage source associated with the intermediate conversion impedance (Z_c), results from the current flow in the earth due to its finite conductivity. This source appears as an additional incremental voltage source in series with the load. All of these incremental contributions must be summed in the proper time-phase which takes into account the earth parameters and the angle-of-arrival.

For long runs of cable which run over or within the ground, ground parameters as a function of frequency are important. Also important for the pickup for these long runs is the angle-of-arrival and both the low frequency and the high frequency content of the EMP waveform.

If the cables are buried within the ground, the principal pickup mechanism to cause current to flow on the cables is the common impedance mechanism. Electric and magnetic fields cause currents to flow in the earth, and the resistance of the earth causes a voltage drop to appear along the cable.

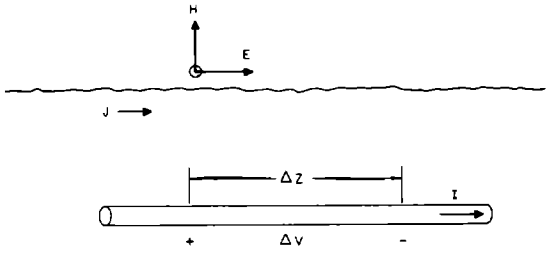

BURIED CABLE

For shielded cables, the shield is viewed as a cylindrical shield. The wires inside the shield interact with the penetrating fields through the same mechanisms ($\dot{E}$ and $\dot{H}$) as the unshielded cables. The penetrating fields, however, are altered by the shield to reduce the field amplitude and change the spectral content. A form of intermediate conversion impedance also plays a role. In the case of shielded cables, it is called the surface transfer impedance (Z_T) and is a characteristic of the cable shield.

Shield Penetration Mechanisms

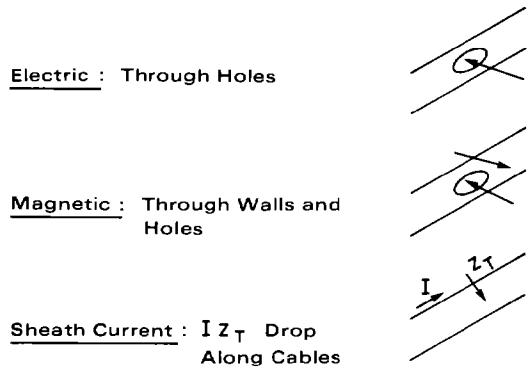

Electric field penetration generally occurs through the apertures or small defects in the exterior shield of the cable. Electric field penetration is also associated with connectors which are not fully shielded. In addition, the electric field is often enhanced at the terminations of long exposed cable runs, and this contributes greatly to electric field penetration effects.

Electric Field Penetration

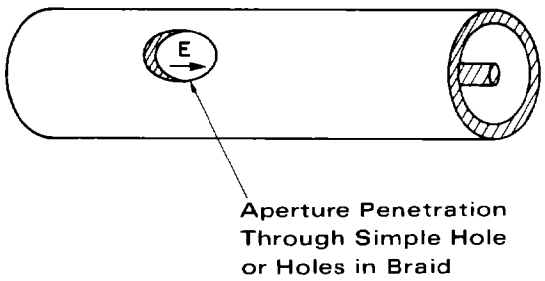

Magnetic field penetration results from aperture coupling and diffusion through the shield, especially for thin, nonferrous shields. The penetration mechanisms for shields is discussed more fully in the shielding section.

In the case of coaxial cables, the interior magnetic field pickup can occur because of the asymmetry, Δ, between the idealized position for the center conductor and the actual position of the center conductor as it occurs in the manufactured cable. This asymmetry essentially results in loops of unequal area and therefore unequal voltage being induced.

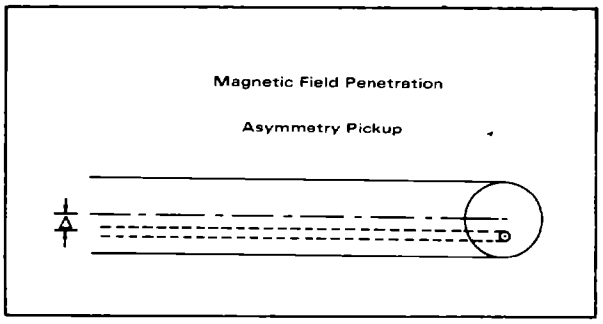

The primary pickup mechanism for shielded open wire pair cables is also through the $\dot{B}$ mechanism. The loop in this instance is closed by the terminations at both ends of the cable.

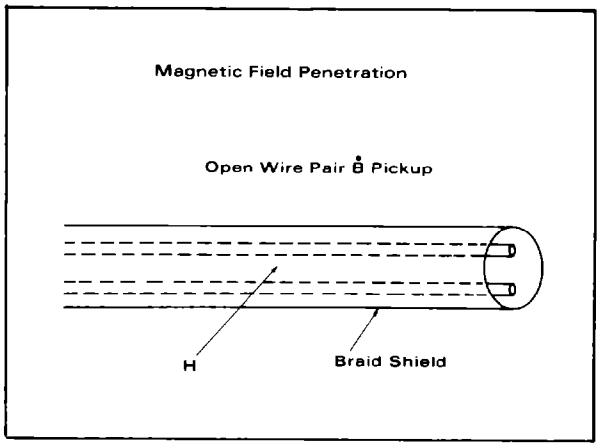

Here we see the definition of the intermediary conversion impedance between the external fields and the inside voltage of a particular cable. The surface transfer impedance is defined as the voltage appearing on the inside of the cable on a per meter basis due to the current flowing on the outside sheath.

Sheath Current Pickup

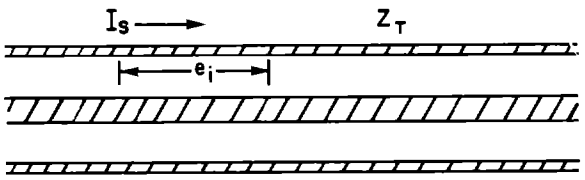

$$Z_T = \frac{e_{inside}}{I_{sheath}}$$

The surface transfer impedance plays a very important role in evaluating the cable performance. Transfer impedance is important for electric field pickup because the $\dot{E}$ field can induce currents to flow on cable runs which are parallel to the electric field as illustrated by the cable which terminates in a UHF antenna mast. Sheath current also flows on inadvertent loops formed by cable runs and other metallic structures.

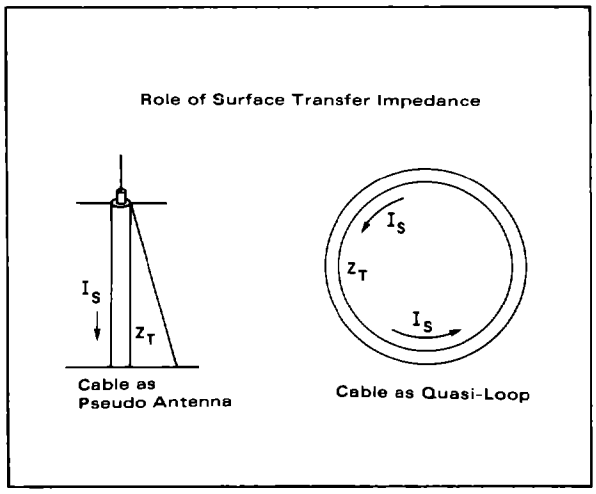

The transfer impedance is very important and at low frequencies is about the same for both braided and solid wall outer shields of the same copper content. However, in the case of the braid, because of the field penetrations through apertures, the transfer impedance increases with frequency, thereby dramatically increasing the pickup characteristics of braided cable. On the other hand, solid wall cable does not exhibit this penetration effect and, therefore, has an improving transfer impedance with frequency primarily because of skin-effect absorption.

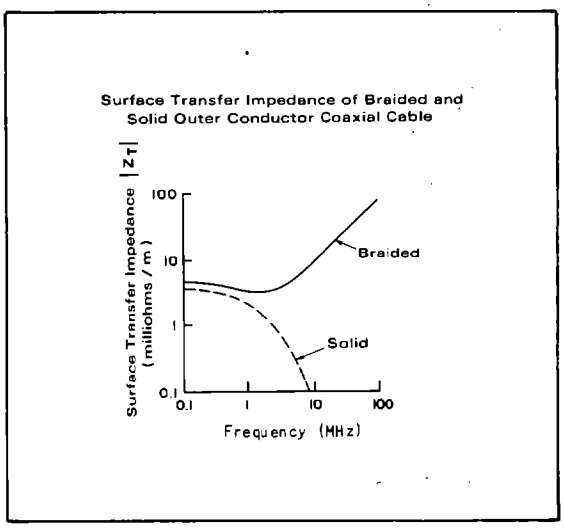

There are some favored approaches regarding cables. One favored approach is the use of twisted wire cable to minimize the $\dot{B}$ pickup. This twisted wire cable is also shielded to minimize the $\dot{E}$ pickup effects. However, the E-field pickups do occur with the presence of sheath currents. The sheath-current-induced inside voltages (common mode pickup) are minimized by the use of balanced terminations which, in effect, are not connected to the external sheath.

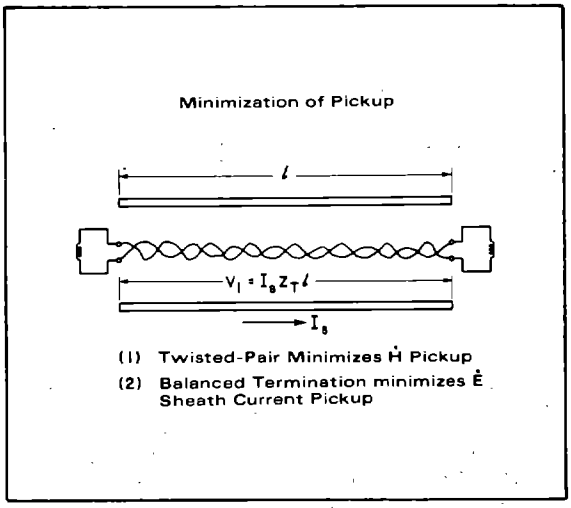

The terminations and splices also can play a major role in enhancing the coupling effects associated with long cable runs. In the case of a balanced pair within a cylindrical shield, the cable should be terminated both for the balance and common mode terminations. Small imperfections along the surface of the cable can convert some of the common mode pickup into differential mode pickup and vice versa. Thus, if the cables are not properly terminated for both modes, the pickup and reverberation effects are greatly enhanced.

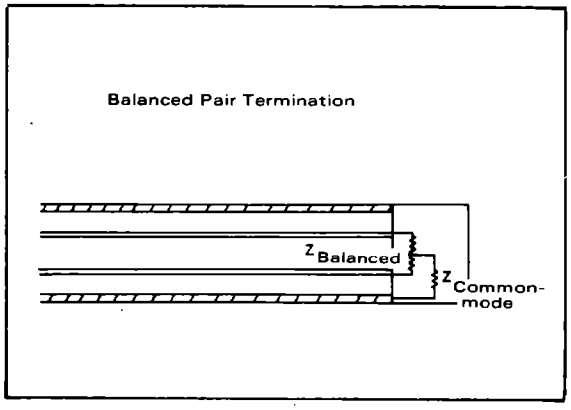

In the case of multi-conductor bundled cables, all sorts of undesirable effects can be produced by cross-talk effects on the terminations.

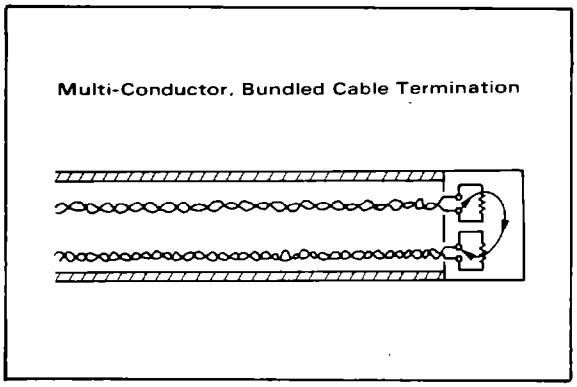

In summary, cable pickup mechanisms are an extension of $\dot{E}$, $\dot{H}$ and Z_c coupling. The same holds for shielded cables except the effect of the shield must be considered. Improper terminations also play a major role in the pickup associated with cable runs. In the case of very long cable runs, time-delay effects become important and give added weight to angle-of-arrival, earth parameters, and the lower or higher frequency content of the EMP waveform.

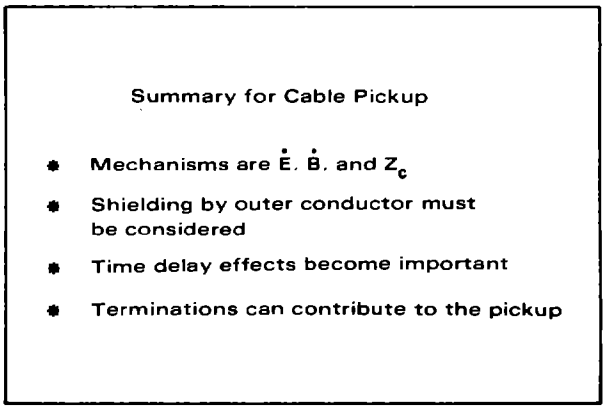

Shielding and Penetration

As discussed previously, propagating EM waves have coupled electric and magnetic fields. In general, whenever you have a time-varying electric field, there is an associated time-varying magnetic field. At low frequencies, however, this coupling is relatively loose and electric and magnetic field penetration effects can be considered separately on a practical basis. This separability of the fields permits defining the figure of merit (shielding effectiveness) of a shield separately for the magnetic and electric field penetration. The inside fields are generally the fields in the geometric center of the enclosure. The outside fields are those fields which would appear at the same spatial point as the inside fields with the enclosure removed.

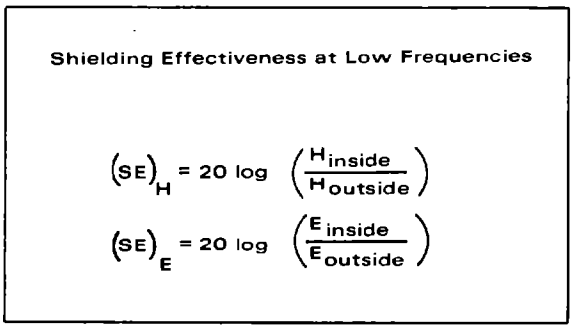

At the higher frequencies, the electric and magnetic fields must be considered jointly. In many instances, the power flow is a convenient form of definition. In this case, the power flow, in the absence of the enclosure, is compared to the power flow with the enclosure present. This is somewhat of an unwieldly definition and a more appropriate definition might compare the energy inside the enclosure with the energy in the absence of the enclosure being taken as a stored energy over a specified volume (the volume of the enclosure).

Shielding Effectiveness at High Frequencies

$$(SE)_p = 10 \log \left(\frac{P_{inside}}{P_{outside}} \right)$$

$$(SE)_w = 10 \log \left(\frac{W_{inside}}{W_{outside}} \right)$$

The shielding effectiveness is generally presented as a function of frequency. This is convenient for many radio frequency engineering-type applications but forms a major stumbling block in translating this rather simple concept into the appropriate EMP requirements.

Shielding Effectiveness Presented as a Function of Frequency

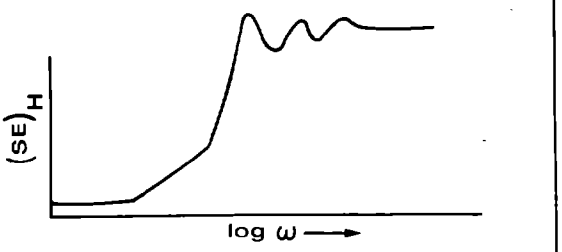

It must also be recognized that the shielding effectiveness often stated is a strong function of the measurement method. For example, if the shielding effectiveness measurement is made with two small loops adjacent to the wall, one value of shielding effectiveness is obtained. If, on the other hand, the shielding enclosure is placed within an EMP simulator, another value is obtained. In general, these measures are each self-consistent with frequency but can have values which differ by as much as 20 or 30 dB. The difference between these two measurements is the small loop technique only measures the shielding effectiveness in a local area. The plane wave technique, on the other hand, provides for current flow simultaneously on all surfaces and thus edge and corner effects are seen. The small loop measurements are, therefore, useful to determine seam leakage, etc., and the plane wave for overall structure shielding effectiveness.

In EMP, we are dealing largely with plane waves where the transient response of the enclosure is important. Thus, the amplitude response, as a function of frequency, must be related to the transient response. There are some rather simple ways of doing this which will be considered in more detail. However, before doing this, let us consider on a qualitative basis how shields actually work.

Shielding Effectivensss as a Function of Measurement Method

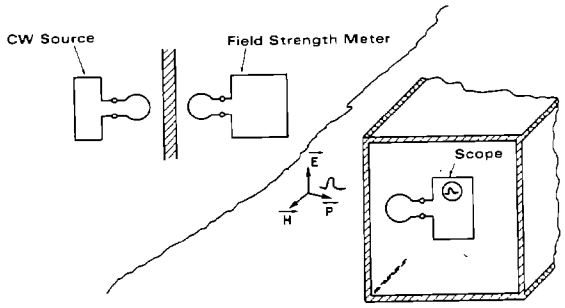

Electric Field Shielding

If a spherical conducting shell is placed within a static electric field, the free charges in the conducting shell will redistribute in accordance with the applied field. This redistribution of charge will be such as to make the force on them zero, or in other words, cancel the applied field. These charges reside only on the surface of the spherical shell and terminate the field lines.

Under these static conditions, once equilibrium has been reached, there is no charge flow and perfect electric field shielding is obtained. This is the well known Faraday Cage effect.

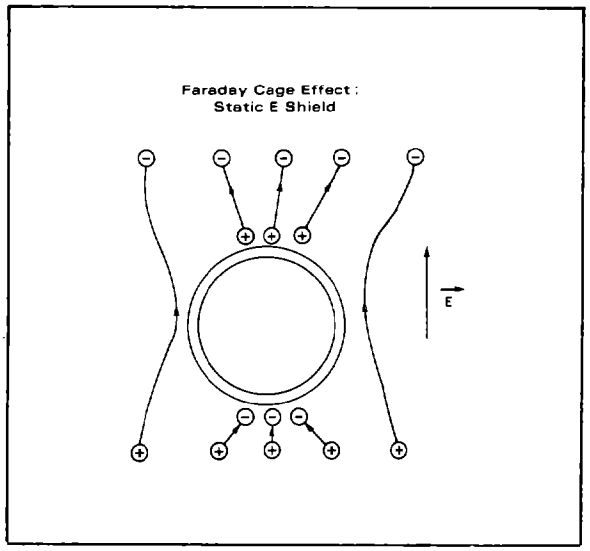

Now allow the applied field to vary slowly with time (a quasi-static field). As in the static case, the free charges will redistribute to reduce the force on them. However, whereas in the static case, equilibrium was reached, in the quasi-static case, the charges will always be in motion since the field is changing amplitude and polarity with time. The result is a time varying current flow on the shell, and since the shell conductivity is finite, a voltage drop results on the surface of the shell. If the shell wall is very thin, the same voltage appears on the inner surface and an electric field is established within the shell.

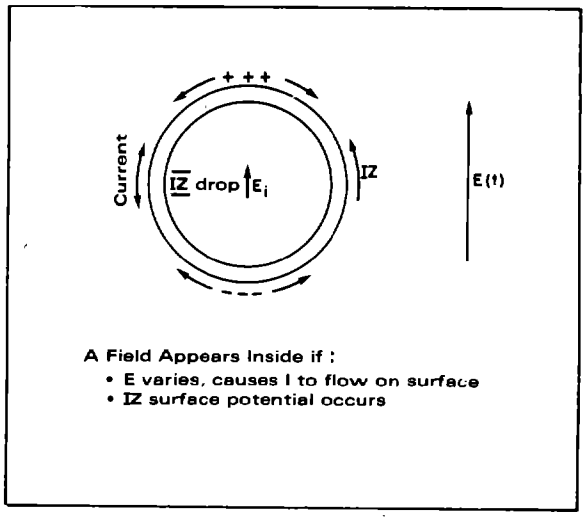

For very thin-walled enclosures and at low frequencies, the interior field has the same potential as the field on the outside of the enclosure. However, for higher frequencies and thick-wall enclosures, skin-effect mechanisms take place which absorb some of the energy. This causes additional shielding by the mechanism of absorption.

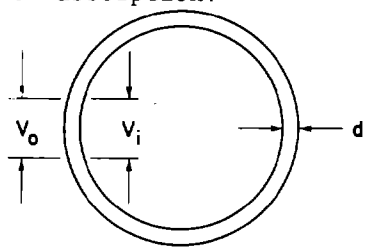

$d \ll \delta$

At Low Frequencies, $V_{inside} = V_{outside}$

$d \gg \delta$

At Higher Frequencies, V_{inside} is Reduced Due to Skin Effect or Absorption

$$\delta = \frac{1}{\sqrt{\pi f \mu \sigma}} = \text{Skin Depth}$$

Typical electric field penetration into an idealized shielded enclosure is shown here. At very low frequencies the charged distribution on the exterior of the enclosure is such as to "cancel" the induced interior fields, giving rise to the Faraday-cage shielding effect. In the case of closed ideal enclosures, this results in almost infinite shielding effectiveness at the very low frequencies. Thus, the electric field is very easy to shield, even with fairly poor conducting materials. On the other hand, if we allow the frequency of interest to increase, we find that the electric shielding effectiveness decreases with an increase in frequency until the absorption losses predominate.

The first three methods are the more rigorous methods and require the use of numerical or digital techniques for their solution. The computer codes for computing antenna and cable response to an EMP are maintained for customer use by the Electromagnetic and Systems Research Group, Lawrence Livermore Laboratory, Livermore, CA. 94550. Maintenance of this computer code library is an ongoing effort funded by the Defense Nuclear Agency.

Generally, the analysis of system response to electromagnetic phenomena is divided into two classes: analysis of linear systems, and the analysis of nonlinear systems. We will consider the applicability of the analytical techniques to these two problem areas.

4.4 ANTENNA COUPLING ANALYSIS - LINEAR SYSTEMS

If a system is linear, or can be approximated to be so, Fourier Transform and ac circuit analysis techniques can be used.

Linear Systems

Antennas

- **Linear**
- **Passive**
- **Distributed**

Antenna Loads

- **Linear**

Simple Energy Collectors

The simplest approach to analyzing the antenna coupling in linear systems is where the antenna (structure) dimensions are small for all wavelengths. Consider a short dipole antenna. The equivalent circuit for a short dipole is a voltage source, a series capacitor (antenna capacitance), and the load.

Equivalent Circuit of a Small Dipole

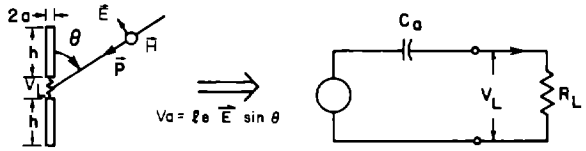

$$Va = \frac{1}{C_a}\int i\,dt + i\,R_L$$

The response of this circuit can be obtained by inspection for the following loads:

HIGH-IMPEDANCE RESISTANCE LOAD

$$R_L >> 1/\omega C_a$$

then

$$V_L(t) = -h \sin\theta\, e^{i}(t)$$

LOW-IMPEDANCE RESISTANCE LOAD

$$R_L << 1/\omega C_a$$

then

$$i_L(t) = -h \sin\theta\, C_a \dot{e}i(t)$$

The antenna capacitance, C_a, is given by:

$$C_a = h/cZ_o$$

where

Z_o = 60 (Ω-2) [average antenna characteristic impedance]

Ω = $2\ell n(2h/a)$ [antenna shape factor]

c = velocity of light

a = antenna radius

h = ℓ_e

The time domain response is approximately the derivative of the incident electric field for the case $R_L << 1/\omega C_a$.

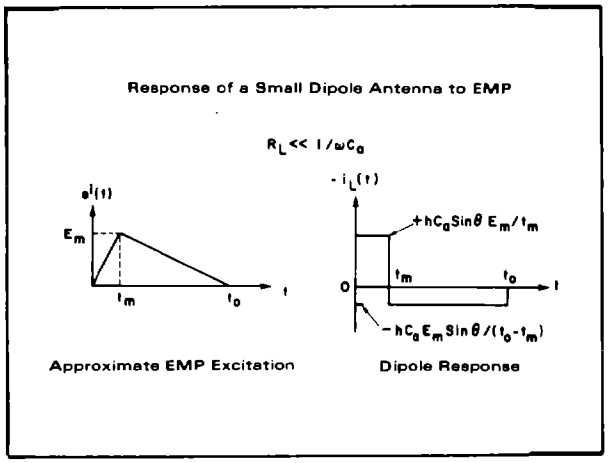

Next, consider a small magnetic dipole (loop) in the presence of an incident EMP field. In the equivalent circuit, L is the low-frequency inductance of the loop and is given by:

$$L = \mu_o R [\ell n (8R/a) - 2]$$

for $R >> a$

where

μ_o = permeability of free space

R = radius of loop

a = antenna wire radius

Equivalent Circuit of a Small Loop

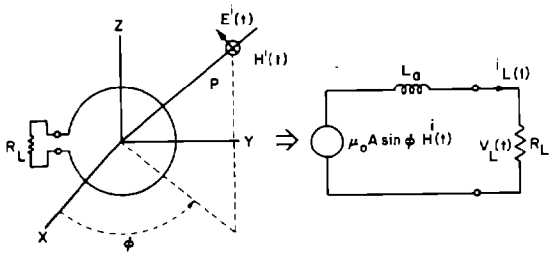

$$Va = L \frac{di}{dt} + iR_L$$

The response of the equivalent circuit is readily obtainable for the following loads:

HIGH-RESISTANCE LOAD

$R_L >> \omega L$

then

$$V_L(t) = \mu_o A \sin\phi\, \dot{H}^i(t)$$

LOW-RESISTANCE LOAD

$R_L << \omega L$

$$i_L(t) = \frac{\mu_o A}{L} \sin\phi\, H^i(t)$$

or

$$i_L(t) = \frac{\mu_o A}{\eta_o L} \sin\phi\, E^i(t)$$

Note that the load impedance does not have to be resistive and it may represent the input impedance of an electronic system such as, for example, a receiver front end. The time domain response for the case of $R_L >> \omega L$ is the derivative of the applied magnetic field. For the small dipole, the open circuit voltage ($R_L >> 1/\omega C_a$) follows the EMP waveform in early time. For the small loop, the short circuit current follows the EMP waveform.

Response of a Small Loop to EMP

$R_L >> \omega L$

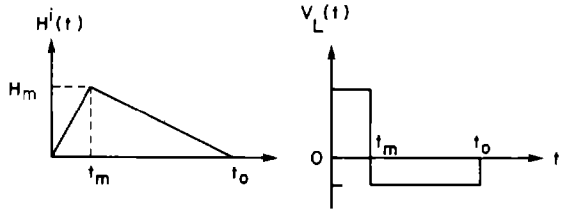

Approximate EMP Excitation Loop Response

A quick look approximate energy analysis can also be performed to determine an estimate of the energy dissipated in the load. In this case, the concept of antenna effective area can be employed. The effective area is related to the power gain by:

$$A_e(\omega) = \frac{\lambda^2 G}{4\pi}$$

where

$A_e(\omega)$ = effective area as a function of frequency

λ = wavelength of wave

G = antenna power gain.

The effective area for various antennas is given below:

EFFECTIVE AREA OF VARIOUS ANTENNAS

Antenna Type	Effective Area
Isotrophic Radiator	$\lambda^2/4\pi$
Very Short Dipole	$3\lambda^2/8\pi$
Half-Wave Dipole	$1.64\lambda^2/4\pi$
Large Aperture Antenna	100% physical area
Pyramidal Horn	50% physical area
Parabolic Reflector	50-65% physical area

The solution for an EMP is obtained by calculating the energy available at the antenna terminals in the frequency domain for each significant frequency component in the pulse. The total energy delivered to the load is then the integral (sum) over the frequency spectrum of the pulse which can be determined through normal Fourier analysis techniques.

For an antenna placed in the field of a linearly polarized EM wave, the power available at the antenna terminals under conjugate matched conditions for sinusoidal fields is given by:

$$W = PA_e$$

where

W = available power (watts)

P = power density (watts/m^2)

A_e = effective area (m^2)

For an EM pulse, the energy available at the antenna terminal is:

$$J_T = \frac{1}{2\pi} \int_{-\infty}^{\infty} A_e(\omega)\, J(\omega)\, d\omega$$

where

J_T = available energy (joules)

$A_e(\omega)$ = effective area (m^2)

$J(\omega)$ = energy density spectrum of the pulse (joules/m^2 Hz)

It should be noted that all the available energy will be transferred to the load only when the load impedance presents a conjugate match to the antenna impedance over the frequency range where the excitation has significant components. Such a wide band match is physically unrealizable and would result in too much of a worst case. To accurately calculate the load energy, one would need to know the system transfer function. An approximation can be obtained by making appropriate assumptions.

Assume a transfer function, $T(\omega)$, of the form:

$$T(\omega) = \begin{cases} A_e(\omega_o) \left[\dfrac{\omega}{\omega_o - \omega_1}\right]^{2n} & 0 \le \omega \le (\omega_o - \omega_1) \\ A_e(\omega_o) & (\omega_o - \omega_1) \le \omega \le (\omega_o + \omega_1) \\ A_e(\omega_o) \left[\dfrac{\omega_o + \omega_1}{\omega}\right]^{2n} & (\omega_o + \omega_1) \le \omega \end{cases}$$

ω_o = center frequency of the system response

$(\omega_o - \omega_1)$ = lower cutoff frequency of the system response

$(\omega_o + \omega_1)$ = upper cutoff frequency of the system response

and n determines out-of-band attenuation.

Under this assumption, the energy dissipated in the load is:

$$J_T = \frac{1}{2\pi} \int_{-\infty}^{\infty} T(\omega)\, J(\omega)\, d\omega$$

The energy available at the load will be distributed as shown below:

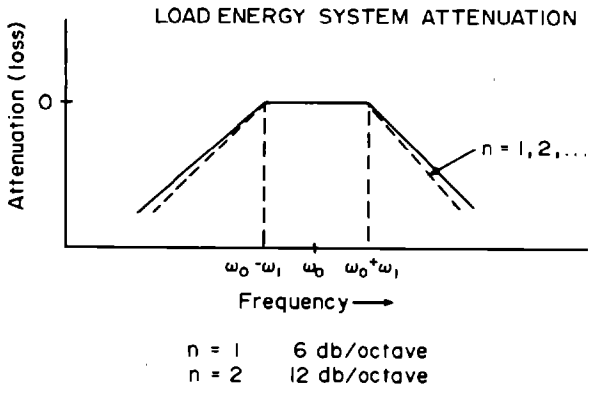

n = 1 6 db/octave
n = 2 12 db/octave

For ideal preselection, the rectangle formed by $(\omega_0 - \omega_1)$ and $(\omega_0 + \omega_1)$ dotted lines would be obtained. The case of n = 1 (6 dB/octave) is considered a worst case and the bandwidth chosen is the turning range of the system. If additional information is available, a different value of n may be more appropriate.

Fourier Transform Method

The response of a linear system to pulse or transient excitation can be determined by the use of Fourier Transforms (FT), provided the complex transfer functions are known over the frequency range where the excitation has significant components.

The Fourier transform pair is defined in terms of the following integral expressions:

$$F(j\omega) = \int_{-\infty}^{\infty} f(t) e^{-j\omega t} dt \quad \text{[direct transform]}$$

$$f(t) = \frac{1}{2\pi} \int_{-\infty}^{\infty} F(j\omega) e^{j\omega t} d\omega \quad \text{[inverse transform]}$$

In effect, the direct Fourier transform takes a function from the time domain to the frequency domain, whereas the inverse Fourier transform performs a frequency-to-time domain transformation. Thus, the Fourier transform pair provides a two-way transformation. Note that $F(\omega)$ is the frequency spectrum of $f(t)$.

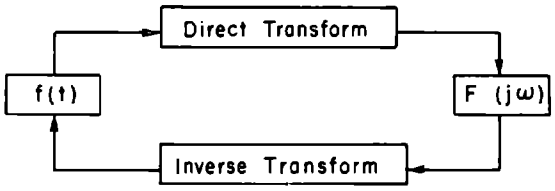

In principle, the solution to the problem of determining the response of a linear system can be obtained by Fourier analysis as indicated. Note that the concept of system transfer function is valid only for linear systems.

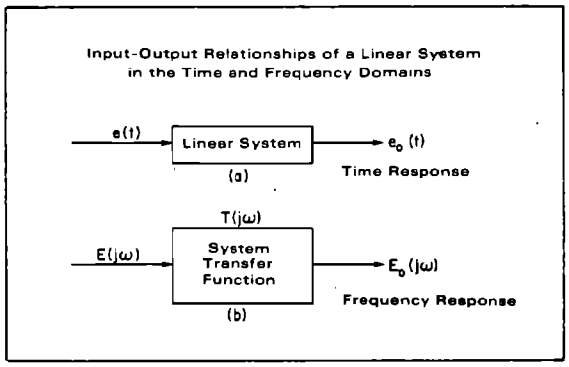

This is a flow chart indicating the procedure for obtaining the time response of a linear system to any excitation using Fourier analysis. In most cases, the Fourier integrations would have to be carried out using numerical techniques with the aid of a digital computer.

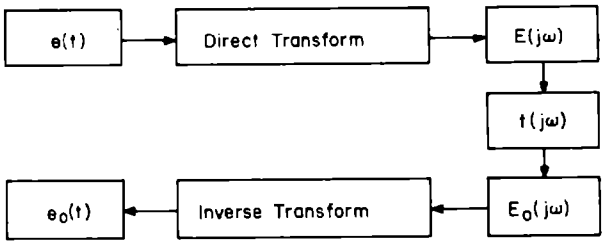

In general, the voltage transfer function is

$$T_V(\omega) = \frac{V_L(\omega)}{E_i(\omega)} \quad \text{(volts/Hz)/(volts/m-Hz)}$$

and the current transfer function is

$$T_I(\omega) = \frac{I_L(\omega)}{E_i(\omega)} \quad \text{(amps/Hz)/(volts/m-Hz)}$$

The time dependence is then determined by

$$V_L(t) = \frac{1}{2\pi} \int_{-\infty}^{\infty} T_V(\omega) \quad E_i(\omega) \quad e^{j\omega t} d\omega$$

(volts)

and similarly for the current.

As an example of the FTM, the equivalent circuit for an antenna is shown in the following figure

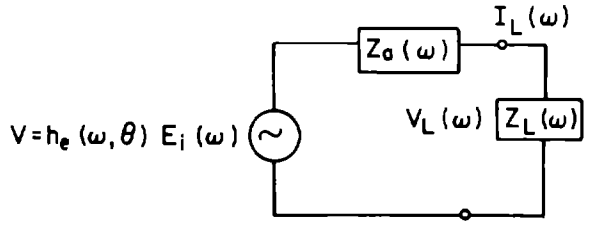

where

$h_e(\omega, \theta)$ = complex effective length of the antenna as a function of polar angle θ and frequency

$E_i(\omega)$ = frequency domain representation of the incident field

$Z_a(\omega)$ = antenna impedance as a function of frequency

$Z_L(\omega)$ = load impedance as a function of frequency

$I_L(\omega)$ = load current as a function of frequency

$V_L(\omega)$ = load voltage as a function of frequency

The cases which will be considered will be for monopole antennas with the following load conditions:

Z_L = 50 Ω

Z_L = 0 (short circuit)

Z_L = ∞ (open circuit)

The antenna configuration is shown in the following figure:

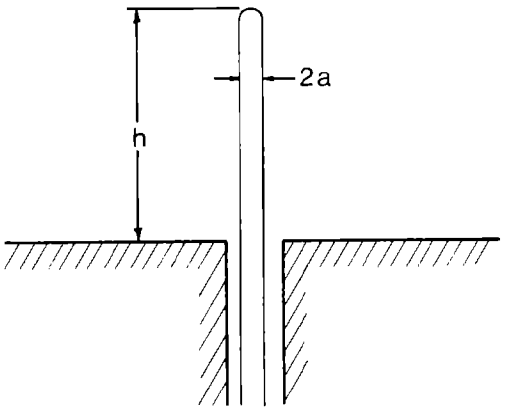

CYLINDRICAL MONOPOLE ANTENNA

The antenna impedance is a complex function. For

$$\beta h = \frac{2\pi h}{\lambda} \leq 1.0$$

where

$$\beta = \frac{2\pi}{\lambda}$$

the theory of R.W.P. King, C.W. Harrison, Jr., and D.H. Dentor, Jr., can be applied. For $\beta h \geq 1.0$, Wu's formulae apply. The antenna impedance for a representative antenna is shown in the following figure.

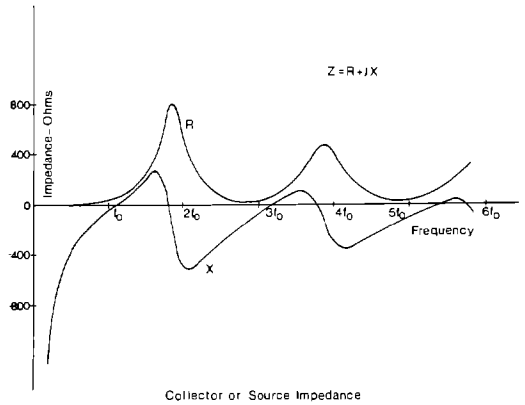

Collector or Source Impedance

Assuming a typical incident high altitude EMP waveform, the time histories of the antenna load voltage and current were calculated using Fourier Transform Techniques.

The time history for the load voltage for Z_L = ∞, and for antenna lengths of 750 meters (f_o = 100 kHz), and 7.5 meters (f_o = 10 MHz) are shown below.

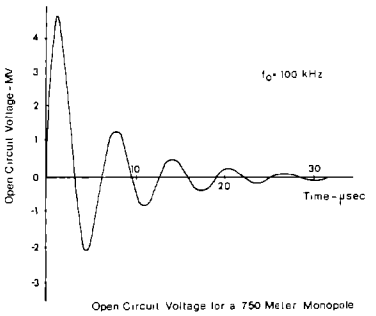

Open Circuit Voltage for a 750 Meter Monopole

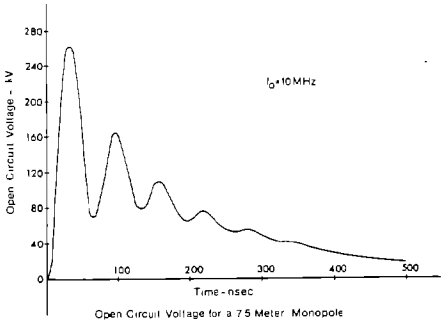

Open Circuit Voltage for a 7.5 Meter Monopole

It should be noted that these antennas basically ring at twice their resonant frequency (damped sinusoid) under matched load conditions. The current distribution approximates that of a shorted dipole in free space under open circuit conditions. In the case of the 7.5 meter antenna, a capacity effect can be seen. This is due to the fact that the antenna is electrically short over most of the frequency spectrum and acts as a capacitance.

The load current for the case of $Z_L = 0$ is shown for these antennas in the following figures.

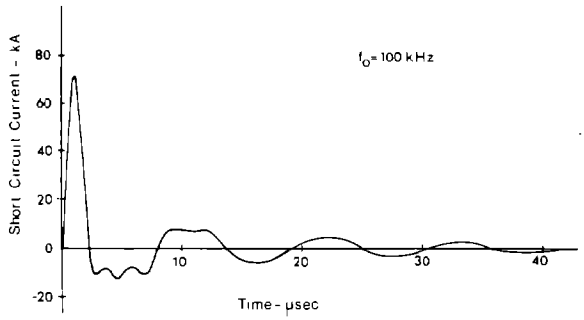

Short Circuit Current for a 750 Meter Monopole

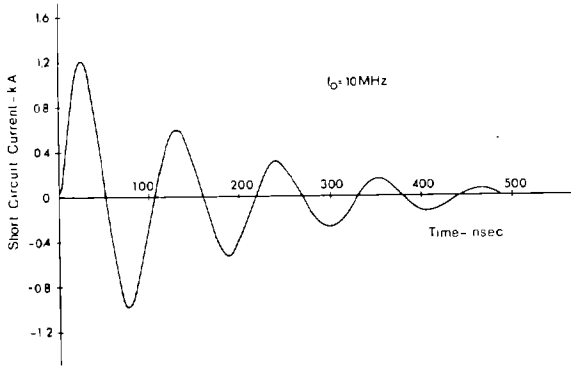

Short Circuit Current for a 7.5 Meter Monopole

The load voltage for the case of $Z_L = 50\ \Omega$ is shown in the following figures.

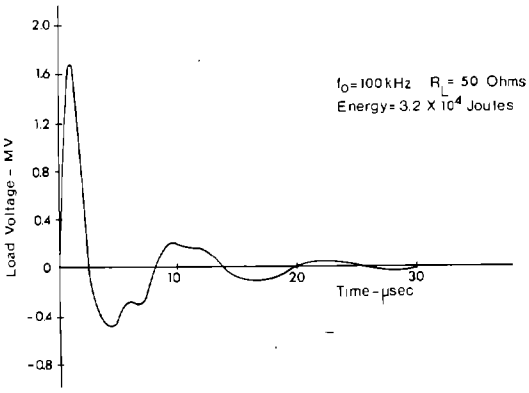

Load Voltage for a 750 Meter Monopole

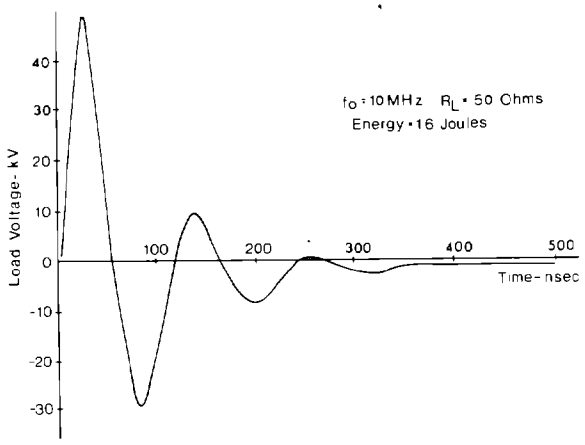

Load Voltage for a 7.5 Meter Monopole

Again, the antenna ringing at the resonant frequency is noted.

This information can be presented in a more useful manner for system hardening. Of primary interest are the peak voltages, rise times, rate of rise, decay time, and energy for the case of $Z_L = 50\ \Omega$.

The peak voltage for the case $Z_L = 50\ \Omega$ as a function of the resonant frequency of the antenna is shown in the following figure.

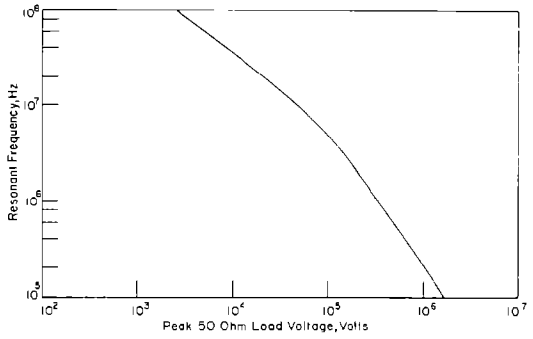

As can be seen, the peak voltage is a direct function of the resonant frequency (antenna length).

The rise time (defined as the time for the amplitude of the initial cycle to increase from 10% - 90% of the peak value) is also of interest for hardening design. This is shown for the case of $Z_L = 50\ \Omega$ in the following figure.

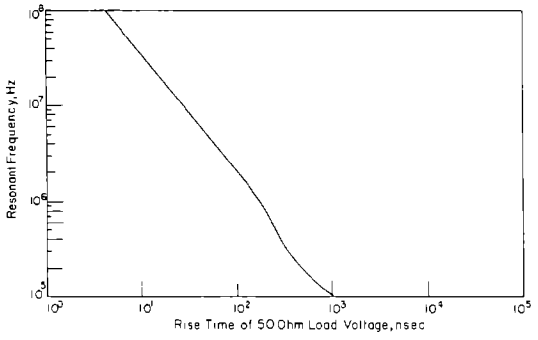

As can be seen, the total rise time is also a direct function of the antenna length as one would expect, since the wave is a resonant ringing damped sinusoid.

Surge protection devices (Section VI), however, are primarily sensitive to the rate of rise of the voltage. The rate of rise as a function of antenna length (resonant frequency) is shown in the following figure.

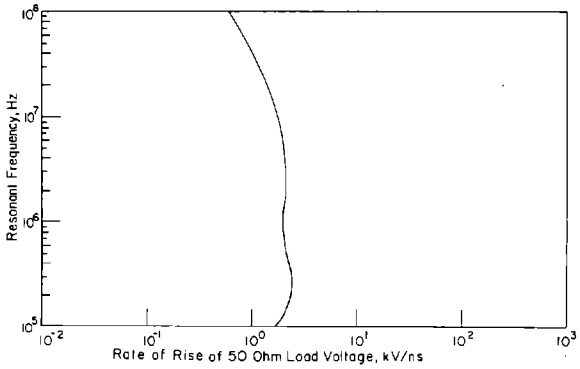

As can be seen, the rate of rise (kV/ns) is relatively independent of the antenna length. Consequently, surge arrestors must have essentially the same response characteristics regardless of the resonant frequency of the antenna.

Of equal importance is the decay time of the pulse in order to determine the energy coupled into the system. This is shown in the following figure for $Z_L = 50\ \Omega$.

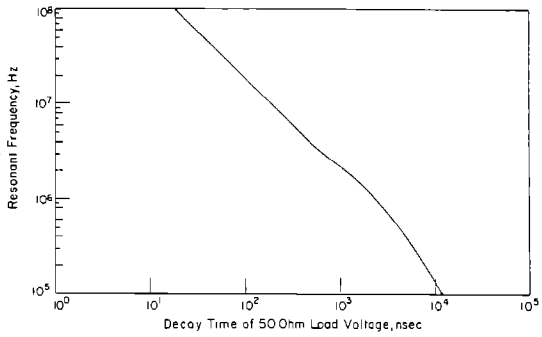

Again, the decay time is a direct function of the antenna length.

The total energy dissipated in the load, Z_L = 50 Ω, is directly related to antenna length (resonant frequency). This is shown in the following figures.

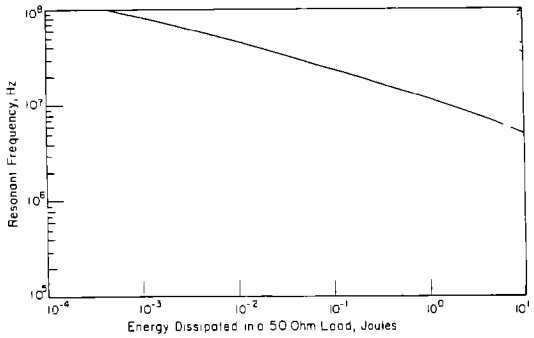

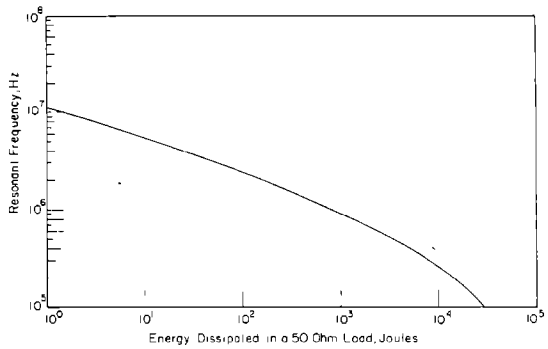

4.5 ANTENNA COUPLING ANALYSIS - NONLINEAR SYSTEMS

If a given system is nonlinear, Fourier Transform methods are not applicable and one must solve the resultant differential equations describing the behavior of the system. Sometimes standard circuit analysis computer codes, such as SCEPTRE, are suitable for this purpose, if the system can be characterized in terms of lumped parameters, i.e., resistors, capacitors, inductors, and controlled sources. Most electronic systems are, in fact, nonlinear since they contain such devices as diodes, tubes, transistors, etc. The major difficulty is deriving this lumped parameter network. The network must have the same transient response as the distributed system it is to represent. Both analytical and experimental techniques have been utilized to obtain the system transient response. Having the transient response, standard circuit synthesis approaches can be used to define the LPN which would produce this response.

In such cases, standard circuit analysis computer codes, such as SCEPTRE, CIRCUS, or others can be employed. This creates the need for a lumped-parameter network (LPN) representation of an antenna, which is basically a distributed network.

Response of a Nonlinear System using the Lumped-Parameter Network Method

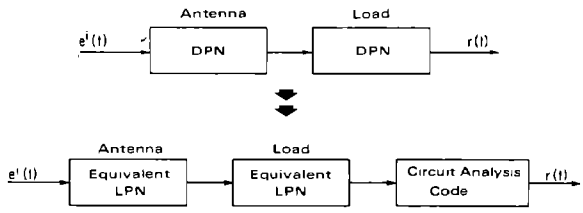

It is to be noted that:

1) Frequency domain techniques are not valid when nonlinear elements are incorporated into a system.

2) If the lumped-parameter network (LPN) representation of a system is given, standard analysis computer codes can be used for a nonlinear system.

A flow chart of the lumped-parameter network method for obtaining the transient response of an antenna system would be:

Flow Chart of Lumped-Parameter Network Method

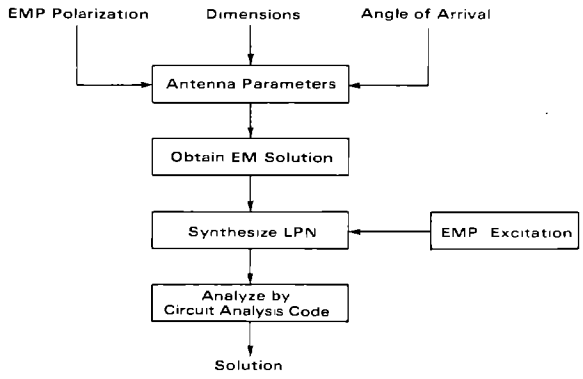

To obtain the lumped parameter network (LPN) equivalents of the effective lengths and impedances for monopole and dipole antennas, the expressions given by Wu were analytically continued over the complex frequency plane, and the poles and zeros of these functions were found numerically. The Singularity Expansion Method (SEM) is one alternative way of determining the required poles and zeros. From a truncated set of poles and zeros, the functions resulting were optimized over finite frequency ranges. Using these functions, conventional network synthesis procedures were used to find the network element values.

Another alternative approach to determining the effective length and impedence for an antenna would be experimentally. The experimental data could be fit by again using conventional synthesis approaches.

At the present time, a catalog of equivalent circuits only exists for monopoles and dipoles. Effort is continuing to develop equivalent circuits for more complex antennas.

Availability of LPN Representations of Antennas

- Complete tables of element values are available only for monopole, dipole and folded dipole antennas. These tables take into account antenna dimensions and any angle of arrival.
- Tables of element values for other antenna configurations are presently under development.
- Tables of element values are also available for the ground reflection coefficient. Such tables are used in calculating the transient response of antennas in proximity to ground.

As an example of the use of the LPN method, the transient response of an 8 foot monopole over a perfectly conducting ground was computed using both the Fourier Transform Method and the LPN Method for a linear 50 Ω load. These calculations were performed for the antenna parameters, angle of arrival and incident field shown in the figure.

EMP Excitation of a Monopole Antenna

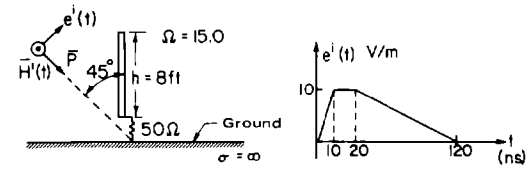

Monopole Antenna EMP Excitation

An LPN representation of this antenna is shown. The element values of the circuit model have been obtained from available tables.

Monopole Antenna Equivalent Circuit

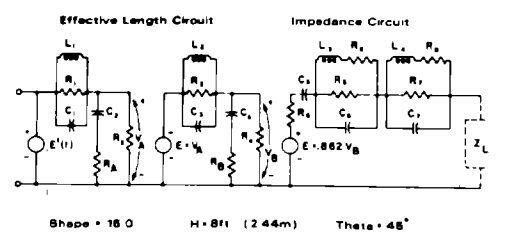

Shape = 16.0 H = 8ft (2.44m) Theta = 45°

The results of the analysis using SCEPTRE are compared to those obtained from the Fourier Transform Method.

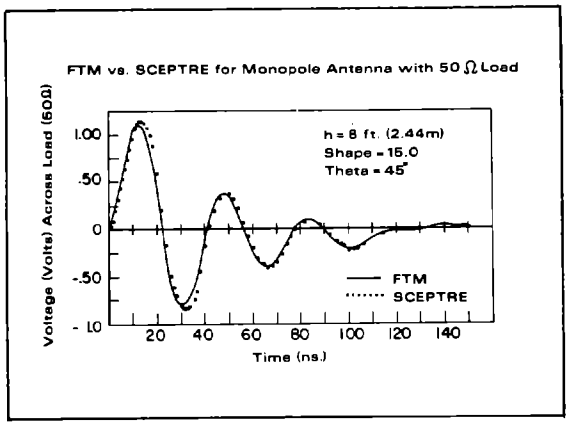

A second example deals with the analysis for a nonlinear load. In this example, an 8 foot monopole over a perfectly conducting ground is loaded with a field-effect transistor (FET) amplifier. The input trapezoidal pulse is limited to a 10 V/m maximum amplitude to keep the gate bias reversed, since the FET network model is not valid when the gate is forward biased. The purpose of this example is to demonstrate the implementation of SCEPTRE using a receiving monopole connected to a receiver front end.

FET-Loaded Monopole Antenna

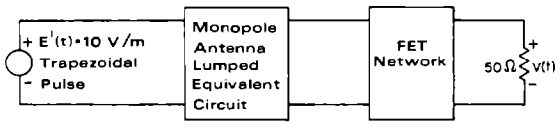

This model of the FET is used in the calculations.

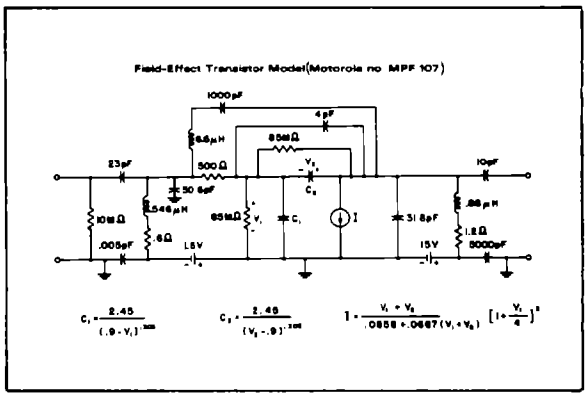

The response of the FET amplifier is shown here.

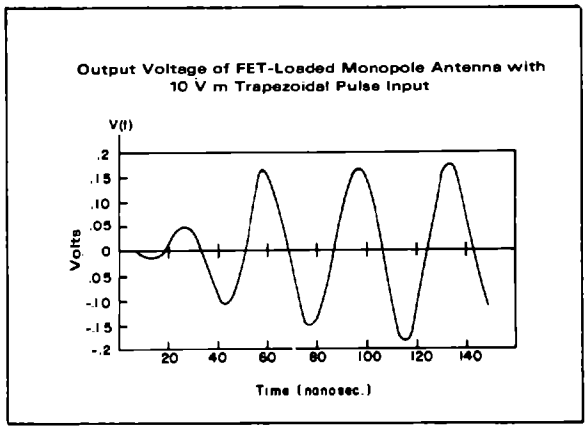

This shows the early time response. The ring up is due to the Q of the circuit. A similar ring down would be seen in late time.

Parabolic Antenna Example

The EMP response of a parabolic reflector antenna with a dipole feed has been considered. The basic geometry considered was a 25 foot paraboloidal antenna, 6 meters above ground with its axis tilted 30 degrees with respect to the ground.

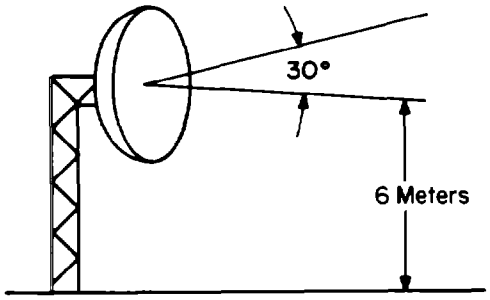

Integral equations for the current distribution on a parabolic cylindrical reflector were derived using superposition methods. These integral equations were solved numerically using an iterative method. As expected, the frequency domain focal-plane scattered fields are poorly focused for most frequencies of the EMP spectrum. This implies that the feed antenna sees a practically uniform incident field.

The calculated open circuit voltage and load current for this case are shown in the following figures for both the over ground and free space conditions.

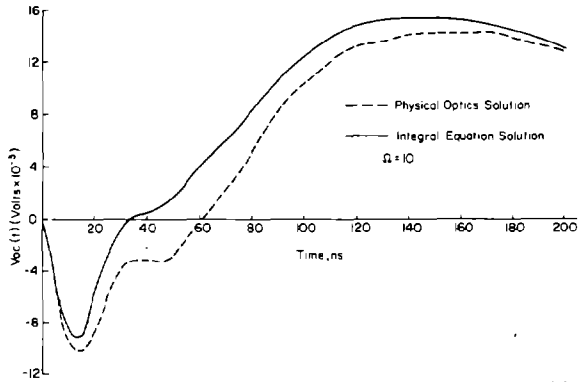

TIME HISTORY OF THE OPEN CIRCUIT VOLTAGE, $V_{OC}(t)$, FOR A RECEIVING DIPOLE FEED ANTENNA TO HIGH ALTITUDE EMP

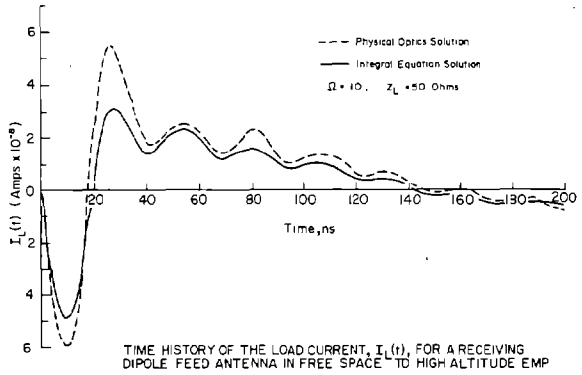

TIME HISTORY OF THE LOAD CURRENT, $I_L(t)$, FOR A RECEIVING DIPOLE FEED ANTENNA IN FREE SPACE TO HIGH ALTITUDE EMP

4.6 STRUCTURES MODELED AS ANTENNAS

Missile in Flight

A useful model for a missile in flight is a short circuited cylindrical dipole antenna. For shape factors (Ω) greater than ten (10), the missile can be considered as a thin dipole antenna and solved by the Fourier Transform techniques.

The current distribution induced by an incident EMP on the surface of a missile body can, in principle, be determined on the basis of scattering or antenna theory. The computational effort required depends to a large degree on the analytical model and degree of accuracy required. In general, the current density on the surface of a missile structure has two tangential components (for a perfectly conducting surface) which are related through a system of two coupled integral equations. Solutions to such integral equations are indeed very difficult and will not be considered here. A great deal of simplification results if a cylindrical model for the missile structure is chosen. It is usually assumed that no circumferential currents are induced, which is valid provided the diameter of the cylindrical antenna is less than a quarter wavelength. It should be recognized that for structures whose length-to-diameter ratio is not large (shape factor > 10), the circumferential currents can be as large as the axial currents. Moreover, first order approximations to the current (axial) distribution are possible using thin linear antenna theory. This antenna theory requires that

$$h >> a \text{ and } 2a/\lambda << 1.$$

If these conditions are violated, the resulting current distribution is expected to be only a rough estimate of the actual one. Fair agreement (a factor of 2) in terms of peak current can sometimes be obtained. The major discrepancy occurs in the actual distribution of the currents on a complex structure due to the superposition of the various components comprising the total current.

Model for Missile Structure

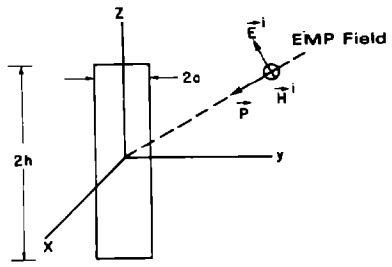

The predicted response of a 12-meter cylindrical structure to a 10,000 V/m double-exponential environment for broadside incidence are presented in the figure. The shape factor of the structure is Ω = 10.0 which corresponds to a length-to-diameter ratio of 75.0. As expected, the amplitude of the current at the center of the antenna is greater than that three meters from the center. Otherwise, the current waveforms are almost identical. Note that the fundamental frequency of the current ringing is 11.2 MHz whose period is 89 μsec and is approximately the time it takes a current wave to traverse the length of the antenna twice.

Having determined the missile skin current, the next step is to calculate the electric field on the inside surface of the missile skin through its surface transfer impedance, as discussed later. This surface field may be viewed as a distributed source, which excites the interior of the missile body, resulting in voltages and currents appearing at various terminals of electronic equipment. The missile skin current also contributes to the antenna excitation and can couple to the interior via apertures or penetrants in the missile skin.

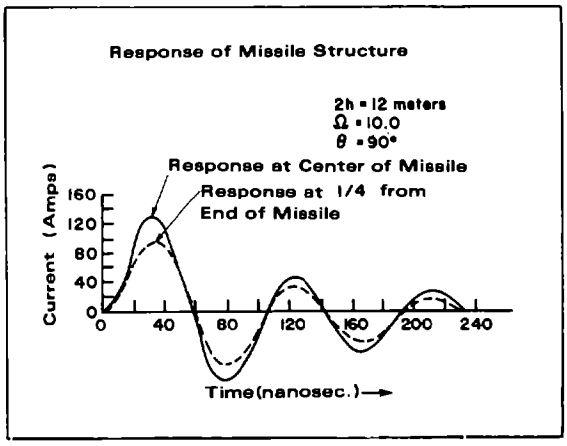

Microwave Tower

An open type microwave tower structure can be approximately modeled as a fat monopole to calculate the tower current due to EMP. An effective radius (a_e) can be determined for the monopole which depends on the tower geometry. Assuming a cylinder (and, consequently, a_e) that is the same size as the base of the tower gives an upper bound on the tower current. A lower bound is obtained by assuming a cylinder equivalent to the size of the waveguide. The difference between the upper and lower bounds is approximately a factor of 3.

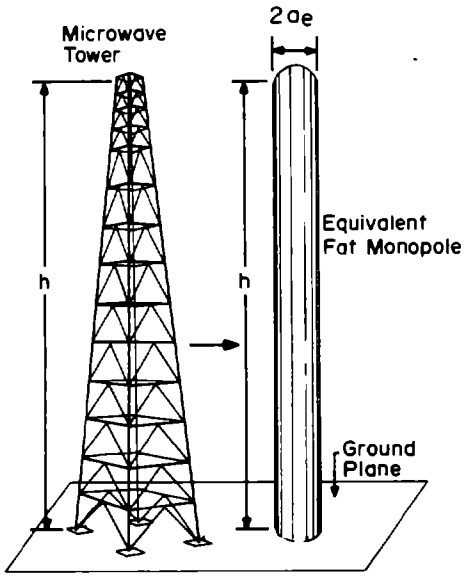

MICROWAVE TOWER AND EQUIVALENT FAT CYLINDRICAL MONOPOLE (ADAPTED WITH PERMISSION OF BELL TELEPHONE LABORATORIES)

To simplify the calculation and determine an upper bound for the tower current two assumptions are made: (1) tower monopole and earth (ground plane) are perfectly conducting; and (2) that the incident EMP electric field vector is parallel to the axis of the cylinder. The effect of these assumptions is to provide an upper bound which is within a factor of approximately 2.

For purposes of analysis, a monopole which is perfectly conducting over a perfectly conducting ground plane can be considered as a dipole of half-height equal to the height of the monopole.

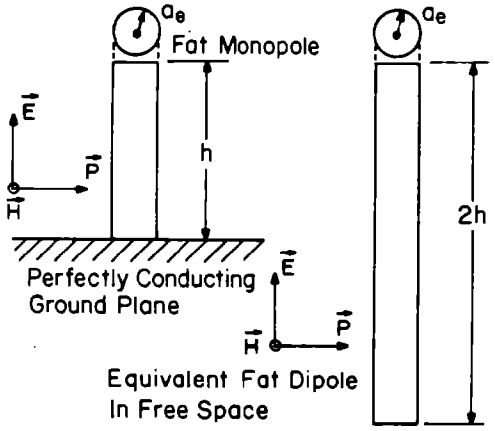

TOWER MONOPOLE AND EQUIVALENT FAT DIPOLE (ADAPTED WITH PERMISSION OF BELL TELEPHONE LABS)

The approximate EMP induced current normalized to the dipole half-height on a normalized time scale for four shape factors is shown.

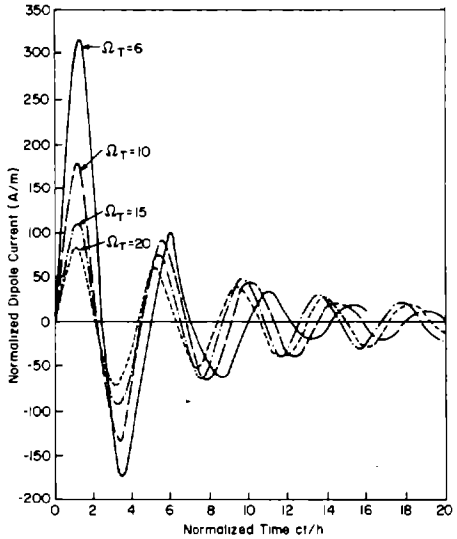

EMP-INDUCED TOWER CURRENT (ADAPTED WITH PERMISSION OF BELL TELEPHONE LABORATORIES)

The ringing frequency is approximately equal to the fundamental resonant frequency of the dipole.

P-3C Aircraft

Another example of EMP predictive modeling has been the P-3C Aircraft. Typical modeling of aircraft utilizes thin wires. The simplest approximation is the wire cross model where the fuselage and wings are modeled by wires, neglecting the tail structure.

This was done for a P-3C aircraft as depicted below.

The shape factor used for this analysis was $\Omega = 2 \ln L/a = 7.0$ (a = wire radius). The wire radius used was somewhat smaller than the average occurring on the real aircraft due to numerical calculation difficulties. This results in slightly higher peak currents due to the higher Q associated with the smaller radius.

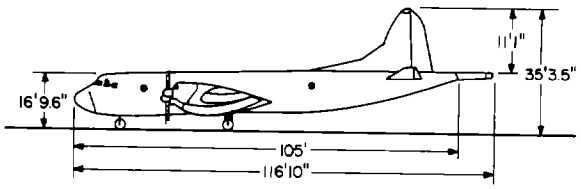

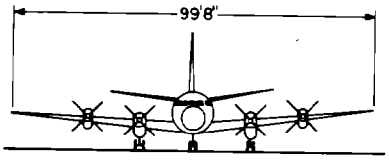

P-3C Aircraft Overall Dimensions

The wire model and calculated response data are shown in the following figure. The data points are located at: (1) Point 1 at Z/L = 0.47, (2) Point 2 at Z/L = 0.71, and (3) Point 3 at X/L_2 = 0.55. The excitation used was a 50 kV/m step drive field.

The analysis was performed using dipole models in free space for each wire of the cross wire model. Calculations of this type have shown reasonable agreement in terms of principal ring frequencies and to a lesser, but acceptable, accuracy for peak currents and current distributions with experimental data. The circumferential currents are not predicted using the thin wire model approximation.

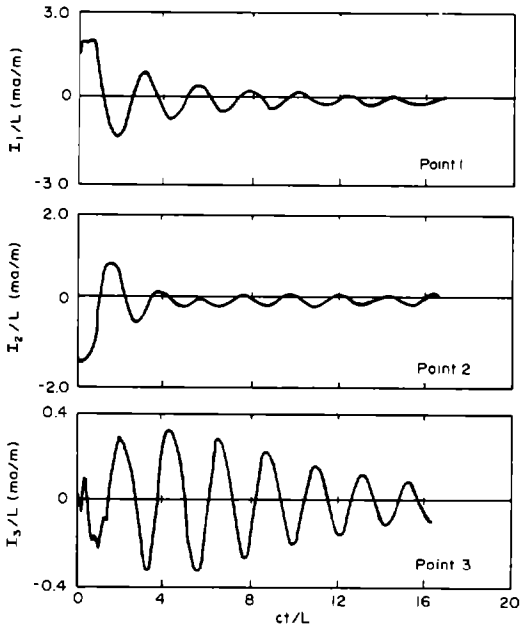

$c = 3 \times 10^8$ m/sec

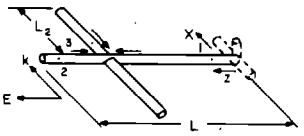

Wire cross currents at points 1-3 (fuselage excited by a unit step electric field.)

4.7 CABLE ANALYSIS

As in the case of antenna coupling, to determine the load voltage, current, or energy due to EMP excitation of cables, it is necessary to calculate the current voltage distribution on the cable. Depending on the cable construction and physical configuration, the current distribution can be determined by either antenna theory or transmission line theory.

In this section, we will look at simple cables and geometries to illustrate the analytical methods employed.

Cables in Proximity to Conducting Surfaces

In general, for cables in close proximity ($d << \lambda$) to a conducting surface (i.e., earth or other conducting surface) antenna currents can be neglected. Due to the reflection from the conducting surface in close proximity, the net field at the cable for use in antenna theory is nearly zero. The cable current (for unshielded cables) or the sheath current (for shielded cables) is totally due to transmission line currents.

Nature of Current Distribution on Cables

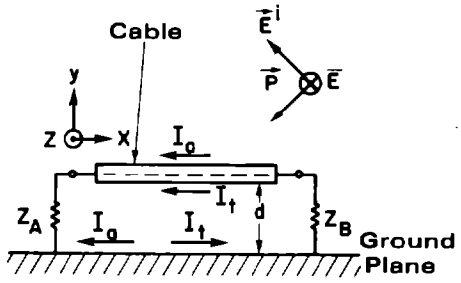

Total Sheath Currents

$I(x) = I_a + I_t$

I_a = **Antenna Current**

I_t = **Transmission Line Current**

$I_t \approx 0$ for $d >> \lambda$

$I_a \approx 0$ for $d << \lambda$

Horizontal Cable Over Ground

The transmission line equivalent circuit of a small cable section over a finitely conducting ground plane is shown in the figure.

Incremental Equivalent Circuit of a Horizontal Cable Configuration

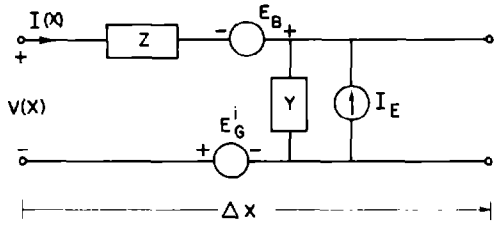

$$I_E = Y \int_o^d E^i_y \, dy$$

$$E_B = j\omega\mu \int_o^s H^i_z \, dy$$

E^i_G = Tangential Electric Field at the Surface of the Earth with No Cable Present

The transmission line equations are given by:

$$-\frac{\partial V(x)}{\partial x} = ZI(x) - E_B - E^i_G$$

$$-\frac{\partial I(x)}{\partial x} = YV(x) - I_E$$

where

Z = cable impedance per unit length in proximity to the ground plane

Y = cable admittance per unit length in proximity to the ground plane

E^i_G = tangential electric field at the surface of the ground plane and in the absence of the cable

$V(x)$ = voltage at point x due to incremental sources

$I(x)$ = current at point x due to incremental sources

E_B = incremental voltage source

I_E = incremental current source

It is to be noted that in this formulation antenna currents have been neglected.

If the incident EMP field is known, the point-source generators shown can be evaluated by

$$I_E(x) = Y \int_o^d E^i_y \, (x,y) \, dy$$

$$E_B(x) = j\omega\mu \int_o^d H^i_z \, (x,y) \, dy$$

The transmission line equations are solved for a point voltage and current generator located at some general point $x = \xi$ along the cable. The result will give the Green's function solution, $G(x, \xi)$, to this problem for prescribed loading conditions (Z_A, Z_B). Then the total current, $I(x)$, at any point along the cable is obtainable by use of the superposition integral:

$$I(x) = \int_o^L G_I(x, \xi) \, I_E(\xi) \, d\xi + \int_o^L G_V(x,\xi) \left[E_B(\xi) + E_G(\xi)\right] d\xi$$

where

$G_I(x,\xi)$ = Green's function due to a point current source

$G_V(x,\xi)$ = Green's function due to a point voltage source

L = length of cable.

The Green's functions are the solution of the transmission line equations for a point voltage source or current source at a point "ξ" on the line. The total current on the line is then the summation (integral) of the contributions of each of the point sources.

A typical time history of the current in a long cable above ground is shown in the figure. This waveform was produced for a vertical electric field at a grazing angle of incidence. The time history exhibits a high-amplitude spike with a long decay (tail). This indicates the low-frequency pickup is highly important.

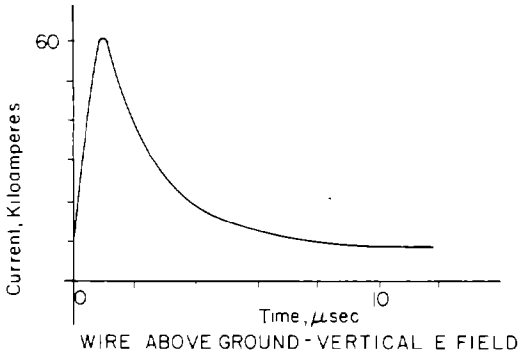

WIRE ABOVE GROUND - VERTICAL E FIELD

If the antenna current distribution on a cable configuration is not available from antenna theory, the transmission line approach may be used to calculate the approximate current distribution. This is based on the close analogy that exists between wire antennas and transmission lines. This analogy is shown in the figure.

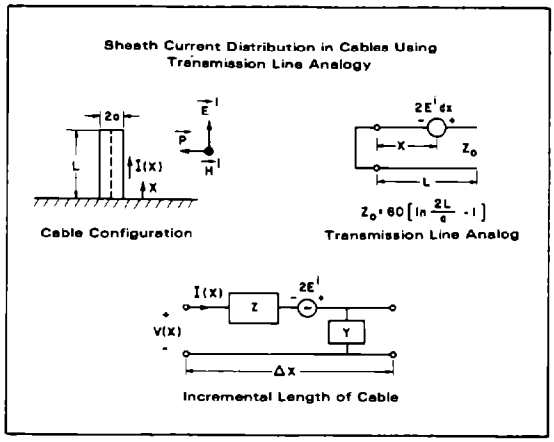

Cables in Proximity to a Non-Conducting Surface

For cable runs which are close to non-conducting surfaces, or far removed from conducting surfaces, the transmission line currents are quite small (negligible) compared to the antenna currents.

To determine the sheath current for shielded cables, or the pickup by unshielded cables (single wires), the cable can be viewed as an equivalent dipole. In this case, the antenna analysis discussed previously, can be used to determine the current distribution.

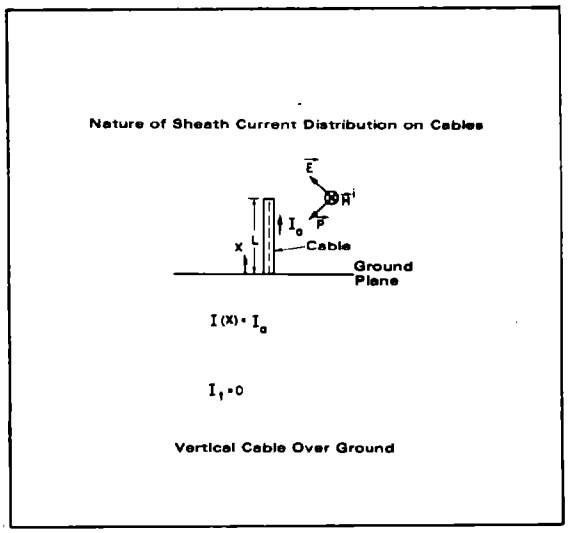

Buried Cables

For buried cables, the principal pickup mechanism to cause sheath currents is the common impedance mechanism. Electric and magnetic fields cause currents to flow in the earth, and the resistance of the earth causes a voltage drop to appear along the cable.

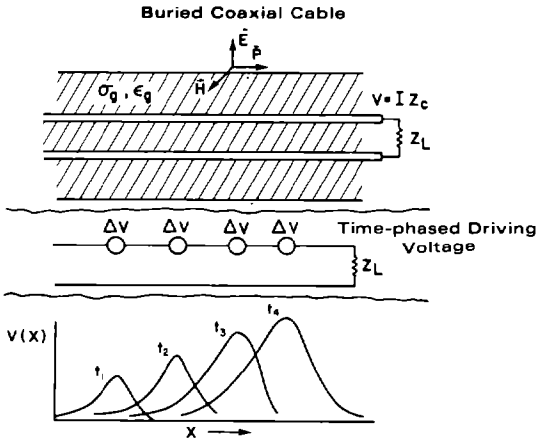

For buried cables, the current induced is obtained from a transmission line model in which the soil surrounding the cable is the return conductor. To model this configuration as a transmission line, it is necesaary to have the characteristic impedance (Z_o) and propagation (γ) of the cable. These are given by:

$$\gamma = \sqrt{ZY}$$

$$Z_o = \sqrt{Z/Y}$$

$$Z = Z_g + Z_i + j\omega L$$

$$Y = j\omega C\ Y_g / j\omega C + Y_g$$

where

Z_g = soil impedance

Z_i = cable impedance

$j\omega L$ = inductive reactance of insulation gap

$j\omega C$ = capacitive reactance of insulation

Y_g = soil admittance.

For near surface burial (a few meters) the incident field is approximately that at the earth's surface. For deep burial, the propagation loss in the earth must be taken into account. The surface field or transmitted field can be determined from the reflection and transmission coefficients, given in a later section, and the earth propagation constant.

Depending on the angle of arrival, the incremental voltage drops appear to be progressively excited along the cables so that a time-phased effect of the driving voltage must be considered. In the case of a tangential angle of arrival with the direction of propagation parallel to the axis of the buried cable, there is a tendency toward a traveling wave buildup of the sheath current or the cable as the wave progresses along the cable. Fortunately, in general, this is counteracted by the differences in propagation time in the earth and in the wave above the earth. The peak amplitude and energy are greatly reduced by earth absorption. Due to the earth parameters, the time history of the current in the cable (deep burial > 10 meters), indicates the primary pickup is low frequency and of low amplitude.

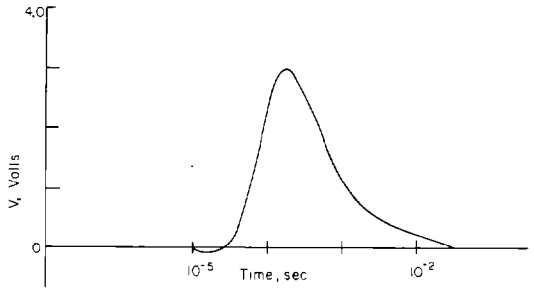

WIRE BELOW GROUND-HORIZONTAL E FIELD

Surface Transfer Impedance for Shielded Cables

Once the sheath current distribution is known, the voltage induced into a shielded cable because of imperfect shielding can be calculated.

The shielding effectiveness of a cable can be represented quantitatively by surface transfer impedance, which relates the sheath current flowing on the cable shield to the voltage drop per unit length (surface electric field) appearing at the inner surface of the shield.

A current, I_s, flowing on the outer sheath of the cable causes an incremental voltage drop, ΔV, to appear across an incremental length, Δx, on the inside of the sheath. This voltage is given by

$$\Delta V = Z_T I_s(x) \Delta x$$

where Z_T is defined as the surface transfer impedance of the cable. The surface transfer impedance is determined by the construction of the outer shield. Analytical expressions are available for solid-shell and braided coaxial cables. Since braided cables present a geometry that is quite difficult to analyze in detail, their transfer impedance is most easily determined experimentally.

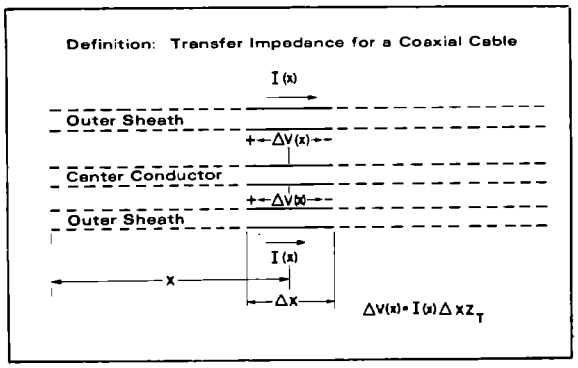

Before presenting expressions for the surface transfer impedance of a solid-state coaxial cable, it is useful to consider the problem qualitatively. In the limit of zero frequency, a current flowing on the outer shell of a coaxial cable will see the dc resistance of the shell. At very low frequencies and thin wall shields, there is little attenuation due to skin effect. Therefore, at zero frequency, the voltage drop appearing inside the shell will be the shell current multiplied by the dc resistance of the shell given by

$$R_{dc} = \frac{1}{2\pi b t \sigma} \text{ ohms/meter}$$

for thin-wall shells, where

- σ = the conductivity of the outer conductor
- t = the thickness of the outer conductor
- b = the inside radius of the outer conductor.

As the frequency of the shell current is raised, less and less of it will penetrate the shell, and thus one would expect the surface transfer impedance of the solid-shell coaxial cable to become smaller.

Schelkunoff has developed an approximate expression for the surface transfer impedance of a solid-shell coaxial cable using the assumption that the thickness of the shell, t, is much less than its inner radius. It is of the form

$$Z_t = \frac{\eta}{2\pi \sqrt{bc} \sinh(\Gamma t)} \quad \text{for } t \ll b$$

where

- η = intrinsic impedance of the shield
- Γ = propagation constant of the medium
- c = outer radius of outer conductor
- b = inner radius of outer conductor.

Surface Transfer Impedance of Braided and Solid Outer Conductor Coaxial Cable

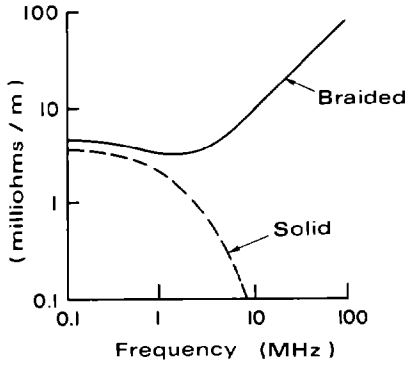

The figure also shows the surface transfer impedance for a typical coaxial cable with a braided outer conductor. Note that at low frequencies, i.e., less than 1 MHz, the behavior tends to follow that of the solid outer conductor, and at zero frequency the surface transfer impedance is given by the dc resistance per unit length of the wires that make up the braid. Above about 2 or 3 Mhz, the surface transfer impedance begins increasing with frequency. Kruegel investigated braided coaxial lines in great depth. He found that this high-frequency behavior was strongly influenced by details of the braid construction -- optical covering factor, number of carriers, and braid angle to name three important factors. These factors determine the size and shape of the holes in the braid and, thus, the magnitude of the magnetic fields which can fringe into the interior of the cable. It is apparently these fringing fields which determine the high-frequency behavior of the cable.

Based on experimental results, the surface transfer impedance for braided shell coaxial cables is characterized by a diffusion term representing diffusion of EM energy through the metal and an inductance term representing penetration of the magnetic field through the holes.

$$Z_T = Z_D + j\omega M_{12}$$

where

Z_D = diffusion term equal to the dc resistance of the braid per unit length at low frequencies

M_{12} = the leakage mutual inductance of the braid per unit length (may be positive or negative).

The diffusion term, Z_D is given by

$$Z_D \simeq \frac{4}{\pi d^2 N C \sigma \cos\alpha} + \frac{(1+j)\, d/\delta}{\sinh (1+j)\, d/\delta}$$

and the mutual inductance term is given by:

$$M_{12} \simeq \frac{\pi\mu_o}{6C}(1 - K)^{3/2} + \frac{e^2}{E(e) - (1-e^2) K(e)} \qquad \alpha < 45^o$$

$$\simeq \frac{\pi\mu_o}{6C}(1 - K)^{3/2} + \frac{e^2 \sqrt{1-e^2}}{K(e) - E(e)} \qquad \alpha > 45^o$$

where

K = optical coverage

C = number of carriers

N = number of ends

d = diameter of individual wires

α = weave angle

δ = skin depth = $\frac{1}{\sqrt{\pi f \mu \sigma}}$

σ = wire conductivity

μ_o = free space permeability = $4\pi \times 10^{-7}$

K(e) = complete elliptic integral of the first kind

E(e) = complete elliptic integral of the second kind

$e = \sqrt{1-\tan^2\alpha}$ $\qquad \alpha < 45^o$

$= \sqrt{1-\cot^2\alpha}$ $\qquad \alpha > 45^o$

These expressions have been found to be very accurate at low frequencies ($d/\delta << 1$) and accurate to within a factor of 3 or less at high frequencies ($\omega M_{12} >> |Z_D|$).

Several coaxial cable types have been investigated to determine their surface transfer impedance. The results for two of the more common cable types are given below:

Cable Type	Resistance (ohms/m)	Inductance (Hz/m)
RG-8A/U	4.5×10^{-3}	$+ 8.75 \times 10^{-1}$
RG-9A/U	3.2×10^{-3}	$- 1.91 \times 10^{-1}$

EMP Response of Typical Cable

We will now consider an example of EMP penetration into a coaxial cable. Let a coaxial cable be exposed to an incident field, E_i, parallel to its axis. With the outer conductor considered as a linear antenna, the external incident field induces an axial current distribution on this conductor. If the current, $I_s(x)$, is known as a function of x, the coupling into the cable can be represented by a continuous distribution of incremental generators each with voltage $Z_T I_S(x)dx$, where Z_T is the surface transfer impedance of the cable shield. To determine the current distribution inside the cable from which the load current through Z_1 can be obtained, it is necessary to have expressions for the current and voltage at any point on the line with arbitrary loads (Z_1, Z_2) for an arbitrary location of a series point generator; this is the Green's function solution to the problem. Then, by the superposition integral, the current distribution due to a voltage source distribution is readily obtained.

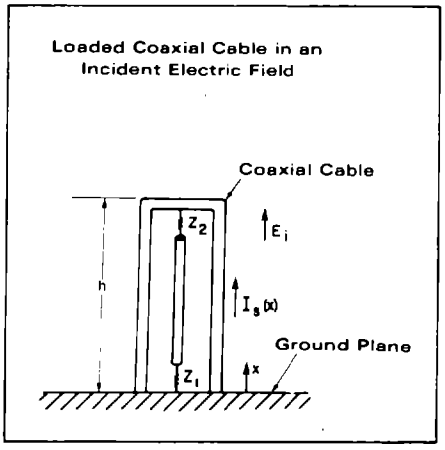

Let a section of the line h be terminated in Z_1 and Z_2, and $V_1(x,\xi)$ and $I_1(x, \xi)$ be the voltage and current at point x when a point source, $V_g = Z_T I_S(\xi)\, d\xi$, is impressed at $x = \xi$ in series with the line. Note that this transmission line corresponds to the interior of the coaxial cable. The voltages and currents in this line are given by Schelkunoff. Let the current Green's function be expressed as:

$$G_I(x,\xi) = I_1(x,\xi)$$

Then by the superposition integral

$$I(x) = \int_o^h G_I(x,\xi)\, I_s(\xi)\, d\xi$$

and

$$I(o) = I_L =$$

$$\int_o^h G_I(o,\xi)\, I_s(\xi)\, d\xi.$$

In order to perform this integration, the sheath current distribution, $I_s(\xi)$, must be known. Since the shield (outer conductor) of common coaxial cables satisfies the conditions of linear antenna theory ($h/a >> 1$, $2a/\lambda << 1$), it may be treated as an unloaded receiving antenna in a uniform field. The total axial current (sheath current) distribution is approximated by the following expression:

$$I_s(\xi) = I_s(o)\, \frac{\cos\beta\xi - \cos\beta h}{1 - \cos\beta h}$$

where

β = propagation constant of the medium surrounding the antenna (cable)

$$I_s(o) = -h_e E_i(j\omega)/Za.$$

In this relationship, h_e is the effective length of a monopole antenna of physical length, h, and Z_a is its input impedance. In the equation concerning the frequency-domain transfer function, the current in the load, Z_1, is related to the incident electric field $E^i(j\omega)$, the time history of the load current is determined by taking the inverse Fourier transform. Let

$$I_L(\omega) = I_{LR}(\omega) + j\, I_{LI}(\omega)$$

be the spectrum of the load current decomposed into its real and imaginary parts. The time history of the load current is

then

$$i_L(t) = \frac{1}{\pi}\int_o^{\omega_c} [I_{LR}(\omega)\cos\omega t - I_{LI}(\omega)\sin\omega t]\, d\omega$$

where, in obtaining the second part, use has been made of the relation $I_L(j\omega) = I_L(-j\omega)$, which is the case for any time invariant, linear system. The radian cutoff frequency, ω_c, is used for computational purposes and is determined on the basis of the high-frequency content of the excitation pulse. For example, the highest significant frequency contained in a Gaussian pulse is usually taken to be $f_c = 2.6\, f_1$, where $f_1 = 1/2\pi t_1$ and t_1 is a measure of the pulse width, ($t_1 = 0.4246\, t_\omega$ where t_ω is the pulse width at the half amplitude points). Numerical techniques may be used to integrate this equation with the aid of a digital computer.

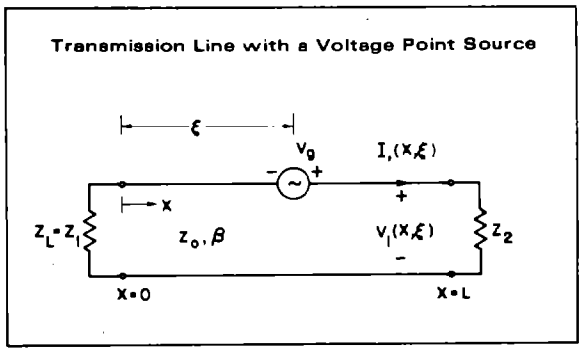

The description of the incident electric field pulse assumed here is a Gaussian pulse of unit amplitude and of width t_ω = 100 nsec at 1/2 amplitude point. It is given by the expression

$$e_i(t) = \exp\left[-\frac{t^2}{2t_1^2}\right]$$

where $t_1 = 0.4246\, t\omega$ sec is a measure of the pulse width. The spectrum of the pulse described is

$$E_i(j\omega) = \frac{\sqrt{2\pi}}{\omega_1}\exp\left[-\frac{\omega^2}{2\omega_1^2}\right]$$

where $\omega_1 = 2\pi f_1 = 1/t_1$ rad/sec. For this example, a 25-meter RG-8A/U and a 25-meter RG-9A/U cable were considered. The electric field vector was parallel to the axis of the cables and broadside incident. The pulse width assumed corresponds to a cutoff frequency $f_c = 9.75$ MHz.

The transient response of the load current was obtained numerically for the following special cases:

Case I

RG-8A/U Cable

$h = 25$ meters

$t_\omega = 100$ nsec

$Z_1 = Z_o = 50$ ohms

$Z_2 = 0$

Case II

RG-9A/U Cable

$h = 25$ meters

$t_\omega = 100$ nsec

$Z_1 = Z_o = 50$ ohms

$Z_2 = 0$

Case III

RG-8A/U Cable

$h = 25$ meters

$t_\omega = 100$ nsec

$Z_1 = Z_o = 50$ ohms

$Z_2 = \infty$

Case IV

RG-9A/U Cable

$h = 25$ meters

$t_\omega = 100$ nsec

$Z_1 = Z_o = 50$ ohms

$Z_2 = \infty$

Shown are the time histories of the load currents for Cases I and II for a Gaussian pulse whose amplitude is 1V/m defined previously. Note that the time scale is normalized with respect to the pulse width. The results indicate that the ringing of the transient response is mainly due to the fundamental resonant frequency of the cable when viewed externally as an unloaded scattering antenna. The fundamental period of current oscillations is determined by the time it takes the current wave to travel four times the cable length, with the propagation velocity of free space.

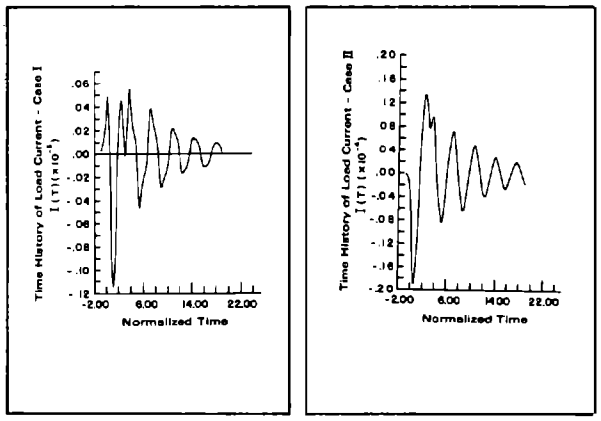

The time histories for Cases III and IV are shown here.

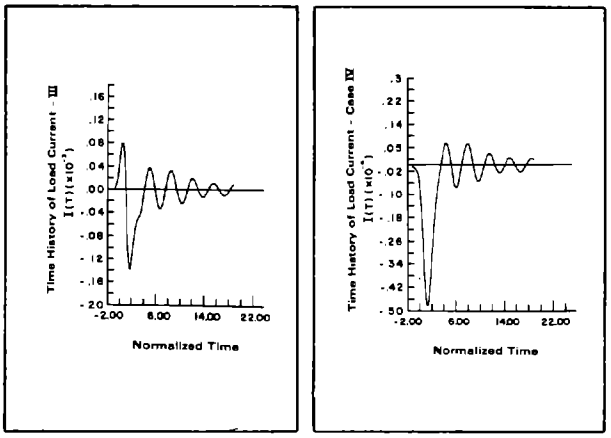

4.8 SHIELDING ANALYSIS

There are about as many analytical approaches to calculating shielding effectiveness as there are shielding engineers. In general, the rigorous approaches involve some simplifying assumptions which are sometimes pertinent to the EMP problem area. In this case, they assume the conductivity of the shield to be such as to permit first solving for the current distribution on the exterior of the shield, as we have done in the previous sections. It also assumes that the shield is reasonably good so that any equipment configurations inside the shield are not a dominant factor.

Thus, the shielding approaches have been boiled down to the three basic groups; exact approach based on scattering theory, approaches which involve some implicit assumptions which can be shown to give rise to the lumped circuit approximation, and the Schelkunoff plane wave approach which gives rise to the so-called transmission line equivalent. The rigorous or lumped-circuit approximation appears to be a satisfactory approach for most EMP-type shielding applications. It does tend to break down where the conductivity of the wall material is low; for example, the conductivity of coke or wall material made out of seawater.

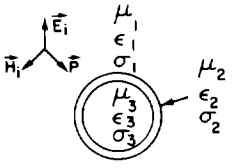

Scattering theory

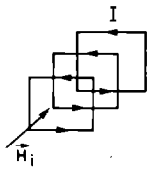

Lumped-circuit approximation

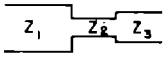

Plane wave, transmission line equivalent circuit

Scattering Theory Solutions

For simple geometries such as spherical, and cylindrical shells and parallel plates, scattering theory solutions have been obtained. These are presented in the form of transfer functions as a function of frequency.

Based on the exact scattering theory, for frequencies greater than a few Hertz, the transfer function for magnetic field shielding is of the form:

$$T_H(\omega) \equiv \frac{H_{in}(\omega)}{H_{ex}(\omega)}$$

and is given by:

$$T_H(\omega) = \frac{1}{\cos(k_2 d) - \frac{k_2 b}{2}\sin(k_2 d)}$$

$\omega = 2\pi f$

f = frequency of incident field

$k = (\mu_o/\mu)k_2 b$

$k_2 = \sqrt{-j\omega\mu\sigma} = \frac{\sqrt{-j2}}{\delta}$

$\delta = 1\sqrt{\pi f\mu\sigma}$ = skin depth of material

d = thickness of enclosure walls

μ_o = permeability of free space

μ = permeability of enclosure walls

σ = conductivity of enclosure walls

The factor "b" in the equation is a geometric variable that characterizes different enclosure geometries as follows:

b = the separation distance between plates for large area parallel plate shields

b = the radius for cylindrical enclosures

b = 2/3 the radius for spherical enclosures

At high frequencies, where the wall thickness is greater than the skin depth ($d > \delta$), the transfer function reduces to

$$T_H(\omega) = \frac{2\sqrt{2}\ \delta\ e^{-d/\delta}}{b}$$

At low frequencies ($d < \delta$) the magnetic shielding becomes

$$T_H(\omega) = \left| \frac{1}{\frac{j\omega d\sigma\mu b}{2} + 1} \right|$$

The transfer function for electric field shielding is given by:

$$T_E(\omega) = \frac{2\ (k_1 b)^2}{k \sin k_2 d}$$

$$k_1 = 2\pi/\lambda$$

λ = wavelength of impinging field

for $d > \delta$, high frequencies:

$$T_E(\omega) = \frac{9\ \omega\varepsilon_o b e^{-d/\delta}}{\sqrt{2}\ \sigma\delta}$$

$\varepsilon_o = 10^{-9}/36\pi$ farads/meter

for low frequencies, $d < \delta$:

$$T_E(\omega) = \frac{9\omega\varepsilon_o b}{4\sigma d}$$

A conservative approximation for other geometries (cubes, rectangles, etc.), modeling a structure as a sphere with b being the minimum dimension of the enclosure is good practice.

Low Frequency Lumped Circuit Approximation

The very low frequency magnetic field penetration characterization for a sphere is given in the form of an R-L circuit. The shield is regarded as a good antenna with inductance L. The Thevenin equivalent voltage generator is equal to the magnetic field intensity incident on the shield. The various circuit parameters are related to the parameters of the spherical shell:

$$R = \frac{2\pi n^2}{3d_\tau}$$

$$L = \frac{2\pi\mu a n^2}{9}$$

a = radius of sphere

d = wall thickness

σ = wall conductivity

μ = free space permeability

n = equivalent number of turns (this cancels out in the final expression for shielding effectiveness).

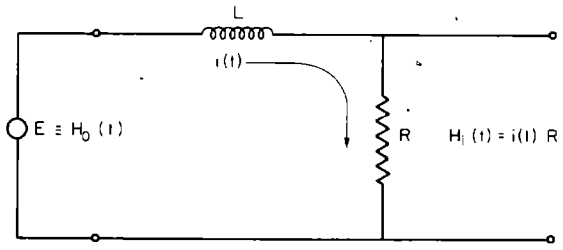

ANALOG CIRCUIT CHARACTERIZING SHIELDING EFFECTIVENESS OF SPHERES

Using the circuit approximation, the time history of interior field with a Gaussian pulse of $120/\pi$, amperes/meter peak amplitude incident on the shield was calculated. The shield was an 18 inch radius, 1/16 inch wall thickness aluminum sphere. The calculation, using the circuit approximation, was compared to one using exact scattering theory.

The early time-history of the interior field is shown in the figure. The maximum interior magnetic field intensity is proportional to the integral of the incident field. This maximum interior field is reached with a rise time approximately equal to the incident field duration.

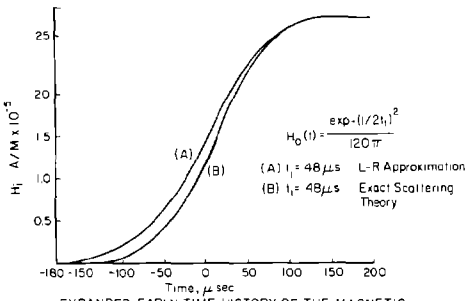

EXPANDED EARLY TIME HISTORY OF THE MAGNETIC FIELD INTENSITY AT THE CENTER OF AN 18 inch RADIUS ALUMINUM SPHERE WITH A 1/16 inch WALL TO A GAUSSIAN PULSE

An exponential decay describes the long time response after the initial rise. The decay time constant is R/L.

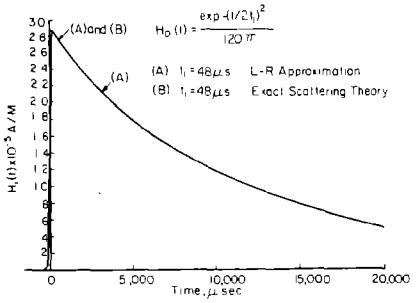

LONG TERM HISTORY OF THE MAGNETIC FIELD INTENSITY AT THE CENTER OF AN 18-inch ALUMINUM SPHERE WITH A 1/16-inch WALL

The very low frequency electric field penetration characterization for a sphere is given in the form of an R-C circuit. The shield is regarded as a dipole antenna with effective height h_e and capacitance C. The Thevenin equivalent voltage generator is proportional to the electric field intensity incident on the shield. The various circuit parameters are related to the parameters of the spherical shield:

a = radius

d = wall thickness

σ_a = wall conductivity

The electric field at the center of the sphere is proportional to the voltage across R_s.

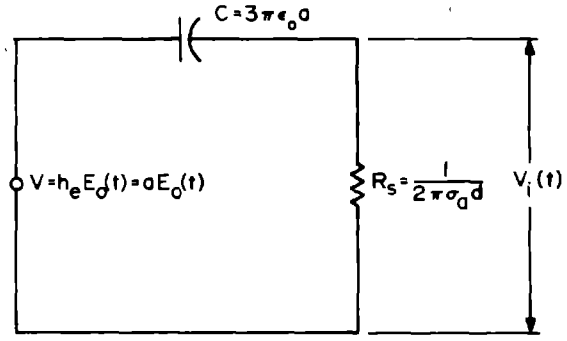

For $8 >> d$ and $\frac{2\sigma_a d}{3\epsilon_0} > \omega$

VERY LOW FREQUENCY ELECTRIC FIELD PENETRATION CHARACTERIZATION FOR A SPHERE

Using the low frequency circuit approximation, the time history of the interior field with a Gaussian pulse of 1 volt/meter peak amplitude incident on the shield was calculated. The shield was an 18 inch radius, 1/16 inch wall thickness aluminum sphere. The calculation using the circuit approximation was compared to one using exact scattering theory.

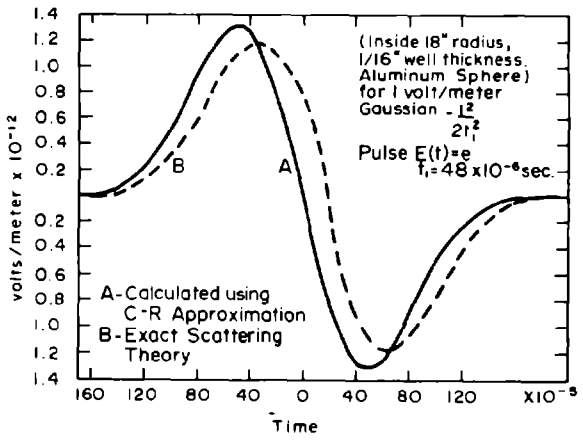

TIME HISTORY OF THE ELECTRIC-FIELD INTENSITY AT THE CENTER OF A SPHERE

Apertures

Obviously, if the enclosure has holes, this provides a means for the exterior fields to leak into the interior. Typically, if we assume the enclosure aperture to be very small compared to the general size of the enclosure, the effect of a small aperture can be calculated. In this case, a magnetic dipole is assumed to appear in the aperture hole which is polarized in such a way as to cancel the exterior current flow. However, since this dipole is coupled both to the exterior and interior, this provides a source of interior fields which tends to fall off at the low frequencies inversely proportional to the cube of the distance away from the aperture. In the case of real enclosures, the effect of the enclosure walls must also be considered.

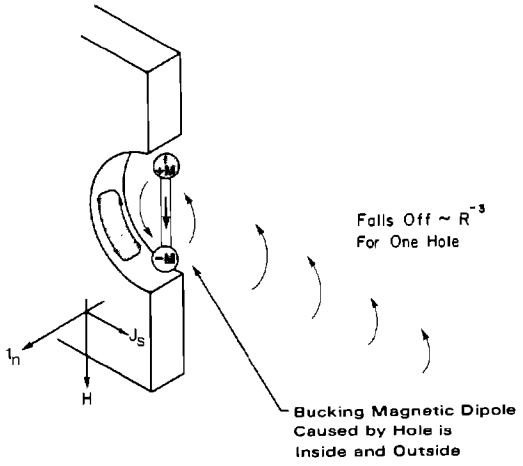

For a plane wave incident on the structure, both the electric and magnetic fields will penetrate. The EMP propagation is in a direction parallel to the shielding plane. The geometry is depicted in the figure. The penetrating fields are given by:

$$E_r = 2/3\pi \left(\frac{a}{r}\right)^3 E_o \cos\theta$$

$$E_\theta = \frac{1}{3\pi} \left(\frac{a}{r}\right)^3 E_o \sin\theta$$

$$E_\phi = 0$$

$$H_r = \frac{4}{3\pi} \left(\frac{a}{r}\right)^3 H_o \sin\phi \sin\theta$$

$$H_\phi = \frac{2}{3\pi} \left(\frac{a}{r}\right)^3 H_o \cos\phi$$

$$H_\theta = \frac{2}{3\pi} \left(\frac{a}{r}\right)^3 H_o \sin\phi \cos\theta$$

where

E_ϕ, E_r, E_θ = internal electric field components in spherical coordinates

H_ϕ, H_r, H_θ = internal magnetic field components in spherical coordinates

a = radius of the aperture. In analysis of non-circular apertures, "a" should be set equal to 1/2 the largest dimension of the opening under consideration

r = radial distance from the point in the enclosure at which the field strengths are to be determined to the center of the hole.

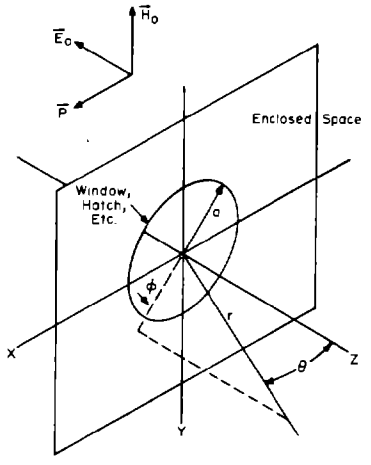

PENETRATION OF ELECTRIC AND MAGNETIC FIELDS THROUGH A CIRCULAR HOLE

Special Problems

There are many special problems which we have not covered in this very brief discussion on shielding. As mentioned previously, there is a problem using the so-called rigorous or lumped-element approaches, wherein the parameters of the wall material are quite comparable to the ground parameters. Another case not considered, but one that must be considered in any shielding, is the collection of the additional current arising from attached cables as illustrated here. Obviously, we can get a lot more penetration if an exposed cable runs through an otherwise shielded enclosure.

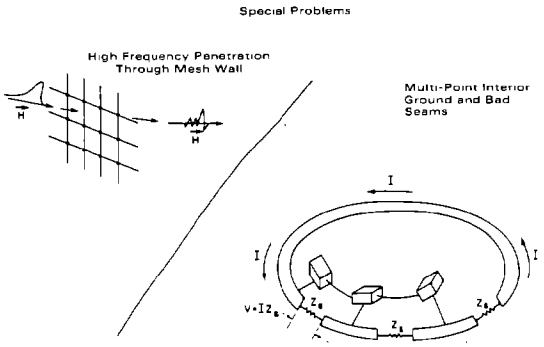

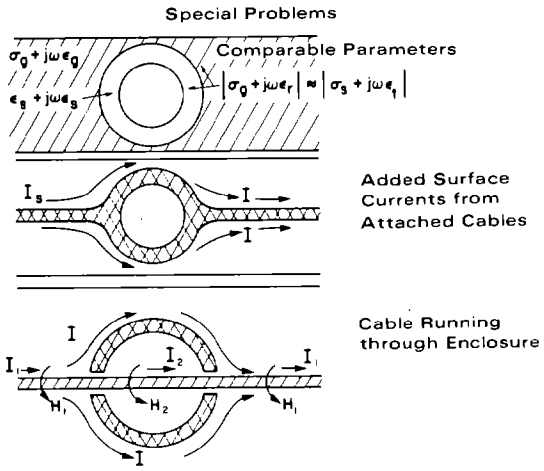

The mesh or loop-type shielding is valid only up to the point wherein the circumference of the loop is significantly smaller than the wavelength. Where the circumference of the loop is larger than the wavelength, various distorted types of penetration can occur, such as illustrated here.

We also have a multi-point ground problem. In many instances it is necessary to ground equipment to the walls of the enclosure at different points. If the inside wall of the enclosure is used as a return current path, serious problems may occur and may arise from lack of symmetry in the conductivity in construction of the wall enclosure. Specifically shown is the effect of seam resistance. If this enclosure is exposed to exterior fields, currents will flow on the outside of the enclosure. Due to the seam imperfections, a voltage drop occurs both on the outside and inside near the seams. This voltage drop can, in turn, then be injected into the circuits via a common ground or common impedance.

As mentioned in the previous section, field enhancement also plays a major role in coupling. The enclosure itself can also enhance the fields, especially near corners and edges.

For certain situations, saturation and nonlinear effects of the wall material may be important. However, if the wall is designed of ordinary cold-rolled steel, copper, or aluminum and is of sufficient thickness to begin with, this, in general, is not a problem for the radiated or more distant fields.

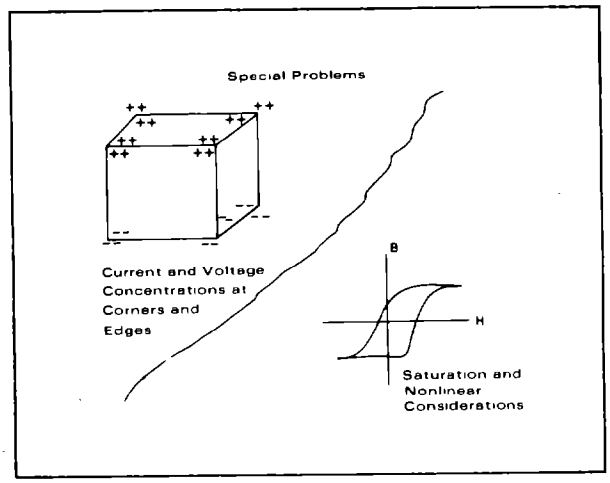

Reflection and Transmission of EM Waves

To determine the response of an underground coupling structure to EMP, it is necessary to first calculate the sub-surface EMP fields in the absence of the structure. An approximate method for calculating the transmitted EM fields into the ground is to assume a plane surface and use ray theory in conjunction with

appropriate boundary conditions. Consider now a vertically (E field in the plane of incidence) polarized EMP plane wave incident on the earth's surface at an elevation angle ψ.

Reflected and Refracted Waves at the Air-Ground Interface

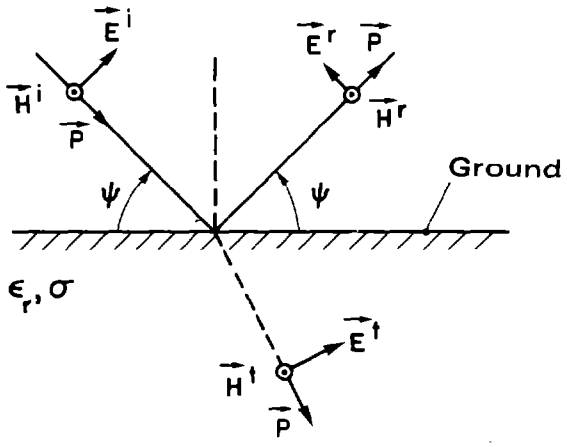

It can be shown that the ground reflection coefficient for the vertically polarized case is given as:

$$R_v = \frac{E^r}{E^i} = \frac{(\epsilon_r - jx)\sin\psi - \sqrt{(e_r - jx) - \cos^2\psi}}{(\epsilon_r - jx)\sin\psi + \sqrt{(e_r - jx) - \cos^2\psi}}$$

where

$x = \frac{\sigma}{\omega\epsilon_o}$

σ = ground conductivity

ϵ_r = relative dielectric constant of ground

ψ = elevation angle.

The transmission coefficient is defined as:

$$T_V = \frac{E^t}{E^i} = (1 - R_v) \frac{\sin\psi}{\sqrt{1 - \frac{1}{\epsilon_r - jx}\cos^2\psi}}$$

The geometry for the case of horizontal (E field normal to the plane of incidence) polarization is shown in the following figure.

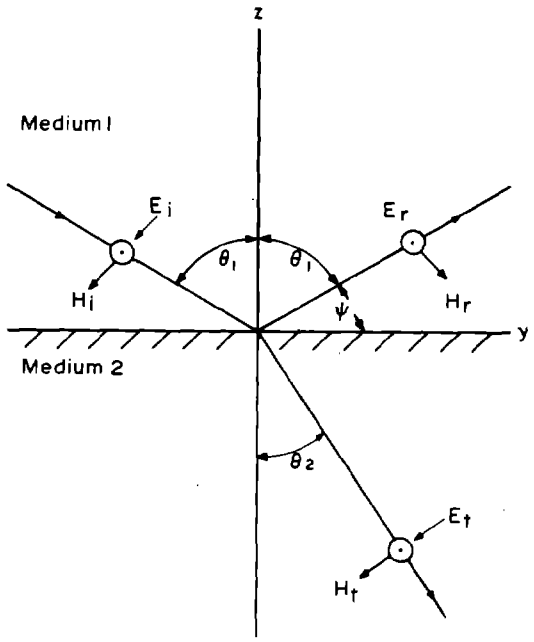

REFLECTED AND REFRACTED WAVES--HORIZONTAL POLARIZATION

The reflection coefficient for this case is given by:

$$R_H = \frac{E_r}{E_i} = \frac{\sin\psi - \sqrt{(\epsilon_r - jx) - \cos^2\psi}}{\sin\psi + \sqrt{(\epsilon_r - jx) - \cos^2\psi}}$$

and the transmission coefficient is

$$T_H = \frac{E_t}{E_i} = 1 + R_H$$

REFERENCES

"Electromagnetic Pulse Handbook for Missiles and Aircraft in Flight," EMP Interaction Notes 1-1, AFWL TR-73-68, Air Force Weapons Laboratory, Kirtland AFB, New Mexico.

"EMP Design Guidelines for Naval Ship Systems," Naval Surface Weapons Center/White Oak Laboratory, Silver Springs, Maryland (to be published).

"EMP Engineering and Design Principles," Bell Laboratories, Loop Transmission Division, Technical Publication Department, Whippany, New Jersey.

Jordan, E.C., Electromagnetic Waves and Radiating Systems, Prentice Hall, 1968.

Vance, E.F., "Prediction of Transients in Buried, Shielded Cables," Stanford Research Institute, SRI Project 2192.

King, R.W.P., Theory of Linear Antennas, Boston, Howard University Press, 1956.

King, R.W.P., Harrison, C.W., Jr., and Denton, D.H., Jr., "The Electrically Short Antenna as a Probe for Measuring Free Electron Densities and Collision Frequency in an Ionized Region," Journal of Research of the National Bureau of Standards, - Radio Propagation, Vol. 65, No. 4, pp. 371-383, July-August 1961.

Gooch, D.W., Harrison, C.W., Jr., King, F.W.P., and Wu, T.T., "Impedance of Long Antennas in Air and in Dissipative Media," Journal of Research of the National Bureau of Standards, - D. Radio Propagation, Vol. 670, No. 3, May-June 1963.

Toulios, P.P., et al, "Effects of EMP Environment on Military Systems," Technical Report No. E6114 under USAMERDC Contract No. DAAK02-68-C-0377, IIT Research Institute, Chicago, Illinois.

Toulios, P.P., Kaurs, A.R., "Antenna Users Manual for Linear Antennas in an EMP Environment," Volumes I and II, Technical Report E6239, under Contract No. DAAG39-72-C-0192, IIT Research Institute, Chicago, Illinois.

Baum, Carl E., "On the Singularity Expansion Method for the Solution of Electromagnetic Interaction Problems," Interaction Notes, Note 88, December 1971.

Vance, E., "DNA Handbook Revision, Chapter 11, Coupling to Cables," SRI, Menlo Park, Ca.

The voltage across and the current through the junction as a function of time when a high amplitude transient is applied as a reverse bias usually exhibits a high voltage, low current characteristic. When thermal second breakdown occurs, the case when the junction fails, the voltage suddenly decreases and the current rapidly increases.

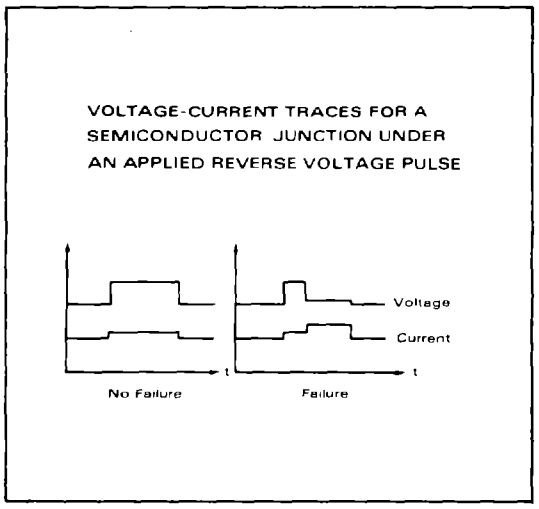

It has been observed that the occurrence of thermal second breakdown, which is an energy dependent process, represents the point of incipient permanent damage for semiconductor devices at submicrosecond pulse conditions. That is, once a thermal second breakdown is initiated with some additional amount of energy being further dissipated in the device, a permanent damage condition results. For most semiconductor devices investigated, device degradation after second breakdown was a result of junction damage, i.e., realloying of the material or the formation of a melt channel. However, for some devices, a low voltage-high current mode of operation was observed due to the migration of contact metalization through the junction thus forming a metallic short. Depending upon the device, either of these phenomena could possibly occur initially, thus precipitating device failure.

Another reverse bias failure mode which has been observed on occasion in transistors is that of current mode second breakdown. Basically, the effect is initiated by relatively high material current densities under the emitter during collector to base junction reverse pulsing resulting in a forward bias on a portion of the emitter. When this bias becomes sufficiently high, the device becomes unstable and is switched to a low impedance, low sustaining voltage mode of operation.

The occurrence of the current mode second breakdown phenomenon in itself generally has not been observed to result in permanent damage. However, if the resulting low impedance currents are not sufficiently limited, then local hot spots form and the resulting failures are produced in a manner similar to that of thermal second breakdown.

The forward biased junction vulnerability to pulsed electrical energy can be understood by considering some of the basic concepts associated with thermal second breakdown. That is, device degradation is a direct result of essentially similar melting and realloying reactions at various current constriction sites within the junction. The significant fact here is that due to the relatively lower junction voltage at forward bias conditions, a correspondingly higher current than that for the reverse direction is required to reach the critical failure energy. This larger current, in turn, results in a significant voltage drop being produced in the bulk material. Hence, a higher energy input is generally required as far as the device terminals are concerned, thus producing much of the apparent decrease in failure sensitivity observed experimentally. Again, since a relatively low initial impedance condition exists, the dramatic switching associated with thermal second breakdown would not generally be observed.

In addition to the single junction mechanisms, another failure mechanism in transistors is possible due to its multijunction nature. This mechanism is called punch-through. The width of the depletion region at a reverse-bias junction will increase as the voltage across the junction increases. Since the collector-base junction of a transistor is usually reverse biased and of small width, it is possible for the depletion region to extend throughout the width of the base which effectively results in a short circuit. Under these conditions, the resulting current may be sufficiently large to damage the junction.

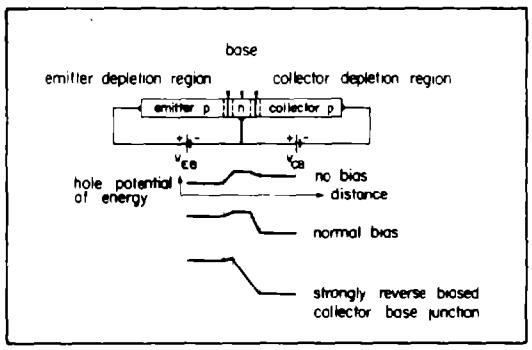

Thermal Failure Model

Many different microscopic mechanisms may contribute to semiconductor failure. However, most of these mechanisms have been found to be linked primarily to the junction temperature. Therefore, in most cases, the treatment of the problem can be reduced to a thermal analysis.

The worst case as far as achieving high temperatures in the junction is when one considers that all of the power dissipated in the device occurs in the junction. This corresponds to the situation where a high-voltage pulse of reverse polarity is applied to a junction with a high reverse voltage breakdown. When the avalanche breakdown occurs, almost all of the applied voltage is dropped across the junction and only a small percentage is dropped across the bulk material (except for a very short pulse on the order of 10 to 100 nanoseconds or less where the high current required for failure causes more voltage drop across the bulk).

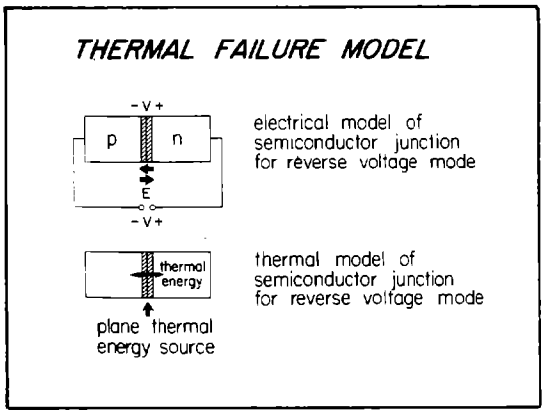

The thermal model for pulses between 100 nsecs and 1 millisec is based on the following assumptions:

- The heat is generated at the junction
- The junction is planar
- The silicon material on either side of the depletion layer of the junction extends out infinitely.

Then the one dimensional heat equation can be used to solve for the junction temperature.

$$\frac{\partial}{\partial x} K \left(\frac{\partial T}{\partial x}\right) - PC_p \frac{\partial T}{\partial t} = 0$$

where

K = the thermal conductivity of silicon (W/Cm^{o}K)

T = the temperature (^{o}K)

x = position measured from the planar heat source in Cm

P = density of the silicon (gm/Cm^3)

C_p = specific heat of silicon (J/gm^{o}K)

If a square pulse of electric power is applied to the junction and all of the electrical power is transformed to heating, the maximum temperature of the junction is given by:

$$T_m = T_i + \frac{P}{A} \frac{1}{\sqrt{\pi KPC_e}} t^{\frac{1}{2}}$$

where

T_m = the maximum junction temperature

T_i = the initial junction temperature

P = the electrical pulse power applied to the junction

A = the area of the junction

t = the pulse width

Rewriting the equation and taking the logarithm of both sides yields an equation which plots as a straight line with a -1/2 slope on log-log paper.

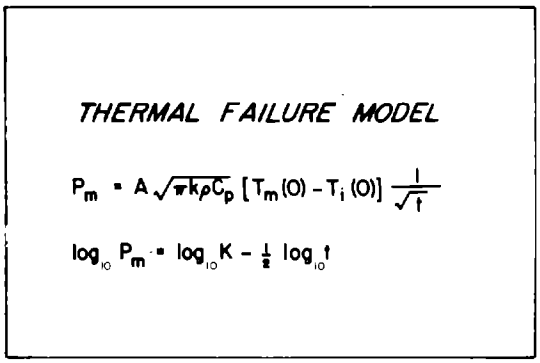

This model allows for determing the peak pulse power as a function of pulse duration if the junction parameters and failure temperature of the junction are known. The theoretical failure curve shown is for a silicon junction with the failure temperature of 675^{o} assumed.

THEORETICAL FAILURE CURVES FOR SILICON JUNCTIONS FOR REVERSE VOLTAGE MODE

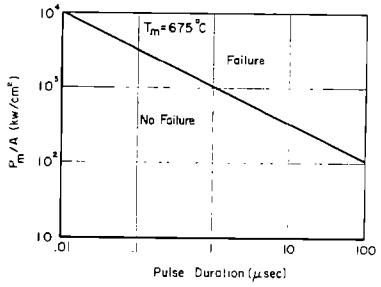

The exact value of the final temperature at which component failure occurs is open to question. Usually, 675° is considered as the temperature at which silicon ceases to be intrinsic. That is, at this temperature, diffusion of impurity atoms across the junction can be expected which tends to nullify junction action. In general, the exact temperature is a function of the doping level and other factors. The melting temperature (1415°C) of silicon, of course, leaves no doubt as to junction destruction. Generally, it would be expected that significant junction degradation occurs before the melting point is reached.

Another problem encountered in attempting to correlate experimental data with the theoretical model, results from the fact that under reverse bias conditions, the current density across the plane of the junction is not uniform. Constriction of the current to a few (hot spot) sites effectively reduces the available junction area. Calculation of the reduced area is beyond the capabilities of a reasonably simple analytical model. Partial experimental results yield an average effective junction area reduction of 20 to 30 percent for some components. A curve for a 10% effective area is shown in the figure with a corresponding reduction in the required failure power density by a factor of ten. Most experimental data appears to be bracketed by these theoretical curves. Typical data is shown for both diodes and transistors in the accompanying figures.

REVERSE VOLTAGE FAILURE CURVES FOR SILICON BASED ON TOTAL ENERGY DELIVERED TO THE JUNCTION

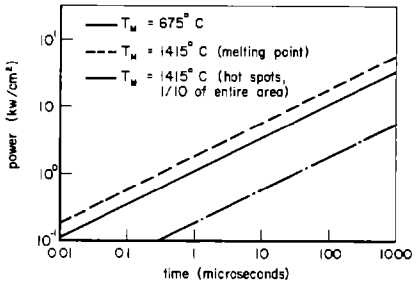

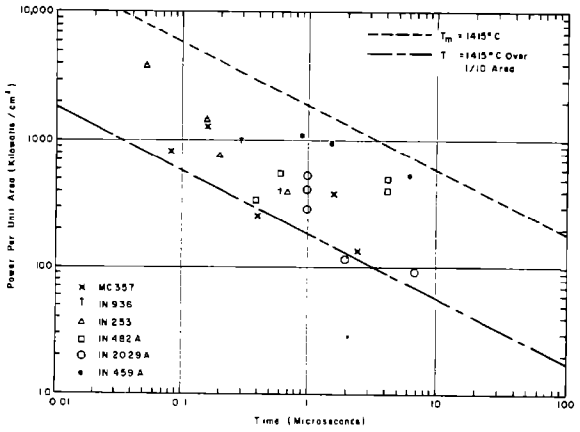

EXPERIMENTAL DATA FOR DIODES

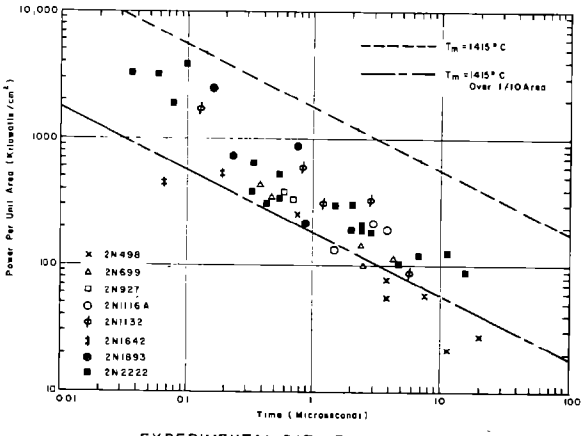

EXPERIMENTAL DATA FOR TRANSISTORS.

The discussion up to this point is for applied pulses with durations between 100 ns and 1ms. In this case, the cause of junction failure is due to localized heating with the heat source at the junction. Using the one dimensional heat flow equation results in the $t^{-\frac{1}{2}}$ relationship as shown. For shorter or longer pulses, the one dimensional heat flow equation and the plane heat source at the junction do not apply.

For short pulse widths (<100 Ns), a constant energy condition independent of pulse width prevails for the initiation of junction failure. From physical considerations, this is the required energy input to a volume of material (the current constriction site) in order for that volume to achieve an increase in temperature under adiabatic conditions. A one-half power of time dependence is obtained for longer pulse widths, which is indicative of heat loss from the (constriction site) volume to its surrounding medium. The direct time dependence for energy found at the longer pulse widths (signifying a constant power input) is indicative of thermal equilibrium resulting in a steady-state temperature at the center of the volume. This constant power level approaches the manufacturer's CW rating for the device as the pulse width becomes very large (>1 ms).

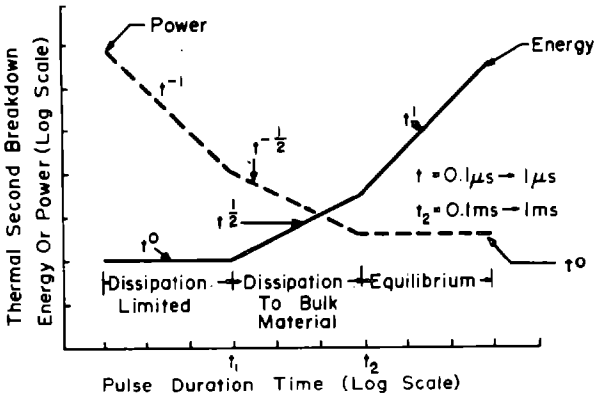

TYPICAL FAILURE LEVEL RELATIONSHIPS FOR THERMAL SECOND BREAKDOWN IN SEMICONDUCTOR JUNCTIONS

For failure due to surface breakdown, no τ dependence results and the failure level is dependent only on the pulse power, or equivalently, the failure level is power or voltage-dependent and not energy-dependent. For example, the failure of microwave diodes for 2-20 nanosecond pulses has been found to be dependent on peak power rather than energy.

Other devices have also been found to be voltage sensitive. This voltage sensitivity seems to occur sometimes across the surface, i.e., surface flashover; and for higher voltage pulses by punchthrough. This voltage sensitivity is a rise-time effect and can occur in some devices with a longer pulse (>30 nanoseconds) provided that the mechanism responsible for the voltage sensitivity occurs before any other effect, viz., thermal failure.

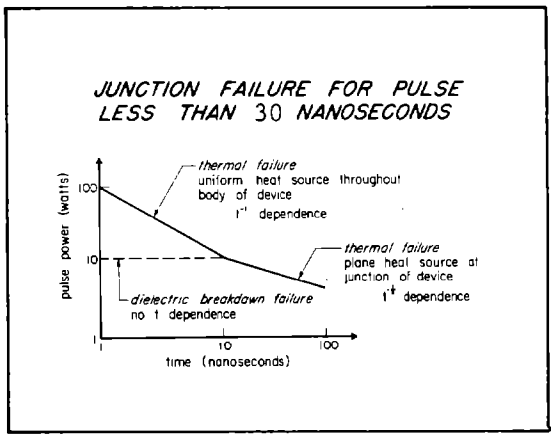

Verification of Wunsch Thermal Model

A number of semiconductor devices (primarily diodes and transistors) have been experimentally tested at various laboratories. Empirical relationships have been derived from the experimental data for the component burnout energy or power as a function of pulse width. It has been shown experimentally that the proportionality between energy or power for component burnout varies as a function of incident pulse width as shown previously.

Typical of data obtained, is the following curve for the 2N2222 transistor showing the single pulse failure power. The change in slope of the best straight line fit to the experimental data for the shorter width pulses is evident.

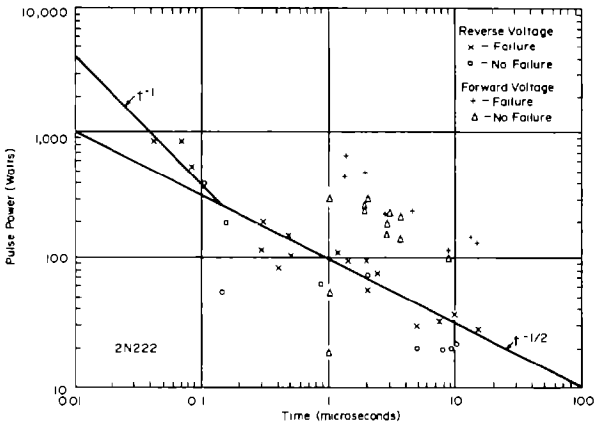

FAILURE OF THE BASE-EMITTER JUNCTION OF A 2N22 TRANSISTER FOR FORWARD AND REVERSE POLARITY VOLTAGE PULSES

Similar data have been obtained for other semiconductor devices by a number of experimentalists. In general, it has been found that the required power level for failure is approximately proportional to the device junction area for areas of up to 10^{-2} to 10^{-1} cm^2. (For larger areas, the failure level becomes more area independent). Because of this proportionality, it has become commonplace to plot power-to-failure per unit-of-junction area versus pulse width. This normalization of the power failure curve allows the convenient comparison of data for more than one device type on one graph.

The general relationship between threshold failure power as a function of pulse width may be considerably more complicated than indicated by the theoretical model. In general this relationship can be obtained experimentally and expressed in the form

$$P_{TH} = At^{-B}$$

where A and B are determined by a least squares fit to the data. Much of the data fits the Wunsch model (B = ½) for simple junction devices fairly well (i.e., within the experimental data spread of approximately 1 order of magnitude).

For pulse widths less than on the order of 100 nsec, the preceding relationship (B = ½) between power failure level and the pulse width does not hold. In this regime, uniform heating of the semiconductor bulk material takes place leading to a modification of the power failure relationship to

$$P \simeq C\, t^{-1} \text{ watts}$$

This form of relationship is plotted in the following figures for 2N336 and 2N2222 transistors, respectively. Two curves with slope proportional to t^{-1} are drawn for comparison with the trend of the experimental data points. These are the $P = C_1 t^{-1}$ curve whose intercept point has been adjusted so as to intersect the $P = Kt^{-\frac{1}{2}}$ curve at t = 1 μsec and the $P = C_2 t^{-1}$ curve which intersects at t = 100 nsec. Inspection of the curves shows that the best fit to the data occurs for different intercept point curves for each device type. In general, the optimum intercept point is a function of device thickness and will tend to move to larger time values for the larger devices.

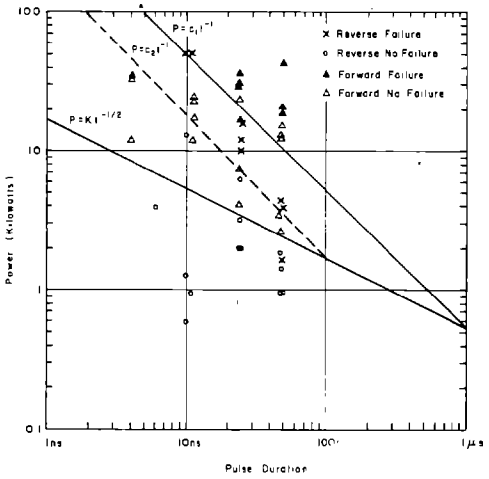

EXPERIMENTAL DATA FOR BASE EMITTER JUNCTION FAILURE OF A 2N336 TRANSISTOR

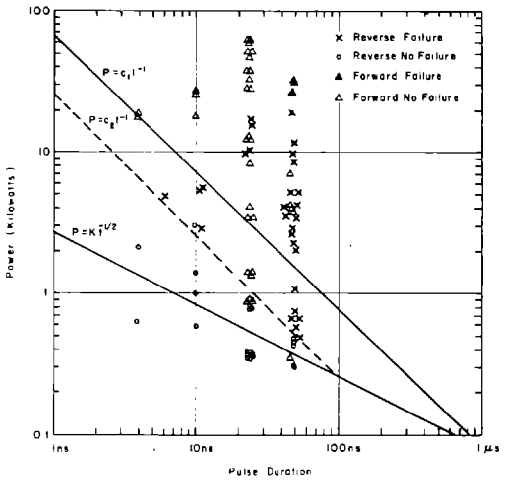

EXPERIMENTAL DATA FOR BASE EMITTER JUNCTION FAILURE OF A 2N2222 TRANSISTOR

The Damage Constant - K

The power failure threshold (P_{TH}) is different for different classes of devices and devices within a class. The power failure threshold P_{TH} is defined as

$$P_{TH} = At^{-B}$$

where

A = damage constant based on the device material and geometry

B = time dependence constant.

The constants A and B may be determined empirically for every device of interest by the least squares curve fit to the data. The theoretical model, however, has a time dependence constant of B = ½. In the mid-range of pulse widths, say from approximately 100 ns to 100 μs, the empirical data for a wide range of devices fits the model within the experimental data spread. In order to be able to directly compare device susceptibility for various pulse widths, and since the data fit fairly well, they are fit to the theoretical equation:

$$P_{TH} = Kt^{-\frac{1}{2}} \text{ Kw/Cm}^2$$

where

t = the pulse width in microseconds

K = the Wunsch model damage constant in kW-(microsecond)$^{\frac{1}{2}}$

It is convenient to express K in these units since the numerical value of K is then equal to the power necessary for failure when a one microsecond pulse is applied to the junction.

In adapting the model for diodes and transistors, Wunsch used experimental data for similar type devices with known junction areas to obtain the best curve fit. The results were:

For diodes:

$$\frac{P_{TH}}{A} = 550\ t_o^{-\frac{1}{2}};\ \text{or } K = 550A$$

For transistors:

$$\frac{P_{TH}}{A} = 470\ t_o^{-\frac{1}{2}};\ \text{or } K = 470A$$

Knowing the junction area, therefore, provides the value for the damage constant, K. Typical range for K for various semiconductors are shown in the following figures. Multiplication of this factor by $t^{-\frac{1}{2}}$ will yield the pulse power threshold.

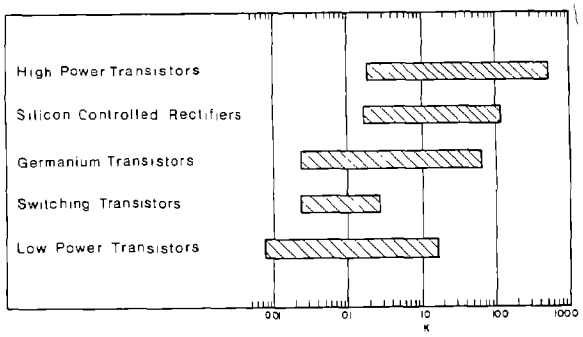

RANGE OF PULSE POWER DAMAGE CONSTANTS FOR REPRESENTATIVE TRANSISTORS AND SCR'S

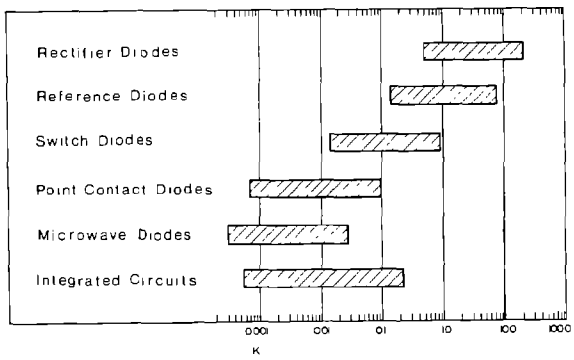

RANGE OF PULSE POWER DAMAGE CONSTANTS FOR REPRESENTATIVE SEMICONDUCTORS

The actual value of K for a specific device may be found, of course, experimentally. Data on some specific diodes and transistors are presented in the tables.

DAMAGE CONSTANTS
DIODES

Type	K	Type	K
IN547	12.1	IN914	0.85
IN625	0.164	IN936	0.14
IN625A	0.045	IN936A,B	7.0
IN645	2.8	IN968B-979B	1
IN660	0.44	IN1200, 1201	62.32
IN662	0.29	IN1317A	0.19
IN689	1.1	IN2808	249
IN702	1	IN2970B	15.0
IN709	0.78	IN3017B	1.9
IN719A	0.1	IN3064	0.02
IN746A-IN752A	1.1	IN3821	1.947
IN754A-IN758A	0.63	IN3976	132
IN761,2,3	1.8	IN4370A	0.625
IN821	0.577	IN4823	0.208
IN823	1.8	D4330	0.001

DAMAGE CONSTANTS
TRANSISTORS

Type	K	Type	K
2N43,A	0.28	2N1480	5.5
2N43,244	0.05	2N1481	2.2
2N274	0.0076	2N1564	0.56
2N339	2.0	2N1602	0.40
2N404	0.05	2N1701	4.5
2N424A	10.0	2N1890	0.27
2N525	0.3	2N1916W	2.22
2N656	0.2	2N2035	3.633
2N687	11.7	2N2218A	0.264
2N717	0.13	2N2219	0.3
2N910	0.218	2N2219A	0.264
2N1039	1.4	2N2222,A	0.1
2N1154	21	2N2223,A	0.21
2N1212	13.129	2N3819	0.22
2N1309	0.087	2N3907	0.165

It should be noted that with a reasonable accuracy, it is possible to calculate the value of K from procedures based on a knowledge of either the semiconductor junction area, its thermal resistance, or junction capacitance. Discussions of these procedures are available in other references. The utility of these procedures lies in the fact that one or more of these junction parameters are normally available from manufacturer's data sheets.

It is interesting to note the relation between the susceptibility (damage) constant K and the dc power dissipation capability for various devices. As can be seen from these curves, there is a direct correlation between the dc power dissipation and the damage constant.

RELATION BETWEEN SUSCEPTIBILITY CONSTANT AND DC POWER DISSIPATION CAPABILITY: TRANSISTORS

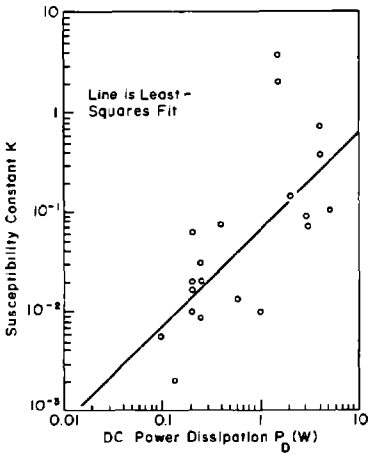

RELATION BETWEEN SUSCEPTIBILITY CONSTANT AND DC POWER DISSIPATION CAPABILITY: DIODES AND INTEGRATED CIRCUITS

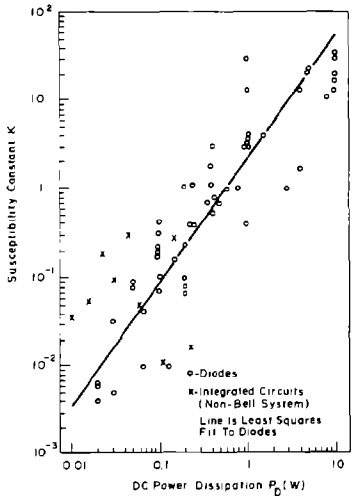

Effect of Multiple Pulses

When a system is exposed to EMP, the components of that system will normally experience a transient that has a damped sinusoidal waveshape. This waveshape may be approximated in the laboratory by a series of single pulses to investigate the cumulative effects with or without a cooling period between the pulses.

The actual input power level at which a junction fails does not seem to decrease significantly with multiple exposure. This is illustrated for the case of the failure threshold for a 2N2222 transistor as a result of single, double, and triple pulse exposure. The interval between pulses was short enough that no junction cooling would take place between pulses. The energy in deriving these curves (double and triple pulse) which results in increasing the junction temperature was estimated as 2 and 3 times the single pulse energy.

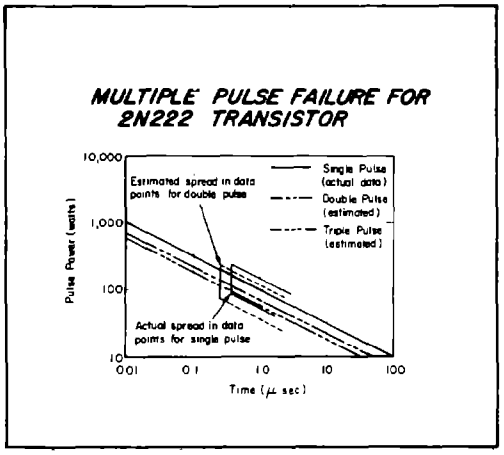

It can be seen that the difference between single-pulse and triple-pulse failure thresholds is less than the experimental spread in data points for single-pulse failure. Hence, failure thresholds which are determined from single-pulse tests are usually adequate approximations for assessing the vulnerability of semiconductors to EMP.

The previous discussion was concerned with the heating effect of multiple pulses affecting the damage threshold level. Next, the cumulative effects of repeatedly pulsing a transistor at and below the damage threshold respectively will be considered. In this case, the pulses are far enough apart so that cumulative heating effects are negligible.

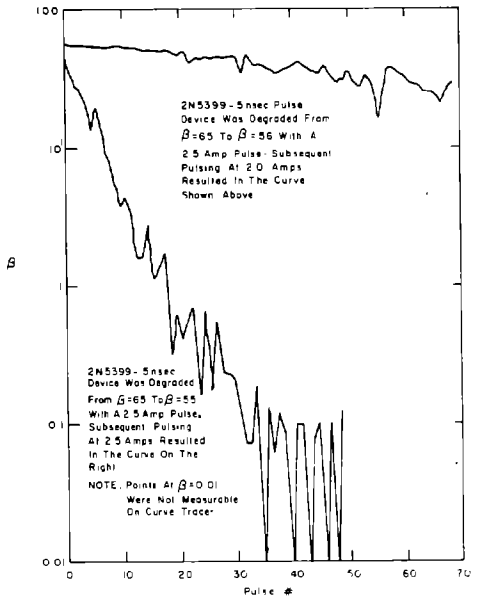

GAIN DEGRADATION FROM CURRENT PULSES FOR TWO CONDITIONS

The figure presents the results of multiple pulsing of a transistor for two different conditions. In each case, the initial pulse applied exceeded the degradation threshold of the transistor resulting in a reduction of the transistor β from 65 to 56. In the lower curve, this same pulse level was utilized for all subsequent pulses. The curve shows that the transistor gain increases and decreases erratically with each subsequent pulse. This indicates that multiple conducting filaments are probably formed across the junction when the device is damaged and subsequent pulses either add to the number of these filaments thus further decreasing the gain, or they cause a re-opening of existing filaments thereby producing an increase in gain.

The upper curve was obtained by pulsing the device at 0.8 times the damage threshold after the initial pulse degradation as in the previous case. Continued degradation occurs for each subsequent pulse. Comparison of the two curves indicates that reducing the amplitude of the applied pulses after damage initiation merely reduces the rate at which additional damage occurs.

Integrated Circuit Failure

Integrated circuits (IC's) employ a large number of junctions on a single clip. Depending on the type of IC, it is possible that the state of the logic (digital logic circuit) voltage at one input will affect the burnout level when a pulse is applied to another input. This was investigated in the case of the MC715 circuit. It was determined for this particular device that the gates fail independently and the state of the logic voltage at the other inputs did not affect the burnout level. This device has isolated transistors forming the 3-input gate. This would not necessarily be true if the input circuits were not isolated.

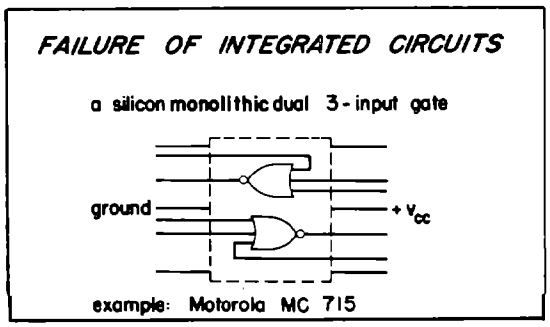

The input and output leads of an IC are more susceptible to transient damage than the positive battery lead. This is not an unexpected result since a transient entering via the positive battery lead would be distributed over a number of P-N junctions in the device.

The pulse power required for damage of an MC 355 G integrated circuit (B-E junction) is shown in the following figure. The line is the thermal failure model curve with a slope of -1/2 fit to the data. As in the case of discrete devices, for pulse widths between 0.1 and 10 microseconds, the thermal failure model is appropriate.

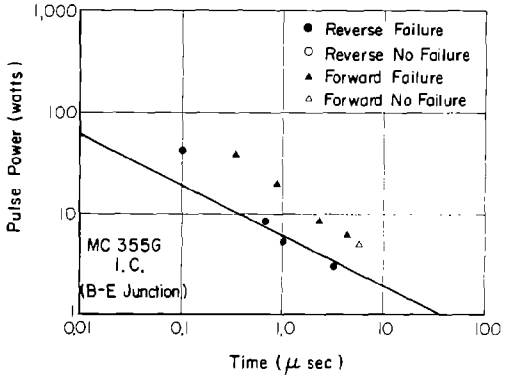

The following table shows the experimental power failure threshold for 15 devices when exposed to a 1 μsec pulse. Data are given for the input lead, output lead, and battery lead. The minimum power for damage on any lead is the controlling threshold value and may be defined as the failure threshold power. On this basis, a K value can be assigned and for the devices indicated ranges from 1.1×10^{-2} to 5.0×10^{-1}. These K values are within an order of magnitude of those for diodes with the same dc power dissipation capability.

INTEGRATED CIRCUITS EXPERIMENTAL DAMAGE POWERS*

DEVICE	TYPE	EXPERIMENTAL FAILURE POWER (W)		
		INPUT LEAD	OUTPUT LEAD	BATTERY LEAD
Fairchild 9930	Dual 4-input gate	230	92	210
Signetics SE 8481	Quad 2-input Nand gate	72	87	390
T. I. 946	Quad 2-input Nand gate	15	20	275
Sylvania SG 140	Quad 2-input Nand gate	54	67	210
Motorola MC 301G	5-input gate	640	300	1400
Radiation, Inc. 709R	Operational amplifier	15	18	65
Motorola MC 1539G	Operational amplifier	280	4600	1700
T. I. 709L	Operational amplifier	500	3600	2650
Radiation, Inc. RD211†	Dual quad-diode gate expander	20	20	--
Radiation, Inc. RD220†	Hex inverter (digital)	35	135	340
Radiation, Inc. RD221†	Dual binary gate	270	180	690
Radiation, Inc. RA239†	Amplifier (analog)	—	50	66
Philbrick Q25AH†	Hybrid amplifier	200	16	320
Philbrick Q25AH†	Hybrid amplifier	100	2000	1000
Fairchild μA709	Operational amplifier	11	30	—

*Applied pulse of 1-μs duration

†Normalized to 1-μs pulse (original data for 0.1 μs)

Interconnection Failure Modes

The vulnerability of device leads, metalization patterns and lead bonds, for the most part, can be considered as a thermal problem. In this case, the problem reduces to that of considering heat dissipation due to system thermal conductivity up to its melting point, together with an assessment of the dynamic stress conditions produced at material discontinuities. In general, one would expect that at least the leads and metalization patterns should exhibit a fairly uniform current density throughout their material cross sections for relatively moderate pulse widths as compared to the current constriction sites in semiconductor junctions which can be altered by defect and bias conditions. For relatively short pulses, such a phenomenon as "skin effect" would, of course, alter the cross sectional current density in such a way as to produce a "peripheral current constriction" condition. These effects, though, are fairly well defined and can be considered in a rather straightforward manner. The lead bonds and any multi-metal metalization patterns can also be considered in somewhat the same fashion. However, bond interface impedance, possible current constriction sites, and hydrodynamic pressure pulses due to interface discontinuities may also have to be considered. In general, it is observed that the vulnerability of the interconnection system usually occurs at current levels in excess of those required to cause significant junction damage in typical semiconductor devices at hundred nanosecond pulse widths.

Typical EMP pulse type experimental data is shown in the following figure. This type of data is in direct contrast with data obtained when a component is exposed to high frequency RF pulses as in the case of testing done to ascertain the hazards to ordnance from electromagnetic radiation (HERO). In this case, much of the energy is shunted around the junction due to its capacitance, and the incipient degradation in most cases is due to lead melting.

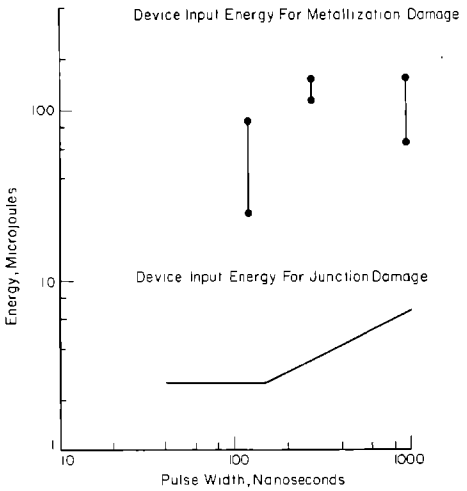

EXPERIMENTAL INPUT ENERGY FOR JUNCTION AND METALLIZATION DAMAGE – RD 211 MICROCIRCUIT

An analytical model and the use of the model are presented in other references.

Synergistic Effects

An additional area of concern in the case of semiconductor failure has been that of synergism between the electrical overstress due to an EMP and the gamma ionizing dose rate ($\dot{\gamma}$). While exhaustive studies of synergism have not been conducted, four independent and reliable investigations have shown no evidence, or only weak evidence, of synergistic effects in discrete semiconductors or IC's.

In the case of complete systems, however, the $\dot{\gamma}$ triggering a circuit into conduction can permit damage due to electrical pulses.

SYNERGISM

COMPONENT LEVEL

THREE INDEPENDENT AND RELIABLE INVESTIGATORS HAVE SEEN NO EVIDENCE OF SYNERGISM BETWEEN ELECTRICAL OVERSTRESS PULSES AND $\dot{\gamma}$

VAULT (HDC) - INVESTIGATIONS ON IC'S SHOWED NO MORE THAN A FACTOR OF 2 DIFFERENCE IN INDIVIDUAL ENVIRONMENT FAILURE LEVELS AND COMBINED ENVIRONMENT FAILURE LEVELS

BUDENSTEIN (AUBURN) - INVESTIGATIONS ON SOS DIODES SHOW $\dot{\gamma}$ COOLS A JUNCTION APPROACHING HOT SPOT NUCLEATION

RAYMOND (NORTHROP-MRC) - EXTREMELY WEAK EVIDENCE OF SYNERGISM IN IC'S

HABING (SANDIA LABS) - REALISTIC ENVIRONMENT TEST SHOWED NO SYNERGISM EFFECT WITHIN A FACTOR OF 2 OR LESS

SYSTEM LEVEL

IONIZING RADIATION CAN TRIGGER CONDUCTION WHICH PERMITS ELECTRICAL PULSES TO CAUSE BURNOUT

SUBJECT TO DESIGN RULE DOCUMENTATION

Resistor Failure

Resistive elements in the form of either lumped resistors or diffused resistors often are the terminating element for long cables. Consequently, information on the way these devices fail and typical failure levels are important. Tests have been conducted on wire wound, metal film, carbon composition and diffused resistors. The failure levels vary with number of pulses, duty cycle, and power or voltage. Conventional ratings indicate that for pulse applications, the pulse power rating is 10 times the dc power rating and the voltage rating is 1000 volts per inch. For low duty cycle, as in the case of EMP, these are far too conservative.

Failure Modes

Four types of failure have been found. These are:

1. Resistance value change - failure is defined as a change in value beyond normal tolerance. The importance of this change is dependent on the circuit function. This mode of failure can be due to thermal effects (energy dissipation) or voltage stress induced.

2. Internal breakdown - this breakdown occurred when the resistor under test opened but did not blow apart or no external evidence of arcing was present. This was due to thermal dissipation with the device.

3. Arc across resistor casing - this type of breakdown was exemplified by an arc across the external surface of the resistor. No damage to the resistor resulted from this failure.

4. Catastrophic breakdown - this type of breakdown occurs when an external arc starts across the resistor, but due to some defect in the ceramic casing, re-enters the core. The pulse energy is then dissipated in only a small fraction of the resistor and causes the casing to rupture (blow off) and the resistor to open.

All of these failure modes have been seen in the resistor tests. To define a safe working voltage level for the resistor, it was given as the level where the resistance did not change as a result of the applied pulses. These data are reported in the next paragraphs.

Resistor Construction

The construction technique plays an important role in the failure mechanisms or level for resistors. Typical resistor constructions are shown in the following figure.

CROSS SECTION OF RESISTOR CLASSES

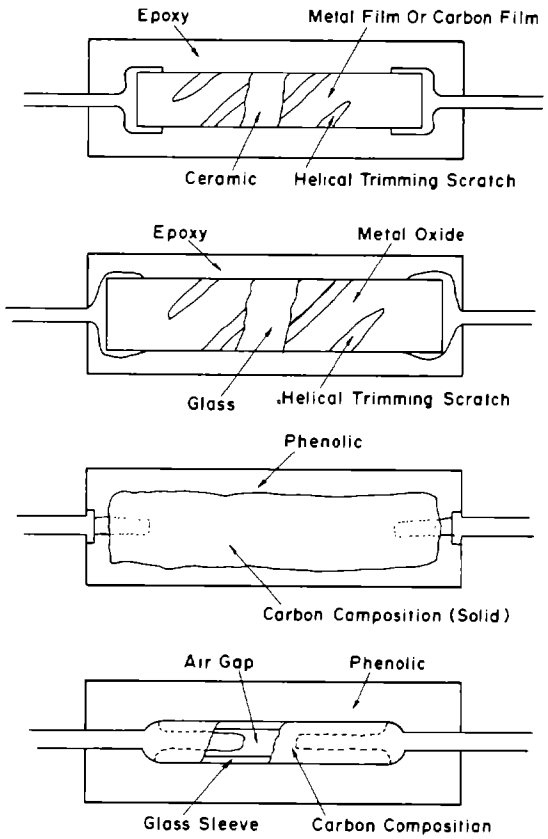

Metal film, carbon film, and metal oxide resistors are constructed with the film deposited, or the oxide grown on a glass or ceramic substrate. The thickness of the film or oxide layer determine the minimum resistance value of the resistor. To increase the resistance, spiral cuts are made in the film to increase the total path length of the current. A very limited family of film thickness is used to cover many decades of resistance value. Spiraling of the film results in uneven voltage distribution across the resistor body which results in voltage breakdown at lower levels than would normally be expected. This breakdown normally occurs at the ends of the spiral where the voltage gradients are highest. The voltage distribution for a typical spiraled film resistor is shown in the following figure.

EQUIPOTENTIAL LINES AND FLOW LINES IN THE RESISTIVE LAYER OF A SPIRALLED FILM RESISTOR. THE NUMBERS REFER TO POTENTIALS (REF 3:14)

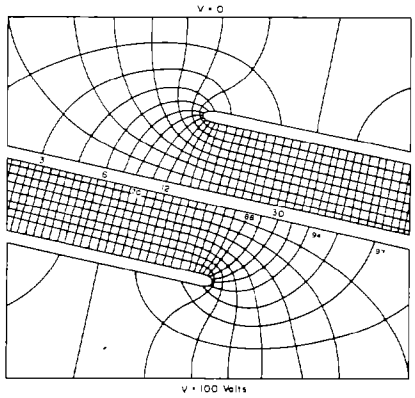

In the case of carbon composition resistors, the entire body of the device is the resistance material, the conductivity of which determines the resistance value and the volume of the power dissipation. The failure level in this type is strongly influenced by the geometry of the lead connection to the body since this determines the current distribution and voltage gradient at the interconnection. Large contact area, that is, expanding the lead at the connection point, results in the maximum useful carbon volume and the minimum voltage gradient.

The composition resistor shown at the bottom of the previous figure utilizes a carbon composition material on a hollow glass substrate. The terminating ends of the lead connections are in the resulting air gap. These type resistors exhibit voltage breakdown in the air gap with no ultimate effects on the resistor.

Resistor Failure Threshold

The susceptibility of resistors can be categorized by resistor type. The data are very consistent for the same manufacturer. Variations between manufacturers is usually due to the geometry of lead connections and construction variations. The susceptibility ranking for metal film and metal oxide resistors is almost equal.

RESISTOR SUSCEPTIBILITY

- Wire Wound ---------- Hardest
- Carbon Composition
- Carbon Film
- Metal Film
- Metal Oxide ---------- Softest

The resistor failure data for all types, with the exception of the wire wound resistors, indicate energy dependence (i.e., adiabatic heating, $t^{-\frac{1}{2}}$) for pulse widths between approximately 100 nanoseconds and 50 microseconds (or greater). This range of pulse widths covers the EMP induced transients anticipated, so for EMP damage thermal failure is usually the normal mode.

Carbon Composition Resistors

For carbon composition resistors, the failure power is proportional to the device rated power. For low wattage rated resistors (< 1 watt) the failure power is directly proportional. Above 1 watt, the failure power does not double as the rated power is doubled. This is due to some nonuseful carbon volume for pulsed signals due to lead connection techniques. The failure mode for thermal failure is a melt (melt fingers being formed) at the boundary between the interconnecting wire and the bulk material. At shorter pulse widths (less than 100 ns) the failure mode is voltage dependent in that surface or internal arcing occurs. This is usually seen as a sharp fracture in the bulk material.

CARBON COMPOSITION RESISTOR FAILURE MODELING

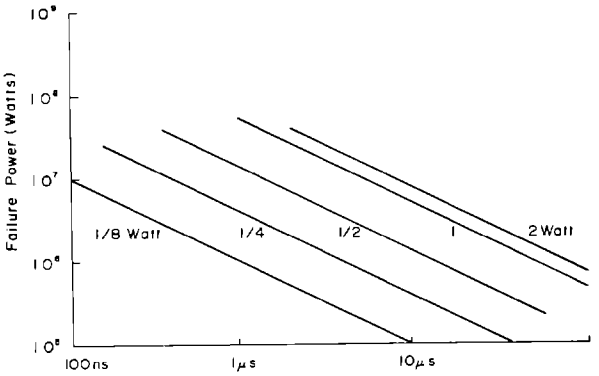

Film Resistors

Film resistor failure breaks from the adiabatic curve ($t^{-\frac{1}{2}}$) at pulse widths between 10 and 50 microseconds. The coating type (metal, metal oxide or carbon) and technique change the thermal properties of the film and, consequently, its failure level. For damage defined as a change in initial resistance, carbon film resistor damage (%ΔR) increases monotonically with pulse power and pulse width (energy). For a given damage level (%ΔR) the pulse power for failure decreases monotonically with pulse width.

RESISTOR DAMAGE EXTENT AS A FUNCTION OF DAMAGE POWER AND PULSE WIDTH FOR DALE MC 1/4 (0.25 WATTS) 49.9 OHM CARBON FILM RESISTORS

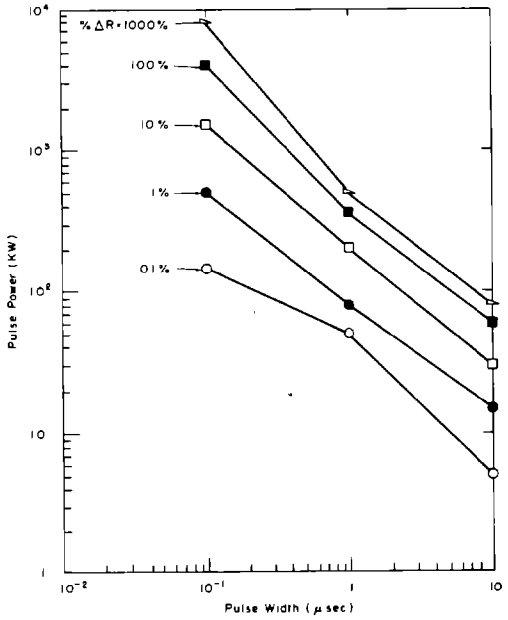

The pulse power required for a given damage level (10% Δ R) is also a function of the initial resistance of the resistor. The damage power decreases monotonically as resistance value increases from 3 ohms to 200 ohms. It then increases for an initial resistance value of 806 ohms. The 3 to 200 ohms resistors had the same film thickness, the resistance value being determined by the amount of spiraling. The 806 ohm resistor was a different film thickness (thinner to increase the resistance) with less spiraling to achieve the final resistance value. It is apparent that the greater the amount of spiraling required to achieve the final resistance value, the lower the failure threshold. This is because of the greater current concentrations due to the spiraling.

DAMAGE POWER DEPENDENCE ON PULSE WIDTH AND INITIAL RESISTANCE VALUE FOR DALE MC 1/10 (0.1 WATTS) CARBON FILM RESISTORS

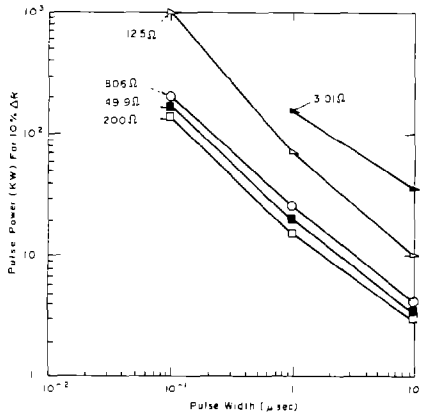

The metal film and metal oxide resistors exhibit lower failure thresholds than the carbon film or composition resistors. The failure power for metal film, metal oxide, and carbon composition resistors is shown in the following figure.

DAMAGE POWER DEPENDENCE ON PULSE WIDTH

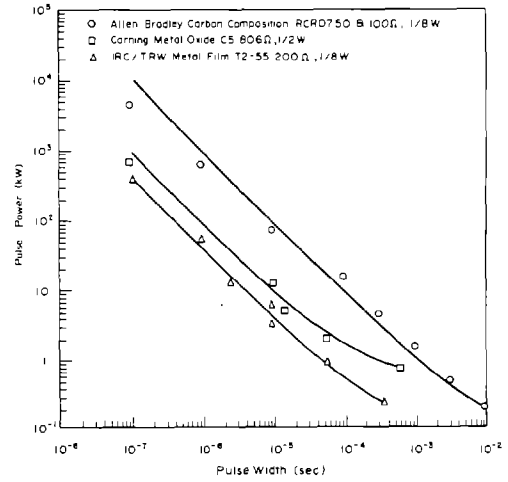

The failure threshold of the metal oxide resistor appears to be higher than for the metal film resistor. Note that the metal film and carbon composition resistors are both 1/8 watt rating while the metal oxide has a 1/2 watt rating.

Diffused Resistors

The failure thresholds for diffused resistors is of the same order of magnitude as for metal film and metal oxide resistors. The failure threshold is energy dependent (adiabatic heating) following a $t^{-\frac{1}{2}}$ slope for pulse widths between 10 microseconds and 0.1 seconds. For pulse widths below 10 microseconds, the failure threshold curve follows a t^{-1} slope.

THERMAL FAILURE IN DIFFUSED RESISTORS

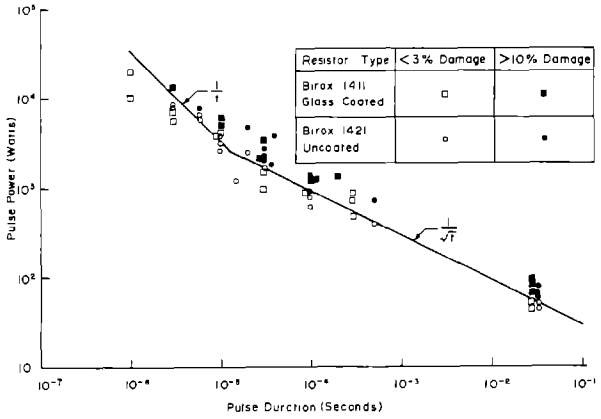

Short Pulse Width Failure

For pulse widths less than approximately 100 nanoseconds, the failure (Δ R) is voltage dependent. This results from the extremely high voltages required to deliver sufficient energy for thermal failure for short pulse widths. This type of failure may be seen in all types of resistors, but is most prevalent in wire wound and film resistors. In carbon composition resistors, the failure is usually surface breakdown. In wire wound or film types, the arcing occurs between turns or across the boundary between spirals. It is manifest in the form of an immediate reduction in the resistor pulse impedance as shown.

VOLTAGE LEVEL EFFECTS ON RESISTOR PULSE IMPEDANCE

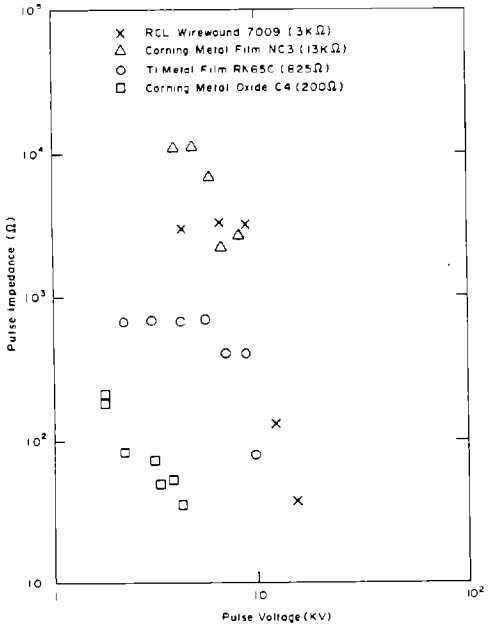

Summary of Resistor Failure Thresholds

A summary of measured resistor failure thresholds is presented in the following figure. Since the data were obtained using 1 microsecond pulses, the power indicated for failure can be equated to a damage constant (K) as for semiconductors. An assigned K value for this pulse width would be numerically equal to the power in kilowatts (i.e., for a threshold of 1 kW, k = 1).

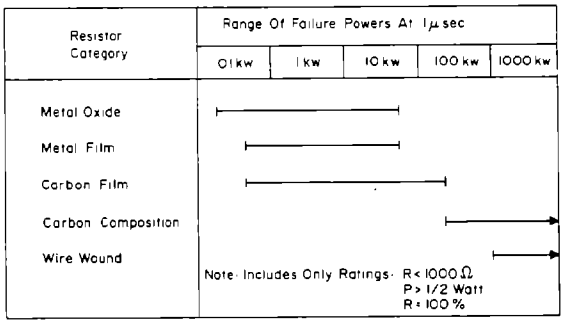

RANGE OF RESISTOR FAILURE POWER

Resistor Failure Thresholds Based on Safe Operating Voltage

The maximum safe pulse voltage for various types of resistors as a function of the resistance value, with the wattage rating as a parameter are presented in the following figures. The average pulse power in no case exceeded the dc power rating for the resistor. The pulse duration used for obtaining these data was 20 μsec.

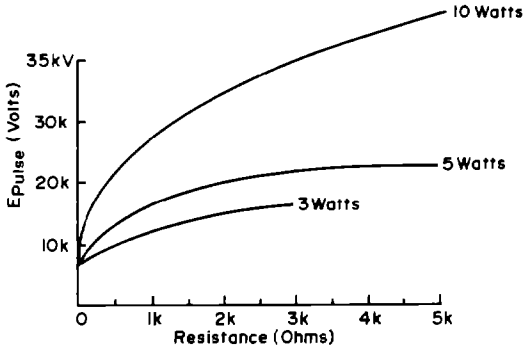

WIRE-WOUND RESISTORS

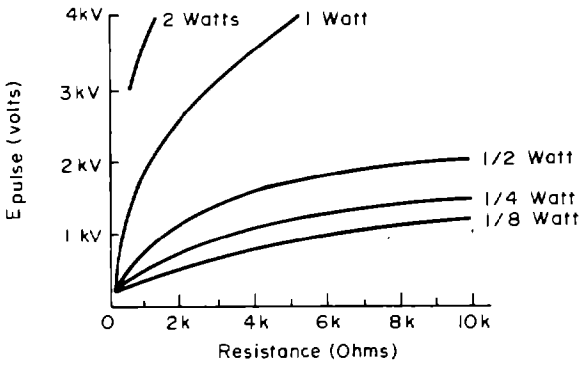

METAL FILM RESISTORS

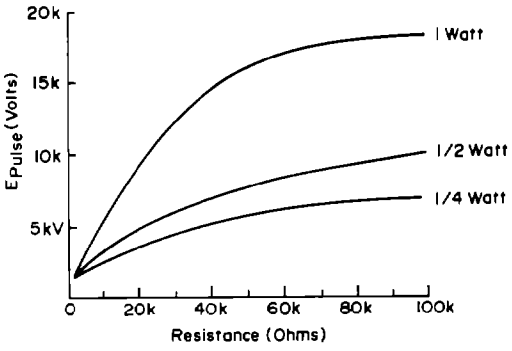

CARBON-COMPOSITION RESISTORS

The pulse power rating is approximately 5000 times the dc rating for wire wound resistors, 1000 times the dc rating for metal film resistors, and 500 times the dc rating for carbon composition resistors. The pulse power rating for these devices can be determined approximately from

$$P_p = \frac{E_p^2 \text{ (volts)}}{R\ (\Omega)} \text{ watts}$$

It should be noted that for carbon composition and metal film resistors of low resistance value and low wattage rating, failure can occur at voltages of a few hundred volts on a single pulse basis. This failure level is further reduced for multiple pulses or increased pulse duration.

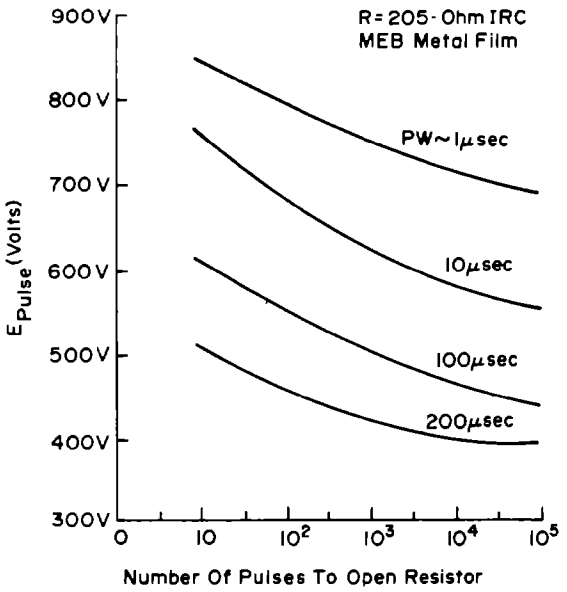

PULSE WIDTH VS MAXIMUM PULSE VOLTAGE

Capacitor Failure

Tests on capacitors have been limited in types of studies and component sample size because they have been considered to be much harder than other electronic components such as semiconductors and thin film resistors. These limited studies have indicated that some capacitor types fail at levels as low as those seen for semiconductors. Therefore, consideration should be given to the failure levels of these components because if the semiconductors in the circuit are protected, the nonsemiconductor components may determine the resulting EMP vulnerability.

Failure Modes

The basic failure mechanism in capacitors is internal (dielectric) breakdown. The parameter that has been found to change is the dissipation factor (D) due to a change in the leakage resistance (R). This relationship is given by

$$D = \frac{\omega C}{R}$$

For ceramic type capacitors this breakdown is very abrupt. The amount of post breakdown degradation was related to the energy dissipated in the capacitor during breakdown. The breakdown voltage was lowered after the initial breakdown occurred (i.e., for subsequent pulses). In some cases (manufacturers' types), no evidence of changes in the capacitor parameter was seen; whereas in other cases, the dissipation factor increased by a factor of 100.

The upper curve shows the characteristic breakdown of most types of capacitors. Once breakdown occurs (in capacitors such as paper or disc ceramics) it is usually sustained. The post breakdown degradation (that is any self healing ability, decrease in breakdown voltage, etc.) depends on the total breakdown energy. The exciting pulse was a double exponential waveform.

BASIC RESPONSE CHARACTERISTICS EXHIBITED BY CAPACITORS FOR SQUARE WAVE CURRENT PULSES

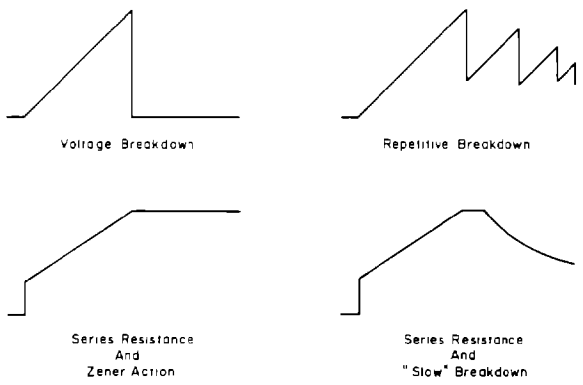

In the case of low voltage tantalum electrolytics, the breakdown characteristics are quite different. The breakdown in this case was a slower process as shown in the lower curves. The abrupt breakdown was not observed but the leakage resistance

decreased progressively until breakdown occurred. As the leakage current increases, dissipation in the device increases, the sustaining voltage decreases. In other tests, abrupt changes were seen but, in all cases, were preceded by large leakage currents. After breakdown shots, dissipation factors often rose by as much as a factor of 600, with the equivalent resistance dropping as low as 1.5 ohms.

Failure Thresholds

The voltage failure thresholds versus pulse rise time for ceramic, paper, glass, mica, and plastic are presented in the following figure. It is apparent from the data that their is only a slight voltage turn up for short (< 100 ns). The failure thresholds are many times (15 to 40) the rated working voltage of the capacitors and, therefore, are relatively hard to EMP induced transients.

PULSE RISE TIME EFFECTS ON VOLTAGE BREAKDOWN IN

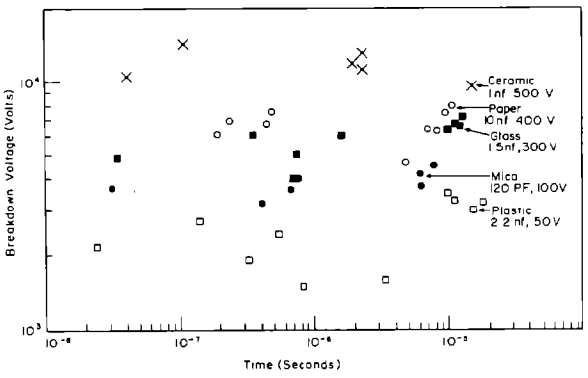

The damage to tantulum capacitors is generally seen as an increase in leakage current. As was seen in the breakdown waveforms, tantulum capacitors have a zener voltage (Vz) characteristic which is equal to the forming voltage (voltage at which oxide was formed). Breakdown occurs slowly (microseconds) when voltage exceeds the forming voltage. The increase in leakage current is a direct function of the total charge transferred during the incident pulse. The increase in leakage current at rated voltage as a function of total charge transferred is shown in the following figure.

LEAKAGE CURRENT DAMAGE IN TANTALUM FOIL ELECTROLYTIC CAPACITORS POSITIVE POLARITY PULSING

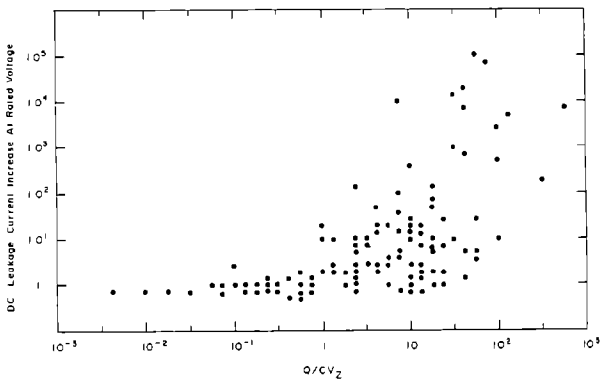

The forming voltage is always higher than the rated voltage. The forming voltage, however, is not a fixed percentage. For higher voltage units, it is a much smaller percentage than for low voltage units and, therefore, has a smaller safety margin. The forming voltage is not normally indicated on data sheets, but may be obtainable from the manufacturers. For the tantulum capacitors tested, the minimum breakdown voltage was approximately two (2) to three (3) times the rated voltage as indicated in the table.

SOLID TANTULUM ELECTROLYTIC CAPACITOR SPECIFICATIONS, TEST CONDITIONS, AND DETERMINED BREAKDOWN VOLTAGES

Sprague Device No	Polarity	Capacitance (μF)	Voltage (WVdc)	Breakdown Voltage			Pulse Width (μs)	Tested Devices (No)
				Mean (V)	Standard Deviation (V)	Minimum (V)		
472X9035A2	Forward	0.0047	35	155.0	43.1	90.0	2.6/4	19
225X9035B2	Forward	2.2	35				4.8/30	24
225X9015A2	Forward	2.2	15	143.0	48.7	68.0	3/30	17
472X9035A2	Reverse	0.0047	35	106.0	19.7	65.0	1/10	15
225X9015B2	Reverse	2.2	35				3/30	15
225X9015A2	Reverse	2.2	15	53.7	6.5	43.0	30	6

Low voltage tantulum capacitors can fail at energy levels comparable to those of semiconductor devices. The minimum energy levels at which failure was seen

for tantulum capacitors is shown along with typical failure energy levels for semiconductors in the figure.

TYPICAL ENERGY FAILURE LEVELS OF SEMICONDUCTORS COMPARED TO THE ENERGY REQUIRED TO DAMAGE LOW-VOLTAGE TANTALUM CAPACITORS

Component	Energy (μJ)
Point Contact Diode IN82A-2N69A	0.7 to 12
Integrated Circuit A709	10
Low-Power Transistor 2N930-2N1116A	20 to 1000
High-Power Transistor 2N1039 (Ger)	1000 and Up
Switching Diode IN914-IN933J	70 to 100
Zener Diode IN702A	1000 and Up
Rectifier IN537	500
Solid Tantalum Capacitor	61 and Up

The Semiconductor Data Were Based On A 1μs Damaging Pulse (From D. Tasca, Document No 70SD401, The General Electric Company (January 1970) And Unpublished Data By J R Miletta)

Inductive Elements

Inductive elements can fail in the way similar to capacitors and resistors whereby a temporary impairment such as an arc-over or saturation occurs such that the characteristics of the inductive elements are not impaired on a long-term basis. Similarly, a catastrophic failure can occur such as an arc-over and punch-through for the insulation similar to the capacitor insulation or semiconductor surface failures.

Studies to date on inductive elements per se have been quite limited owing to the relative hardness of these devices in comparison to the more susceptible semiconductors and passive thin film resistor elements.

Squibs and Detonators

Squibs and detonators can play an important role in the EMP susceptibility or vulnerability of a particular system. Typically, squibs and detonators are not only used to initiate the formation of a final explosive, but also to perform separation of stages in the initiation of rockets. In general, squibs and detonators can fail in two ways. First of all is the premature unwanted ignition of the pyrotechnical devices with obvious catastrophic implications. The other is dudding of the device such that after EMP exposure, the device no longer performs in a satisfactory manner.

Major emphasis in the past has been directed toward protecting the squibs and detonators from either dudding or unwanted pre-ignition from either static charges or energy picked up under microwave illumination conditions. The EMP failures of the device can occur when sufficient energy from EMP pickup is applied to one or both terminals of the pyrotechnical device. Typically, the two terminals of the device are fired via a balanced two-wire cabling system. Here, the differential mode pickup under EMP conditions may be somewhat lower than the common mode pickup. In the case of common mode pickup, one observed failure mode occurs when the arrangement is such that an arc-over can occur between one of the wires to ground and not the other. This, in effect, converts the common mode into a differential mode of sufficient magnitude to cause premature detonation. In other cases, arc-overs can occur within the case between the sensitive elements of the pyrotechnical device and the case.

EED's (electroexplosive devices) are the more sensitive to ignition requiring for the most sensitive devices only a few ergs. EBW's (exploding bridgewires) require considerably more energy, minimum energy values being on the order of five (5) millijoules. Bridgewire burnout always results in ignition of EED's but in the case of EBW's may only result in dudding the device.

Terminal Protective Devices

Terminal protective devices can also be damaged by electrical overstress or excess energy during conduction. These devices include zener type devices, gas tubes, spark gaps, thyristors, etc. As seen in the following table, the voltage failure level and associated pulse durations for typical TPD's are higher than the normally anticipated EMP induced transients. Failure of these devices, however, could possibly occur for very long transmission lines, large antennas, etc.

APPROXIMATE FAILURE LEVELS

DEVICE	V_B(V)	FAILURE LEVEL (V)	PULSE DURATION μS
LOW VOLTAGE ZENER	6.8	11,000	50/500
" " "	20	11,000	50/500
" " "	200	11,000/11,000	50/500
BIASED ZENER LIKE	20	3800	50
" " "	200	3800	50
GAS TUBE	300-500	3800	50
" "	500-900	3800	50
SPARK GAP	470	11,000	50/500
" "	2500	11,000	50/500
THYRISTOR	60	3800	50
"	50A	3800	50

Miscellaneous Devices

A comparison of the test results for a variety of devices is shown in the following table. As can be seen from these data, most of these devices are hard to the the normally anticipated EMP induced transients, although the potential for failure cannot be excluded in all cases.

These data are a summary of very limited test results since most of these devices have been considered to be inherently hard.

TEST RESULTS FOR MISCELLANEOUS COMPONENTS

	Component Type	Test Results	Comments
1	Spark Gaps - Rated 75V to 5kV	No failure 1500 amps, 160 joules	Hard to essentially all EMP trans ents
2	Magnetic Surge Arrestors - Rated 500V to 8kV	No failure to 1000amps, 160 joules	Hard to essentially all EMP transients
3	Neon Lamps Rated 55V to 110V	No failure to 1000 amps, 160 joules	Hard to essentially all EMP transients
4	Varistors		
	• MOV	No failure to 1000 amps, 160 joules, clamping voltage increase 1600 amps, 50 joules	Hard to essentially all EMP transients
	• Thyrite	Failure at 300 amps, 22 joules 10 amps, 50 joules	Possibly susceptible to very high signal levels
5	Relays, Motors, Transformers, Switches, and Potentiometers	No failure at kV 0 8 joule	Hard to at least 1 kV
6	Discrete Filters	Failure at 5kV, 0 8 joule	Hard to 5kV
7	Filter Pin Connectors	Leakage increases at 300V, 0 04 joule	Potentially susceptible at moderate levels (>300V)
8	Tubes	Degradation at 1kV, 0 8 joule	Potentially susceptible at levels > 1 kV
9	EED's	Activation at 2kV, 6 joules	Susceptible at levels > 2kV

5.4 CABLE AND CONNECTOR FAILURE

Other very important system components that may be functionally damaged by EMP induced transients are cables and connectors. This is particularly important for cables that are already electrically stressed such as transmitter output cables. The difference between the voltage applied to the cable by the transmitter and the voltage breakdown rating of the cable may be sufficiently small that EMP induced transients will cause breakdown of the insulation or air space in connectors.

TRANSMITTING SYSTEM CABLE WITH VOLTAGE APPLIED BY THE TRANSMITTER AND ANTENNA

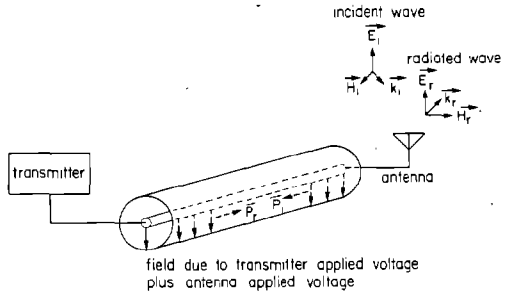

The breakdown strength of cable insulation may be limited by the dielectric strength of small imperfections in the insulation. Within the body of the cable, breakdown starts from a small air pocket. At first, discharges take place in the pocket. This produces local heating. The insulation melts and carbonizes and ultimate failure occurs, either through mechanical effects or due to a short-circuit produced by a carbonized track across the dielectric from one conductor to another. A mechanical effect that can occur is for distortion of the dielectric to occur resulting in the inner conductor becoming eccentric and touching the outer conductor.

The role of dielectric imperfection in producing cable breakdown is shown in the figure which portrays the cross sectional view of a coaxial cable at a site where an imperfection in the cable dielectric is assumed to exist. Here it is assumed that the insulator with a dielectric constant of ε_2 does not touch the center conductor due to a manufacturing defect. Hence, an air pocket with a dielectric constant of $\varepsilon_1 < \varepsilon_2$ exists around the center conductor. Due to the dissimilar dielectric constants, the electric field in the air pocket will be enhanced, thus causing an initial arc in the air and a subsequent breakdown in the insulating material.

ELECTRIC FIELD DUE TO TWO DIELECTRIC MATERIALS IN CONCENTRIC COAXIAL CABLE

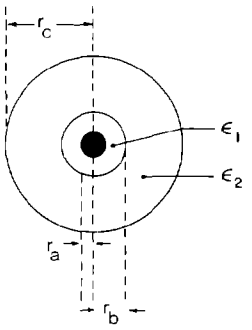

Cable connectors, in many instances, breakdown prior to cable failure. This is because of the inadvertent air paths that exist in many connectors due to the construction techniques. As in the case of cable failure, it is these air paths that result in breakdown.

5.5 OPERATIONAL UPSET MECHANISMS

As mentioned previously, operational upset is primarily a circuit or system problem. In general, it is not related to individual components comprising the circuit but rather depends on the circuit function, circuit operating levels (biases), the circuit type (digital or analog), and the nature of the waveform driving the circuit.

Operational upset can occur in both digital and analog circuits. In analog circuits an EMP transient may be amplified and interpreted as a control signal, or it may be interpreted as a fault current resulting in circuit breaker operation, or result in the opening of fuses if the currents persist for a long enough period and contain sufficient energy. Low level pulses in analog circuits usually appears as noise and does not interrupt circuit operation. In digital circuits, the induced waveform may be interpreted as discrete pulses which are propagated through the system resulting in errors. For example, flip-flops and Schmitt triggers may be inadvertently triggered, counters may record wrong counts, or memories may be altered due to driving current or direct magnetic field effects. These voltage and current thresholds are usually much lower than those required for analog circuit upset so digital circuits and semiconductor or core memories are the most susceptible.

Digital Circuit Upset

Operational upset mechanisms will be briefly illustrated by considering the effects of EMP-induced transients on digital logic circuits and computer memories. A digital logic circuit may be upset by input terminal disturbances or by dc and ground disturbances. The problem is further complicated by whether or not the disturbance propagates through the system.

DIGITAL LOGIC CIRCUIT UPSET

There are two general types of problems associated with upsetting a digital logic circuit:

1. input terminal disturbances
2. DC power and ground disturbances

An example of operational upset is given by considering an inverting gate. An unwanted pulse on such an inverting gate may change its state. This undesired change of state of the output of the inverting gate may be amplified by the following gate and propagated on through a string of digital gates. An error may thus arise in a bit in a data register.

An input disturbance will be propagated by the following gate if the undesired output state of the first gate exceeds the on-threshold of the second gate.

DC TRANSFER FUNCTION OF AN INVERTING GATE

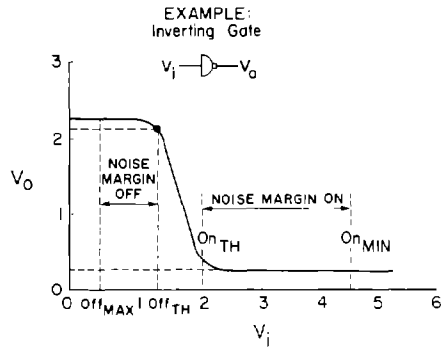

The circuit diagram for a nonsaturating DTL (diode-transistor logic) dual four-input gate, constructed with dielectric isolation and thin film resistors,

is shown in the accompanying figure. It has a low noise margin (1.2 v) and a high speed (10 nsec) propagation time.

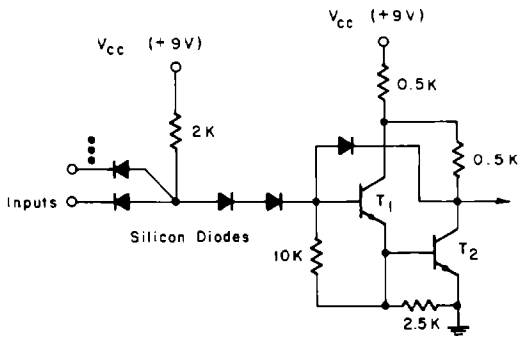

DTL GATE CIRCUIT

If the semiconductor forward voltage drops are all equal to $V_\phi \approx 0.6$ volt, the input dc threshold for conduction of T_1 and T_2 is approximately $3V_\phi = 1.8$v. Conversely, the (largest) threshold for turning T_1 and T_2 off is $3V_\phi - 9 = -7.2$ v This means that the transient necessary for turn on must be at least 1.8 v, and for turn off at least -7.2 v. Unbalance of this sort is undesirable from an EMP hardness standpoint. For transients that exceed the threshold for times less than the specified propagation delay, a higher level can be tolerated before transient upset occurs. Although this level is related to the time duration, the polarity, the input point, and circuit parameters such as noise immunity and response speed, no straightforward way of establishing the relationship is known except to experimentally test the circuit. Experimental results for this circuit for negative and positive upsets on the input lead are shown in the following figures. Once the transient pulse width exceeds the propagation time, the required upset voltage asymptotically approaches the dc threshold voltage. Shorter pulse widths require correspondingly greater voltages.

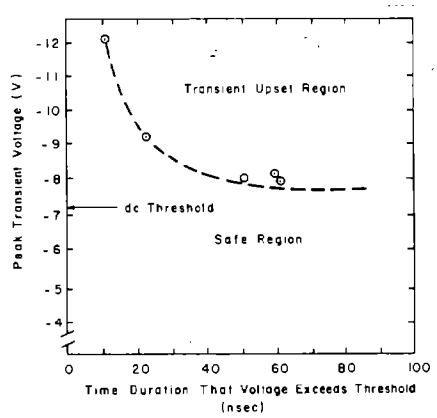

INPUT LEAD NEGATIVE UPSET

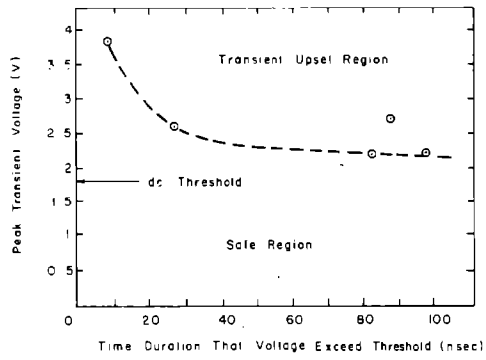

INPUT LEAD POSITIVE UPSET

These results show that the dc threshold establishes a safe measure for transient upset. Observations indicate that transient upset levels appear to be independent of the exact waveshape, depending rather on the peak value. It has also been observed that circuit threshold regions for upset are very narrow. That is, there is a very small amount of voltage amplitude difference between the largest signals which have no probability of causing upset and the smallest signals which will certainly cause upset.

Memory Erasure

Computer memories are also susceptible to EMP induced transients. The level of susceptibility is determined by the magnetic field required to change the magnetization state of the memory element (magnetic memories), or the voltage or current thresholds for semiconductor memories.

In the case of magnetic memories, the magnetic field impressed may be due to direct magnetic field effect (impinging magnetic field illumination) or driving

currents induced in the associated wiring. The direct effects require much higher levels of incident magnetic field than the induced current effects. The table indicates the minimum energy levels required for upset of typical digital circuits and memories due to EMP induced signals.

The minimum energy necessary for operational upset is on the order of one to two orders of magnitude less than for damage of the most sensitive semiconductor components.

MINIMUM ENERGY TO CAUSE CIRCUIT UPSET OR INTERFERENCE

DESIGNATION	MINIMUM ENERGY JOULES	MALFUNCTION	OTHER DATA
Logic Card	3×10^{-9}	Change of State	Typical logic transistor inverter gate
Integrated Circuit	4×10^{-10}	Change of State	Sylvania J-K flip-flop monolithic integrated circuit (SF50)
Memory Core	5×10^{-8}	Core Erasure Via Wiring	Burroughs medium speed computer core memory (FC 8001)
Memory Core	3×10^{-9}	Core Erasure Via Wiring	RCA medium speed core memory (269M1)
Amplifier	4×10^{-21}	Interference	Minimum observable energy in a typical high-gain amplifier

The most susceptible memories are those that require the smallest driving currents to cause a change of state in the memory, such as core or semiconductor memories. It should be noted, however, that if the transients are induced in circuits external to the memory proper, that is, prior to the read/write amplifiers for example, they may be amplified in the same manner as normal signals and written into memory. Under this condition, the hardness of the memory proper is a secondary consideration. It is obvious that under this condition the memory is most susceptible in the write mode of operation. This has been verified experimentally.

Effects of Operational Upset

The effect of operational upset on system performance and mission is highly dependent on the system design and use. In some systems, loss of synchronization for as long as a few milliseconds is of no great importance. On the other hand, loss of stored information in a computer may require restart of a very long computer program, thus delaying the operation of a specific system.

The trajectory control of a spacecraft or missile is an example where operational upset for a very short time may be of considerable significance.

Some functions performed by a computer may be unimpaired by relatively long periods of circuit upset. Others may be impaired by short periods of upset. In this example of a power station computer, functions such as data logging, scan and alarm, performance calculations, and trend recording may be relatively unaffected by operational upset. On the other hand, process control functions such as turbine startup, boiler setpoint control, and combustor control may be affected to a much greater extent.

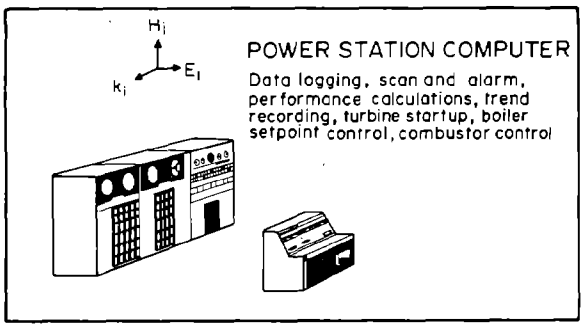

Large amounts of energy may be collected by power lines and cause circuit breakers to open. The time to reenergize the system may cause its function to be seriously impaired. Also, since a considerable amount of a generator's load could be dropped, undesirable effects might occur in the generating and transmission system.

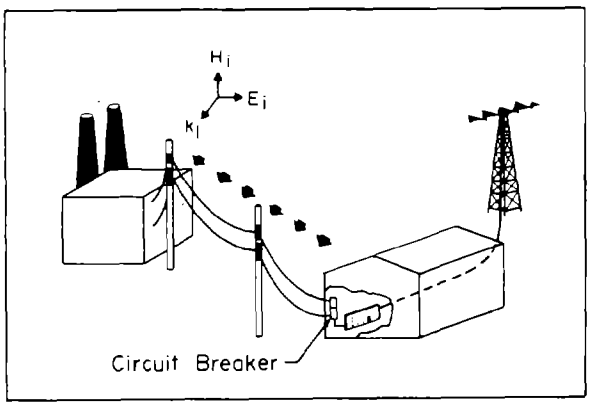

REFERENCES

Burdenstein, Paul P., et al., "Second Breakdown and Damage in Semiconductor Junction Devices," Auburn University, Auburn, Alabama, Report No. RG-TR-72-15, April 1972.

"EMP Engineering and Design Principles," Bell Telephone Laboratories, Loop Transmission Division, Electrical Protection Department, Whippany, New Jersey, 1975.

Lennox, C.R., "Experimental Results of Testing Resistors Under Pulse Conditions," Electrical Standards Division 2412, Sandia Laboratory, Albuquerque, New Mexico (PEM #6).

Case, C., Miletta, J., "Capacitor Failure Due to High-Level Electrical Transients," HDL-TM-75-25, Harry Diamond Laboratories, Adelphi, Maryland, December 1975.

"DNA EMP Preferred Test Procedures," IIT Research Institute, DNA 3286H, Chapter 14 (to be published).

"Electromagnetic Pulse Handbook for Missiles and Aircraft in Flight," Sandia Laboratories, AFWL-TR-73-68, EMP Interaction Note 1-1, September 1972.

Domingos, H., "Pulse Power Effects in Discrete Resistors," Clarkson College of Technology, Potsdam, N.Y., AFWL-TR-76-120, November 1976.

Tasca, D.M., Wunsch, D.C., Domingos, H., "Device Degradation By High Amplitude Currents and Response Characteristics of Discrete Resistors." Work supported by DNA under Subtash R 990 AXE B097, Work Unit 42.

Tasca, D.M., (General Electric), Wunsch, D.C., (AFWL), "Computer Damage Characteristics Due to EMP Induced Transients," (to be published).

Wall Thickness and Material

In the EMP time domain, the dominant mechanism in shielding is the induced surface current. This is concentrated in a surface layer, the "skin depth (δ)," is given by

$$\delta = \frac{\tau}{\mu_o \mu_r \sigma}$$

where

τ = time

μ_o = $4\pi \times 10^{-7}$ permeability of air

μ_r = relative permeability of the material

δ = conductivity of the material

Since the skin depth varies as $\sqrt{\tau}$, it is difficult to significantly reduce the internal $\dot{B}$.

In most practical cases, it becomes difficult to justify a shielding thickness much greater than that required by mechanical strength and rigidity.

Wall Thickness

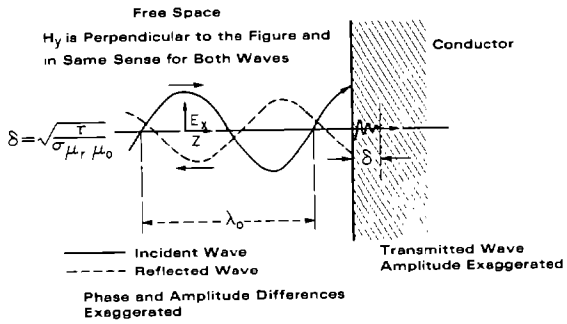

Schematic Representation of the Reduction in Amplitude of an Electromagnetic Wave on Entering a Metal

The skin depth also depends on $\sqrt{\mu\sigma}$ ($\mu = \mu_o \mu_r$). Hence, there is not as much difference between copper and steel as one might think. We see here that the main advantage of steel is to obtain the same attenuation at about one order of magnitude lower frequency. Note also the large attenuations realized for relatively thin sheets. These values are for infinite sheets of material.

Materials

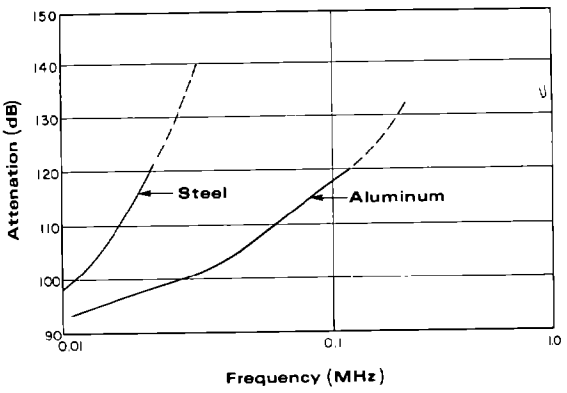

Magnetic Attenuation versus Frequency.

As indicated, the attenuation (shielding effectiveness) for magnetic fields is a function of frequency. The higher the frequency (the greater the $\dot{B}$), the greater the attenuation. Therefore, the shield tends to be a $\dot{B}$ reducer.

A SHIELD = $\dot{B}$ REDUCER

A further implication is the lower the frequency the less the magnetic field attenuation. Therefore, good low frequency shielding requires the use of very high permeability (μ) materials, such as hypernom and conetic, or very thick materials such that magnetic field ducting is realized.

Diffusion Shielding

There is another kind of shield -- the semipermeable type; examples of which are earth cover and rebar grids. Here the effective skin depths may be large (δ = 28m for earth with conductivity of 10-2 mhos/m at a frequency of 100 kHz), and the total attenuation relatively small -- about 30 dB. Usually this is used in combination with smaller, internal,

and more complete shields. Often such a shield appears as a zone enclosure of opportunity, such as in buried or heavily reinforced structures.

The waveform appearing inside such a diffusion zone will generally be a combination of a short spike (possibly associated with apertures) and a longer "tail," related to the induced skin currents on the conductor.

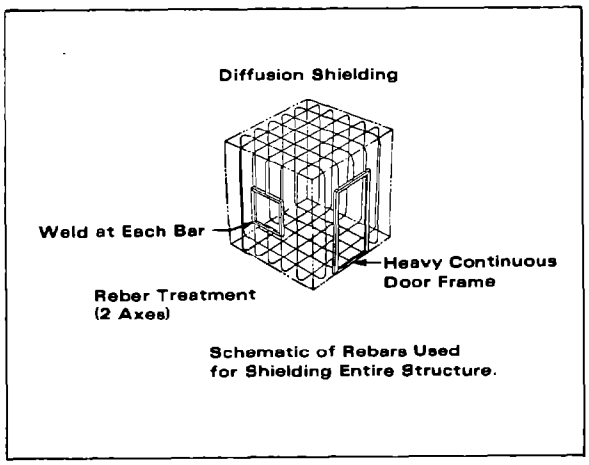

Apertures

There are many different kinds of "apertures." They may be divided as intentional and as unintentional. The single worst class of violations of good EMP protection practice is found in the accidental or unintentional compromise of shielding integrity. Anything which interrupts the skin current path on a shield increases its impedance and acts as a radiator into the internal region. Hence, the effect of a seam crack is not measurable simply by its physical area, which may be quite small. If it is near a region of high surface current concentration, it can couple energy to the interior many times greater than you would superficially guess. In particular, physical breaks -- such as seams and bonds, however well made -- represent a constant threat to integrity and protection value.

Of course, it is almost impossible to fabricate a shield as a single, unbroken, electromagnetic enclosure. Large system enclosures can only be constructed by assembling large numbers of sheets or plates. Technically, the contact lines or seam between such single pieces represent potential apertures.

Depicted is an "idealized aperture"-- a long slit in a shield wall due to a poor panel joint. It behaves approximately like a slot dipole antenna. In effect, it is excited by the EMP fields and the induced skin currents and radiates a wave, characteristic of its length, into the box.

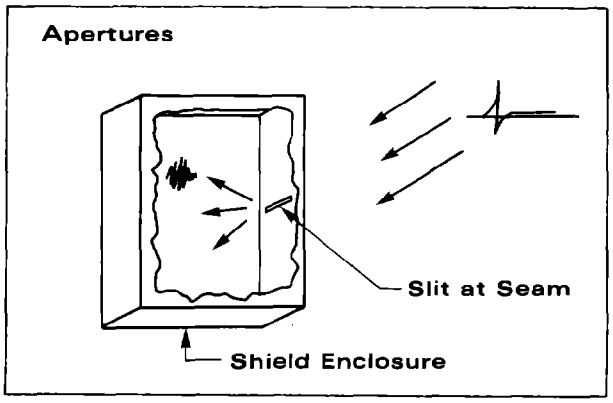

The most common large-scale seam fabrication techniques involve welding for steel or aluminum and soldering or brazing for copper. These fabrication methods in themselves place certain minimum thickness criteria on the material. Thin sheets tend to "burn through" during welding. Therefore, at least two mechanical aspects impose minimum thickness requirements, which may be greater than required by the EMP criterion: strength and fabricability. Such thicknesses run from 60 to 300 mils for medium-large construction. Overlap should preferably be 10-20 times the sheet thickness for thin sheets. Butt joints can be acceptably used for thick plate, but this usually requires welds on both sides, with careful probe tests for weaknesses.

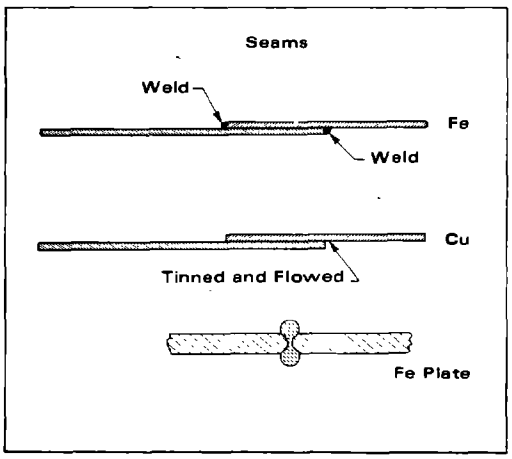

The necessary mechanical thickness provides an implicit (and high) protection level. Inexpensive assembly methods, such as tack welding, may seriously erode the protection level due to aperture leakage at the open seams throughout the structure. The "good shielding" criterion

may require continuous and meticulous welding along all seams in order to match the protection value inherent in the material itself.

As an example of the welding integrity criteria, an ICBM test facility had a shielded room built into its base. This enclosure had a 100 dB requirement in the UHF domain. The construction was such that several large structural I-beams passed through the room. In order to "seal" the room electromagnetically, specially cut plates were welded around the beams and onto the steel walls. These seam areas were tested by using a transmitter loop outside and smaller receiver loop probe inside. A single continuous welding pass proved inadequate to prevent leakage at this seam. Several additional passes were needed around these beams, both inside and out. These were made in such a way as to build up a thick weld. The inner corners were particularly difficult points, as indicated here.

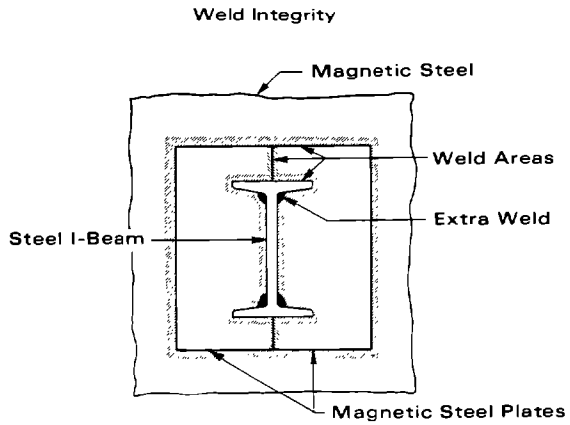

Gaskets and Bonds

Considering the difficulties encountered with such seemingly "tight" apertures as welded seams, it is no surprise that metal-to-metal contact surfaces, held together by simple mechanical pressure, can constitute serious violations of shielding integrity. Such contact areas are unavoidable at functional apertures, e.g., access doors, service hatches, equipment panels, etc.

There is extensive literature on all manners of bonding long, continuous, metallic, contact lines. They deal with a range of bonding permanency, from permanent, once-made joints, through rarely-disturbed service panels, to continuously exercised doorways. Of course, the latter represent the most difficult problem in dependability and maintainability.

The basic mechanical requirements for simple reliable seam bonds are absolute flatness and electrical cleanliness. Neither of these is generally achievable in other than ideal laboratory conditions. The pragmatic hardware problem is then to obtain low-impedance continuous contacts at an acceptable level of "dirtyness" and "deformation."

Electrically clean surfaces can be readily obtained with pure tin, gold, palladium, platinum and silver! Zinc, cadmium, and very thin gold platings are considered as acceptable substitutes. Easily oxidized materials (like aluminum) should be avoided. Lubricants are capricious. In some cases, they will inhibit corrosion and oxidation and facilitate good metal-metal contact. However, motor oils, for example, are more apt to do just the opposite.

Controlled roughness (machine sining and knurling) is generally better than attempting to achieve a smooth surface for mating parts. When controlled roughness is utilized, the total contact area is generally greater, and easily predictable, than for smooth surfaces which mate usually at only three points (no surface is perfectly smooth).

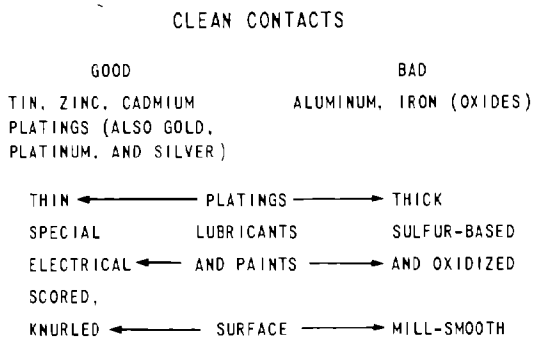

Roughness is one way to compensate for surface irregularity. An ultimate way to do this is to use deformable conductive gaskets. A good way to understand the pressure contact problem is to consider a panel seam, bonded by means of bolts and flange strips, as illustrated here. In the frequency domain of interest, seams of this type require specific contact pressures of 60 to 100 pounds per lineal inch for 80-100 db attenuation. Obviously, this form of seam is best for "once-only" cases, which are expected to be broken very rarely, if ever, during the system's life.

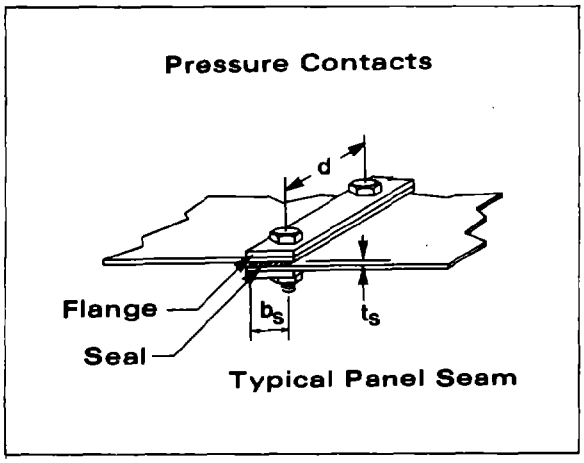

People have also resorted to the "gasket" solution for "bonding" peripheral contacts which would only be occasionally broken. It is also useful for irregular or deformable surfaces.

There are two "fairly" good types:

1. The flat molded metal gasket which deforms slightly under pressure. This is a "throw-away" in the sense that it cannot be reused.

2. The braided cord gasket. A variety of exotic designs appear on the market. The good ones from an attenuation standpoint utilize deformable metal cores. Unfortunately, these have low resiliency and can only be reused two or three times. The synthetic core, double braid gaskets are generally more transparent in a given geometry. The single braid types provide even less attenuation. Braided gaskets are not generally recommended for exposed, unmaintained situations for EMP protection.

Corrosion control of the gaskets and the associated mating surfaces is also a problem. Considerable maintenance is required to insure good electrical contact.

Depicted is a typical application of a knitted mesh gasket for a ship missile loading hatch. Note that the RF gasket is protected from corrosion by a water seal on the hatch.

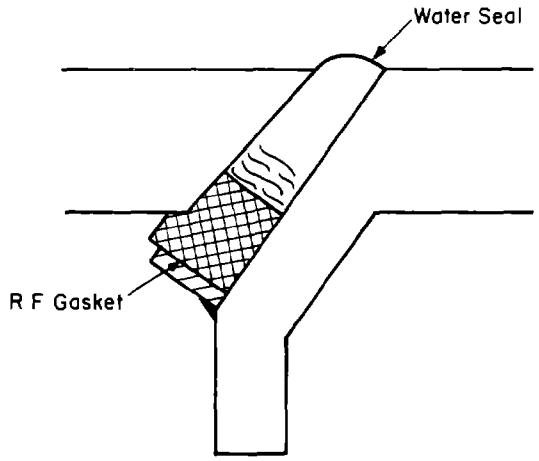

MISSLE LOADING HATCH RF SHIELDING (CLG), (METHOD A)

The average field attenuation that can be obtained with knitted wire mesh gaskets as a function of the applied pressure is indicated here. It should be noted that application of higher pressure increases attenuation, but shortens the lifetime of the gasket as it permanently deforms.

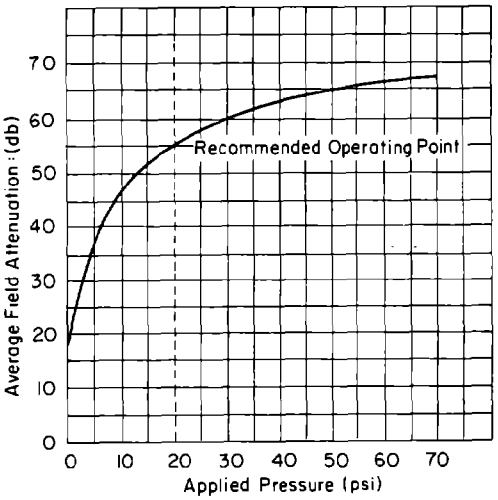

KNITTED WIRE MESH GASKETS, AVERAGE FIELD ATTENUATION

Resilient finger stock is a favorite solution for doors and hatches which must be frequently used. Finger stock should be used in double rows. Some people suggest that the rows should be staggered for maximum attenuation so that the fingers in one are opposite the slots in the other. At the higher frequencies, this seems reasonable when one considers the radiation pattern of each slot, seen as a tiny dipole.

Finger stock is probably the most difficult protection hardware to maintain. Traffic inevitably brings with it dirt and abrasion. The doors and frames must be extra stiff if the fingers and the contact surfaces are to maintain their register.

Finger Stock and Doors

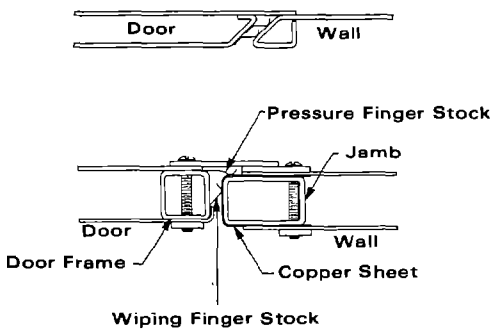

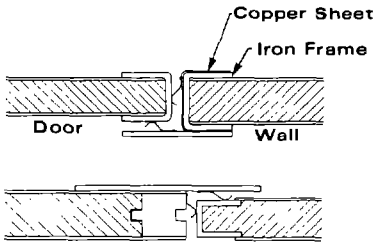

The joint constructions illustrated here show some of the ingenious ways in which shielding engineers have solved the problem of structural flexibility with reliable shielding effectiveness. They typify shielded enclosures for R.F. testing and measurement. At present, at least, it is not likely that military systems would employ such components except as accessories in production and testing phases.

The prefabricated bolt-together enclosure has enjoyed wide acceptance. It does, however, require periodic maintenance. The frame shifts cause open slits and metal-to-metal seam corrosion. Where high shielding requirements exist, serious consideration should be given to the welded seam enclosure.

Shielded Enclosures

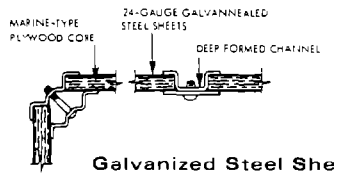

Galvanized Steel Sheet with Plywood Core.

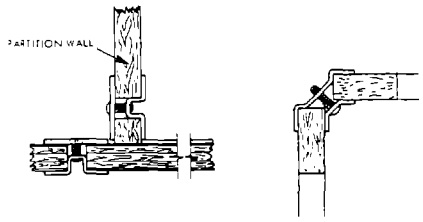

Partition Joint Example.

Open Apertures

So far we have dealt with apertures which could be "closed" electromagnetically by means of conductive materials (sheets) and construction similar to the surrounding shield. The significant problem was with peripheral control. Some mechanical requirements, however, call for a physically open aperture for such things as ventilation, microwave lines, etc. Two broad classes of "solutions" are common for these: screens of various types, and "waveguides-beyond-cutoff." The latter can also be used sometimes for entrance passages and doorways to avoid the finger-stock problem, where penetration of high frequency content is clearly not a problem.

Ordinary heavy-duty screening can provide on the order of 40 dB attenuation. The trouble with ordinary screening lies in corrosion and oxidation which can break the contact between individual wires. Electromagnetically, an old piece of screening may be a good coupler. The specially fabricated materials like "electromesh" are treated to resist this action.

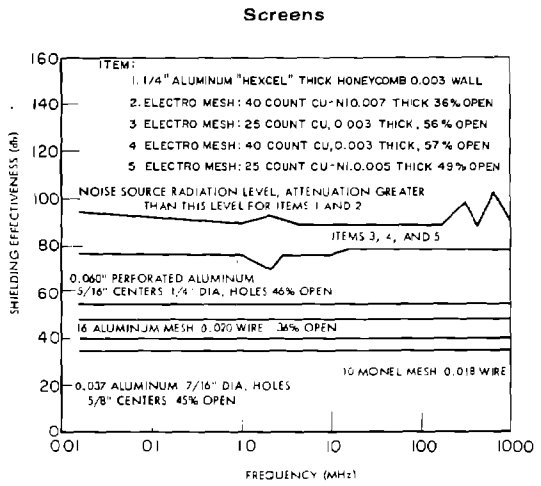

attenuation of various screening materials

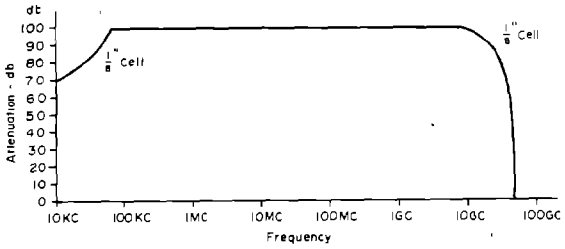

PREDICTED THEORETICAL ATTENUATION

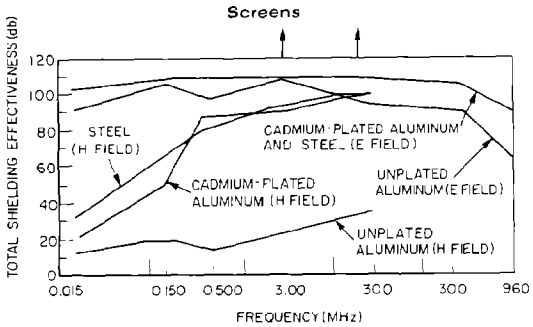

claimed performance of an average commercial honeycomb filter

Hexcel is usually satisfactory, but there have been instances of poor quality control in which the glue between the foils acted as an insulator. True "honeycomb" screening provides the best compromise between shielding and air flow. Where air flow is important, best results are obtained with honeycomb which has soldered, brazed, or welded contacts between foils.

The "waveguide-beyond-cutoff" is somewhat of a misnomer. Over most of the EMP frequency domain, such a geometry is really behaving more like a quasi-static "field-bender." The idea is to design it so that its cut-off frequency is significantly well above the high-frequency "roll-off" in the environmental spectrum. This is not difficult to do if it is under many feet of earth or it is already protected by some partial attenuation, such as a welded rebar cage. These situations tend to move the roll-off to lower frequencies, as we have indicated before. For example, a two (2) meter high driveway would have a cutoff frequency of 75 MHz ($f_c = \frac{c}{\lambda}$, where $\lambda = 2a$ and a is the maximum doorway dimension). For frequencies of less than 30 MHz, the attenuation is between 12 and 13.65 dB per meter length within the guide.

The approach is fine for ventilation, but care must be taken not to make the guide a propagating structure by running cables through it.

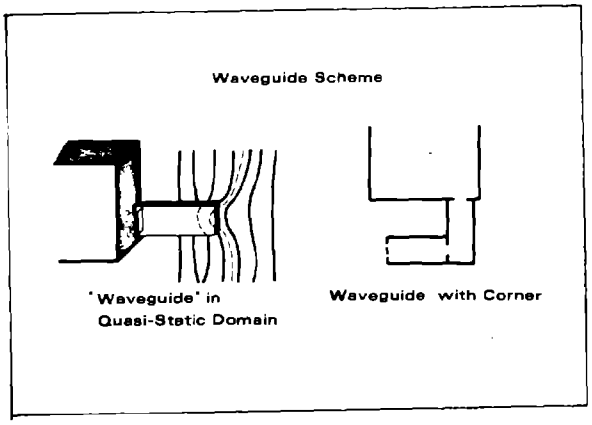

The use of the "waveguide-beyond-cutoff" approach for ventilation shafts in structures is one typical application. High frequency roll-off is obtained by partitioning the overall opening into an array of smaller openings as depicted. This will cause some reduction in airflow depending on the effective area reduction of the overall opening.

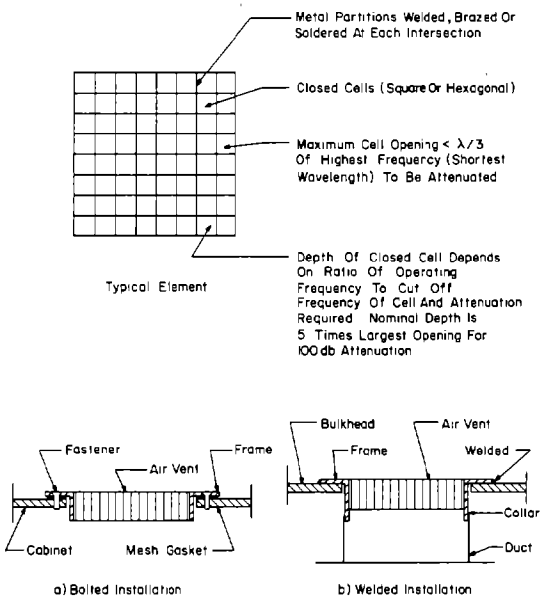

USE OF HONEYCOMB MATERIAL FOR SHIELDING AIR VENTS

Another technique to handle large apertures, such as personnel entry ways into shielded compartments, is through the use of a protected entry. Shown is a technique using a double shielded door hallway type configuration. Interlocks should be provided if critical equipments are housed in the compartment so both doors cannot be open at the same time.

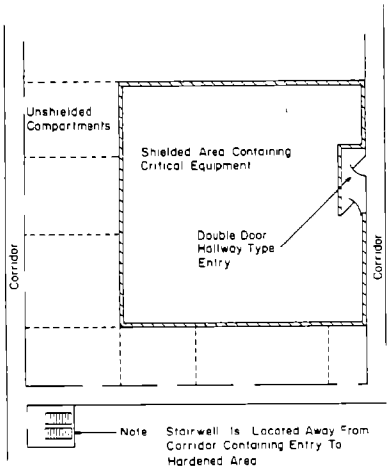

DOUBLE DOOR HALLWAY TYPE ENTRY TO HARDENED AREA

Penetrations

There are many kinds of "penetrations." Most commonly, one thinks of an insulated conductor passing into a facility or system. It may be carrying power or functional signals, but uninsulated, "grounded" conductors, such as motor shafts, can also represent penetrations. Thus, there are two broad classes -- electrical and mechanical. We see here ways in which each can provide paths for coupling and transferring energy from the external to the internal zones. Note particularly that mechanical penetrations can be deceptively protected by innocent-looking bonds, which are really high-impedance couplers.

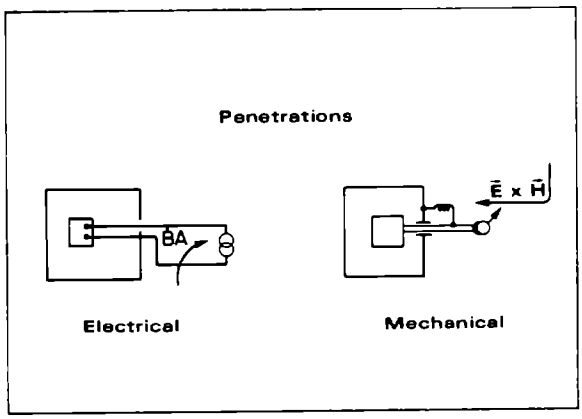

The existence of a true "electrical penetration" corresponds to an intentional or unintentional violation of the zoning concept. If an electrical circuit is carefully confined to a single EM zone, then its penetration through a shield does not, in fact, constitute a violation. In principle, it cannot transfer energy which would not be there in its absence. We make this seemingly simple point to emphasize the necessity for observing zonal hierarchies in providing conductor and cable shielding (as discussed in a succeeding section).

But what about unavoidable conductor penetrations -- such as, for instance, long wire antennas? One thing to do to rectify such situations is to provide entrance protection in the form of filters or active devices (zener diodes, spark gaps, etc.). These are discussed in the section on "Protective Devices." These protective devices should be located in vaults or small shielded boxes.

Since all external conductors are collectors of EMP energy, they must all be terminated at the entry to the shielded compartment (or equipment cabinet). If these terminations are allowed on a haphazard basis, (terminating on all sides

of the enclosure), they will inject additional current on the enclosure resulting in higher fields on the inside. Therefore, to keep this energy from entering, all penetrants are brought into the protected space via a single point of entry into an entry vault. The conductors (pipes, conduits, cable shields, etc.) are peripherally welded to the enclosure at the entry point. All protective devices are contained in the vault and the output electrical leads into the enclosure protected by feed-through capacitors, for example. These terminal protection approaches are discussed in subsequent paragraphs of this section.

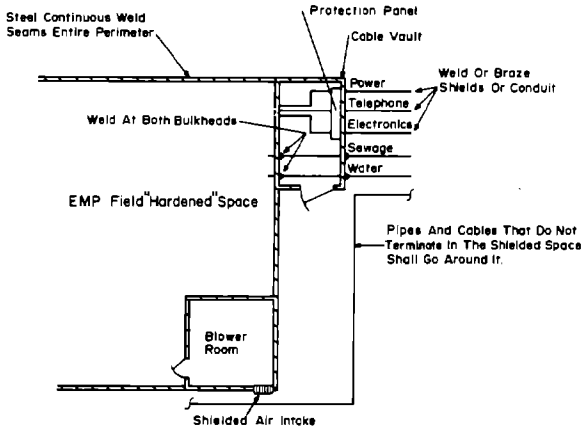

TYPICAL EMP HARDENED SPACE

Finally, one can isolate that portion of the system (which really goes back to systems and circuit layouts) and simply make its terminal circuits very hard.

So we see that the treatment of purposeful electrical penetrations is not really a "shielding" topic.

ELECTRICAL PENETRATIONS

NOT REALLY A "SHIELDING" HARDWARE PROBLEM -- WHY?

ZONE VIOLATION ⟶ GO TO "SHIELDED"

ENTRANCE PROTECTION ⟶ GO TO "PROTECTIVE DEVICES"

TERMINAL HARDENING ⟶ GO TO "SYSTEM ASPECT" AND "COMPONENT SUSCEPTIBILITY"

We noted before that a conductive metallic penetration may be deceptively protected. Consider, for instance, a shaft passing through a bushing. In the case of a metallic shaft with a conductive bushing and a bond strap, it can be treated analytically as a parallel R L circuit as shown. Simple circuit analysis can be applied to determine the fraction of the current which is not shunted by the bond strap or the bushing resistance. If the bushing has a high contact resistance (or is an insulating bushing), at high frequencies ($WL \geq R$) the shaft can act as a probe antenna coupling directly to the interior as a skin current or by reradiation. This type of penetration could easily result in a 30 dB lead in a 60 dB shield.

In the case of a nonconductive shaft, the configuration can be modeled for analysis as a dielectrically loaded circular aperture. The aperture problem becomes important when the aperture diameter is equal to or greater than the half wavelength of the highest frequencies associated with the incident waveform. For small shaft dimensions (5 to 10 cm), the coupling through the aperture would be small (a few dB) over the frequency spectrum of the EMP.

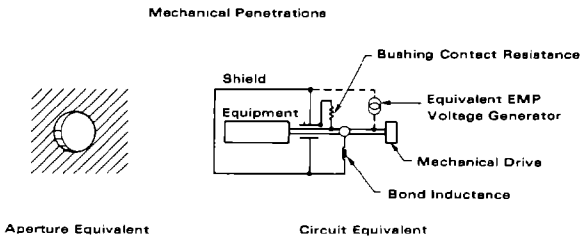

The principle here is to "rectify the obvious." We will discuss some embodiments for these first two types of fixes.

Treatment

- **Break the metallic path**
- **Improve the seal bond**
- **Examine electromechanical servos, relays (plus filters on the wires)**
- **Examine non-conductive, exotic schemes**

The first approach is to break the metallic path. This treatment replaces the continuous conductor by a small capacitance. Its equivalent circuit represents it as a filter between the two EM zones. Note that the separate small enclosure must be well-bonded to the shielding partition between the two zones. An impedance at this point turns it into an effective coupler. This is equally true for filters and for other enclosed protective devices located at a partition between zones. An alternative approach is the use of the waveguide-beyond-cutoff technique. This approach requires the mechanical shaft to be non-conductive. In sizing the waveguide, it must be analyzed as a dielectrically loaded guide with the dielectric being the mechanical shaft.

Break the Metallic Path

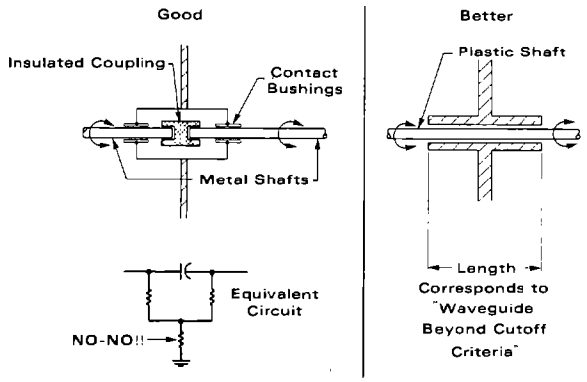

Shown are two examples of unusual treatment. A simple way to improve a leaky manual adjustment shaft is to mount it through a split-bushing with a taper-thread locking nut. When the locking nut is tightened, a low resistance bond is achieved between the shaft and the equipment panel.

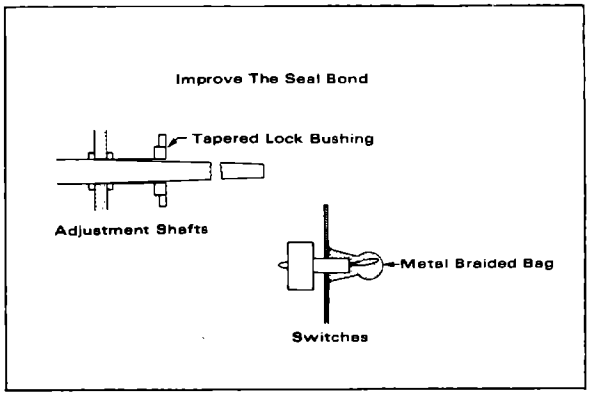

In "explosive proof" hardware, or in equipments with very high shielding requirements, a simple fix is to utilize a braided metal bag to increase the shielding as shown.

Grounding

The primary purpose of grounding is the protection of personnel and equipment. Electrical codes require that electrical and electronic equipment cabinets/frames be connected to the surrounding media (building, earth, etc.) in such a manner that no shock hazard exists due to a voltage difference between the equipment and the surrounding media. For equipment protection, the purpose of the ground is to provide a fault current path so sufficient fault current can flow to cause circuit breaker or fuse actuation. Ground further prevents the buildup of electrostatic or transient voltages that may cause insulation damage. Lightning protection is a special case of transient voltage buildup which is shunted to ground, in most cases, via surge protective devices.

In other words, the purposes of grounding are to provide an equipotential connection between equipments and surrounding structures/media, and a return current path for fault currents. For signal circuits, two-conductor transmission lines are used. Tying the signal circuit to ground prevents electrostatic drift and provides a common reference provided the ground circuit is truly an equipotential plane.

The discussion which follows will divide the grounding problem into earth grounds ("exterior" grounds), and equipotential or reference nodes ("interior" grounds). Emphasis will be placed on meeting system grounding requirements without becoming a major source of EMP pickup.

Both Interior and Exterior Grounds are Needed for Other System Requirements

Both Interior and Exterior Grounds can be a Major Source of EMP PICKUP

Earth/Exterior Grounds

There are at least three reasons for considering how EMP and exterior grounds interact. First, there are long wavelength threat components with which ground circuits can meaningfully couple. Second, system grounds are essential for any number of other reasons; hence, their EMP coupling is a germane issue. Third, it has been pragmatically established that grounds make a noticeable difference -- good and bad -- in nuclear test and nuclear simulation instrumentation.

Of course, a grounding system can be put to advantage in EMP control. But this needs to be integrated with other grounding requirements, i.e., lightning, power, etc.

The basic idea of earth grounding is to provide an equipotential distribution between the structural members of a system and the surrounding natural environment. This concept is perfectly valid only for the ideal case of static fields, infinite earth (ground) conductivity, and no current flow. Thus, earth grounding is an attempt to connect, in a field-significant way, to the large, but poor, conductor. In the cases of shock hazard elimination or lightning protection, only lower frequencies are of interest and this "equipotential surface" concept must only apply for local areas. For EMP, on the other hand, where distributed systems are of concern, this concept must apply over large geographical areas and over a broad frequency spectrum.

Another factor is the connection from the system structural members to the earth. The idea is to couple the electromagnetic energy into the earth and absorb it in the earth. The impedance to earth is a function of the connection from the system to the groundwell, and the impedance of the groundwell to the earth. To minimize voltage buildup due to EMP or other transients, these impedances must be low at all frequencies of interest. All conductors have associated with them in inductance which is a function of the geometry of the conductor. The inductance term produces an IZ_c drop (conductor impedance), in addition to the IZ_g (ground impedance). The groundwell impedance can be reduced by using large contact area ground rods or wells and improving the conductivity of the earth in the immediate vicinity by "salting" (ionic salts). Further, most of the EM energy in a current carrying conductor exists in the field external to the conductor. The impedance mismatch results in the field stored energy being reflected and reverberating on the conductors.

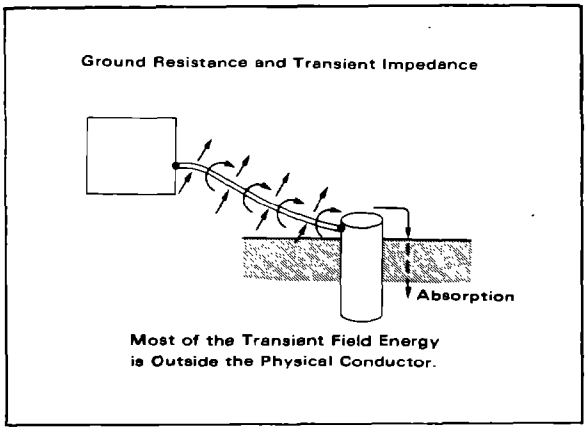

One demonstrated use of controlled grounds was found during atmospheric testing. Here, long duration reverberation currents on the exterior of the cables were present which often interfered with shock wave measurements which occur a few milliseconds to seconds after the blast.

By viewing the long cable run as a transmission line and terminating it in its Z_o, much of the reverberation could be suppressed.

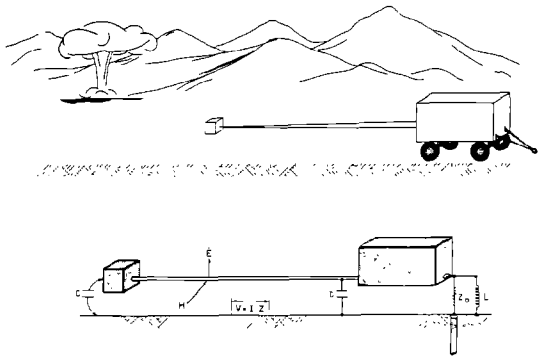

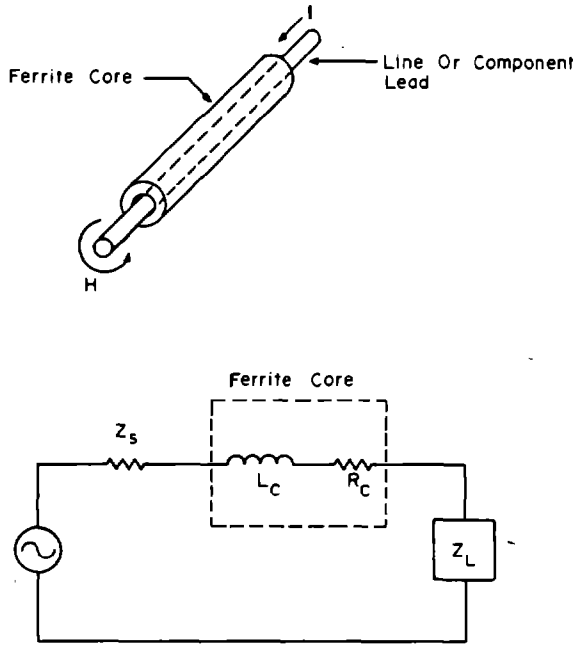

FERRITE CORE AND EQUIVALENT CIRCUIT

Filters

The most common passive, lumped-element device is the terminal filter. It is basically a black-box with input and output connections for insertion into an otherwise continuous two-wire circuit. Its insertion loss is chosen for minimum attenuation in the frequency domain of normal circuit operation and maximum attenuation in the domain of maximum "noise" (i.e., induced EMP signal) content.

The intercepted energy has to be diverted or absorbed. It may be reflected back into the input system, increasing the EMP level there. A better alternative would be to dissipate the energy as heat in an internal filter resistance. This implies a preference for "lossy" filters.

The effectiveness of the filter also depends on the out-of-band responses of the filter. Since the EMP induced energy contains a wide spectrum of frequencies, even the damped sinusoid, the filter must not have any spurious responses over the interfering signal spectrum. Further, if filters alone are used, the components used in the filter must be capable of withstanding the induced voltages and currents without failure.

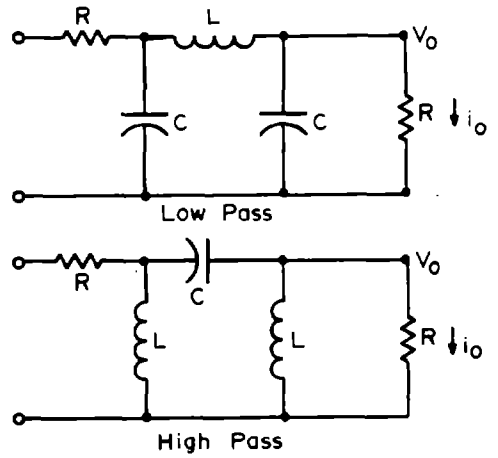

Here is a typical working example of a filter analysis for a very severe exposure situation. One might experience something as bad as this for a completely "naked" megawatt level power line. The figure shows the effect of a simple, three-element filter for various design parameters.

Note the logarithmic scale compression. Obviously, the linearized pulse will be much "more peaked" in appearance.

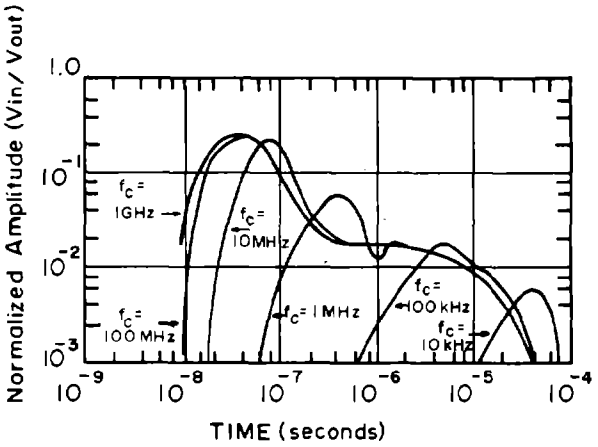

It should be noted that the lower the cutoff frequency of a low pass filter, the more the slope of the wavefront is reduced.

Another example shows the rejection for a typical low pass filter. Shown at the left is a typical power-line EMP surge. Assuming the filter cuts off at about 15,000 Hz, it can pass about 1/5 of the applied energy for certain expected applied waveshapes.

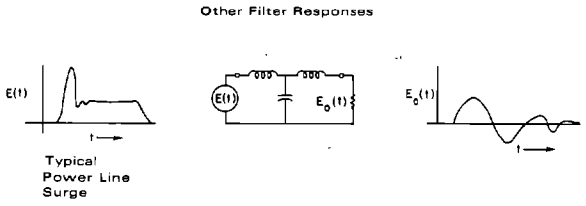

Amplitude Limiting Devices

Amplitude limiting devices are usually nonlinear in nature. Included among these devices are spark gaps, gas and semiconductor diodes, soft limiters such as thyrites and varistors, and mechanical or thermal devices such as fuses, circuit breakers, and relays.

Types of Non-linear Devices

- Spark gaps
- Gas diodes (cold, hot)
- Zener diodes
- Silicon diodes (w/bias)
- Thyrite (sic)
- Fast relays
- Hybrids
- Crowbar circuits

Nonlinear devices can cause some problems. We already indicated under the heading "Filters" that the EMP energy has to go somewhere. This remains true for active elements as well. Furthermore, the switching operation itself can be a source of unwanted EM energy (e.g., RFI) interfering with sensitive downstream components. This is particularly true if the associated circuits contain significant EM energy in normal operation. When the device switches, it must inevitably cause some change in effective circuit impedance and hence in operative current distribution.

In addition, the switching function may generate a spurious pulse in the circuit itself. This is particularly possible if the switching occurs on a time scale short compared to that of the normal operational signals in the system, e.g., on the fast-rise "front" of an induced EMP signal. This is one of the strongest reasons for using "hybrid" (i.e., limiter/filter combination) lumped elements.

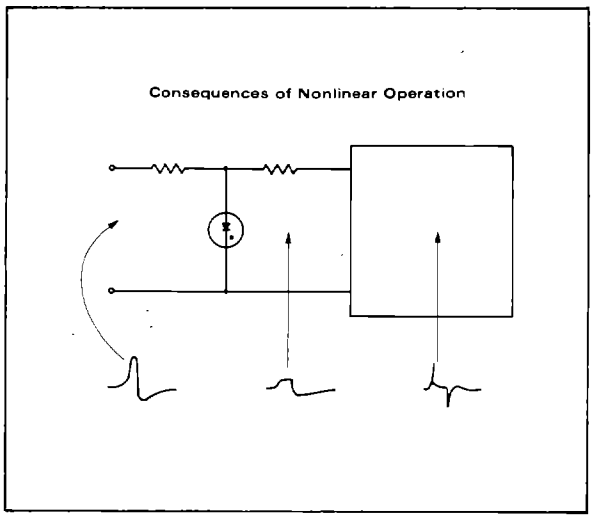

Spark Gaps and Gas Diodes

A spark gap is a voltage-threshold switch with two or more electrodes separated by a dielectric gas. Spark gaps depend on initiating conductive breakdown in a gas. When this breakdown occurs, the device switches from a very low to a very high conduction state.

Spark gap type devices have the advantages of being bipolar in operation and can handle extremely large currents (thousand of amperes). They are available with static initiation voltages of 60 to 30,000 volts. The initiation voltage depends on the gas medium, gap spacing and gas pressure. Arc initiation requires some free electrons and, therefore, there is a minimum for a given gas. The lower voltage devices often use radioactive doping to increase the number of free electrons and thus lower the initiation voltage.

Since these devices require mobilization of the free electrons under the influence of the applied field and generation of secondary electrons due to collisions, it takes a finite time for the arc to occur. Because of this time delay, these devices will fire at the static breakdown voltage for slowly rising pulses, but require higher voltages for rapidly rising pulses. This impulse ratio may be anywhere from a few percent of the static voltage to several times the static volt-

age depending on the steepness of the wavefront slope. For example, a 500 volt gap may have an impulse voltage of 9500 volts for a pulse having a rate-of-rise of 5 kV/ns.

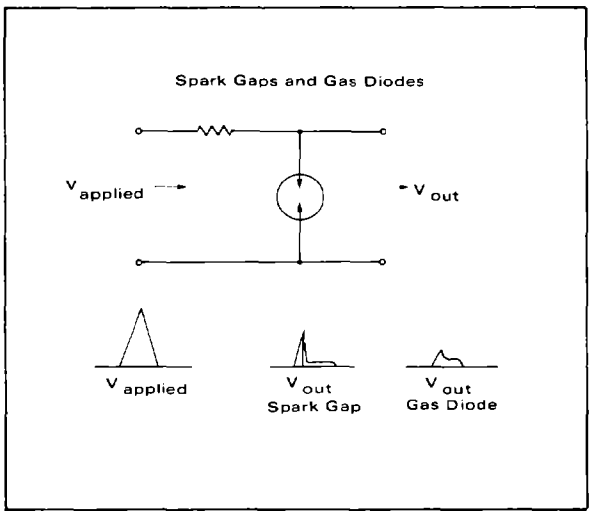

The extinguishing potential must also be considered for spark gap type devices. The voltage at which the device extinguishes is a function of the current through the gap; the higher the current, the lower the extinguishing voltage. This can be a serious problem in dc circuits where the follow current from the source is sufficient to keep the gap ionized. In ac circuits, the gap will extinguish as the signal passes through zero. Special arresters (expulsive arresters) use magnetic fields or gas emissions to extinguish the arc. Resistance in series with the gap (fixed resistors or varistors) can be used to limit the surge current, but this results in higher terminal voltage.

The operation of a typical gap arrestor for a damped sinusoid exciting voltage is shown. The total energy passed is indicated by the shaded area. It should be noted that if the signal amplitude is insufficient to ignite the gap, more energy can be passed to the protected circuit.

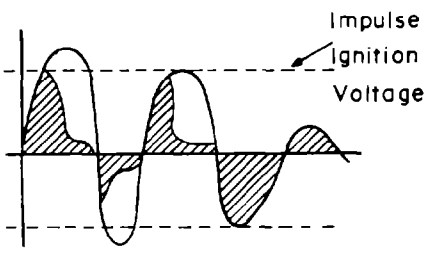

Zener and Silicon Diodes

These are generally smaller, lower power devices. They operate effectively in the voltage-current range of solid state circuitry, so that they are extensively used for such circuit protection. They are voltage-limiting in action (rather than voltage-reducing). Silicon diodes "clip" more effectively -- their "plateau" is flatter. Their operating voltage is generally low -- a few volts -- and the introduction of "hold-off" bias can be an inconvenience. They are generally high-capacity devices, so that there are limits as to the circuit frequency range of applicability. Also, the semiconductor devices have definite limits on the joule energy handling capability (i.e., the protective elements may have low "damage" thresholds).

In general, these devices do not exhibit a turn-up (impulse) voltage characteristic. The p-n junctions in these devices will react sufficiently fast to limit transients even with nanosecond rise times. Caution must be exercised in the application of these devices since if very short lead lengths (less than 1/2 inch) are not utilized, the inductance associated with the leads can result in a voltage drop far in excess of the normal junction voltage.

Semiconductor limiters (diodes) are unipolar devices. The limiting is usually provided by the reverse voltage breakdown characteristic. When breakdown occurs, large currents can result causing a possible failure of the semiconductor if care is not exercised. Zener diodes which are often used for this purpose range in clamping voltage from about 2 to 200 volts. Current handling capability may range as high as a few hundred amperes. For very short (100 of nanosecond to microsecond) pulses.

Extinguishing of these devices is no problem since there are no residual electrons to be swept as in the case of spark gap type devices.

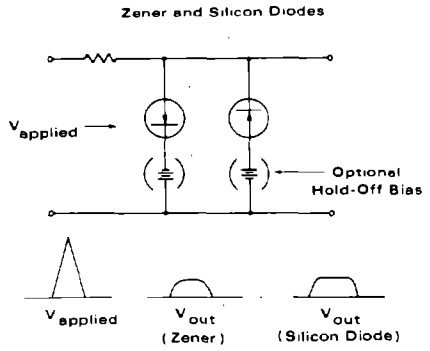

The response of a zener diode limiting circuit to a damped sinusoid incident signal shows the hard limiting features of such a device. The case shown is the same incident signal as that shown previously for the spark gap arrester.

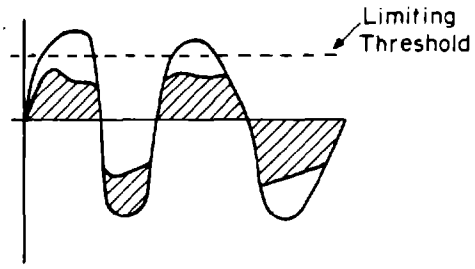

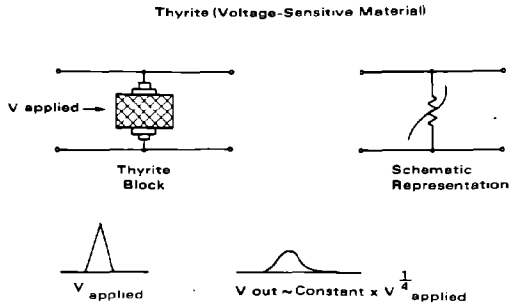

MOV's are available with clamping thresholds of 40 to 1500 volts, response time in the nanosecond regime, and peak energy handling capability of up to 160 joules. SIC's have considerably higher peak energy handling capability, 270,000 joules, and clamping thresholds of 15 to 10,000 volts.

Since these devices are nonlinear resistors, care must be exercised in their application. If they are applied to circuits where normal voltage swings cause a resistance change, the device can generate harmonic and intermodulation type interference which may be objectionable. This could be a problem in RF transmitter output circuits or in power circuits.

Varistors

A varistor is sometimes referred to as a "soft" limiter. It is a bulk semiconductor material whose resistance is varied with the magnitude, but not polarity, of the voltage applied to it. The voltage/current curve is nonlinear but never negative. Therefore, the voltage drop across the device always increases.

There are two basic types of varistors available: (1) the silicon carbide (SIC) type, and (2) the metal oxide varistor (MOV). For very low values of current (less than approximately one microampere) the device acts as a linear resistor with a resistance of hundreds of megohms. At higher values of current, the voltage current relationship is nonlinear and is given by:

$$I = KV^{\alpha}$$

For silicon carbide varistors α ranges between 2 and 7, whereas for metal oxide types an $\alpha \simeq -25$ is typical.

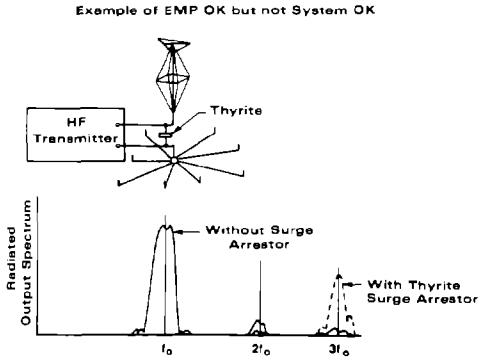

Hybrids

A hybrid circuit, that is, one employing a combination of amplitude and spectral limiting devices, is one of the more favored approaches for terminal protection. A spark gap or other high energy amplitude limiting device can be employed to shunt the bulk of the current. The filter (low pass) following the gap reflects the high frequency energy in the spike resulting in a slowed rate of rise of the wavefront. It also reflects the high frequency noise associated with gap firing. If the pulse out of the filter is still too large, a second, low energy arrester such as a zener diode can be used since the energy in the pulse has been reduced to safe levels for the zener.

The series impedance preceding the surge arrester is a necessary component to assure appropriate limiting; in some cases, the surge impedance of the transmission line can suffice.

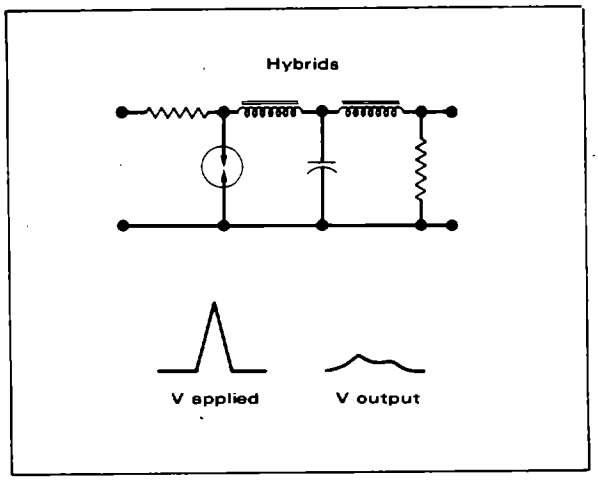

Electromechanical and Thermal Devices

Fast relays, circuit breakers, and fuses have response times that typically are on the order of one (1) to several milliseconds. Their principal value lies in interrupting circuit operation as a result of the current "dumping" of the faster protective devices (arresters). This circuit interruption feature limits the energy which must be dissipated in faster devices and the relays may also be used to initiate restoration to normality from a breakdown condition.

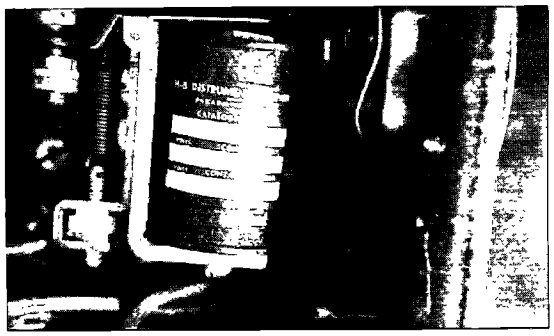

Crowbar Circuits

In these systems, a high-power rating device is operated by a subsidiary sensing/trigger circuit. Thyratrons, ignitrons, spark gaps have been used for the "crowbar." Sensing can come from the circuit itself, from a "threat" sensor, or from an auxiliary breakdown device (e.g., corona optical sensor).

Crowbar circuits are often used to activate the normal system protection interlocks. For example, EMP could "fire" a spark gap or cause an arc-over in the transmitter output. This arc, if not extinguished, could cause excessive plate dissipation in the output tubes. In this case, a thyratron can be "fixed" across the transmitter dc supply to activate the circuit breakers. The thyratron is activated by a corona-sensing photocell near the spark gap or better yet by an impedance sensing circuit.